Journal of Medicinal Chemistry

pubs.acs.org/jmc Article

Template-Hopping Approach Leads to Potent, Selective, and Highly Soluble Bromo and Extraterminal Domain (BET) Second Bromodomain (BD2) Inhibitors

Helen E. Aylott,* Stephen J. Atkinson, Paul Bamborough, Anna Bassil, Chun-wa Chung, Laurie Gordon, Paola Grandi, James R. J. Gray, Lee A. Harrison, Thomas G. Hayhow, Cassie Messenger, Darren Mitchell, Alexander Phillipou, Alex Preston, Rab K. Prinjha, Francesco Rianjongdee, Inmaculada Rioja, Jonathan T. Seal, Ian D. Wall, Robert J. Watson, James M. Woolven, and Emmanuel H. Demont

Cite This: *J. Med. Chem.* 2021, 64, 3249−3281 Read Online

ACCESS | Metrics & More | Article Recommendations | Supporting Information

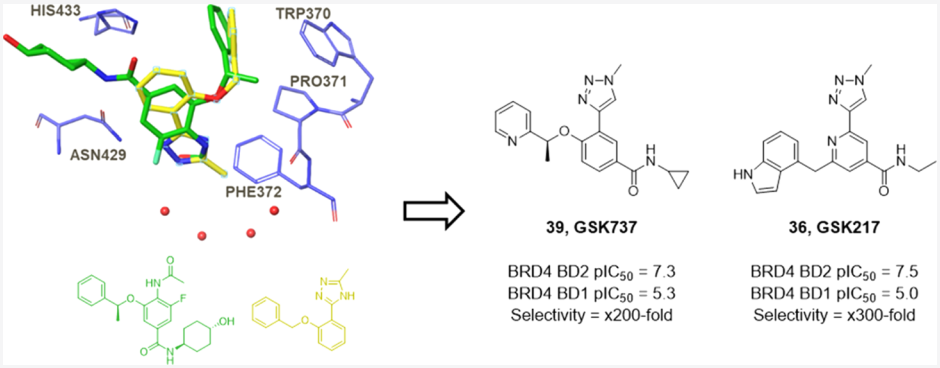

ABSTRACT: A number of reports have recently been published describing the discovery and optimization of bromo and extraterminal inhibitors which are selective for the second bromodomain (BD2); these include our own work toward GSK046 (**3**) and GSK620 (**5**). This paper describes our approach to mitigating the genotoxicity risk of GSK046 by replacement of the acetamide functionality with a heterocyclic ring. This was followed by a template-hopping and hybridization approach, guided by structure-based drug design, to incorporate learnings from other BD2-selective series, optimize the vector for the amide region, and explore the ZA cleft, leading to the identification of potent, selective, and bioavailable compounds **28** (GSK452), **39** (GSK737), and **36** (GSK217).

INTRODUCTION

The bromo and extraterminal domain (BET) family is composed of the germ cell-specific (BRDT) and ubiquitously expressed (BRD2, BRD3, and BRD4) epigenetic reader proteins. All family members contain N-terminal tandem bromodomains, a structural feature that enables the recognition and binding to acetylated lysine residues on histones and other cellular proteins that support their function as key transcriptional regulators.[1] The therapeutic potential of "pan-BET" inhibitors (binding equipotently to all eight bromodomains of the four BET proteins) has been comprehensively reported for oncology[2−11] and immunoinflammation.[12−23] The potential of this epigenetic reader target family is further bolstered by the fact that several of these inhibitors are currently being progressed in the clinic for oncology indications.[24−26] However, it is well-documented that clinical toxicities and dose-limiting findings have been associated with pan-BET inhibition;[25,27−29] hence, some efforts in this target area have focused on enabling selectivity within the BET family in attempts to tease apart efficacy and pharmacology-driven toxicity.[30−38] Additionally, recent studies have shown that the BD1 and BD2 domains have different roles in chromatin binding.[39−42] A number of publications have reported medicinal chemistry efforts toward the identification of molecules with increased selectivity within the BET family. Due to the higher homology between the four BD1 bromodomains and the four BD2 bromodomains compared

Received: December 14, 2020
Published: March 4, 2021

https://dx.doi.org/10.1021/acs.jmedchem.0c02156
J. Med. Chem. 2021, 64, 3249−3281

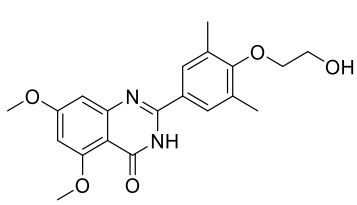

RVX-208
1
BRD4 BD1 K_d = 8.9 μM
BRD4 BD2 K_d = 0.3 μM
BRD4 BD2 selectivity (fold) = 30
(ITC)

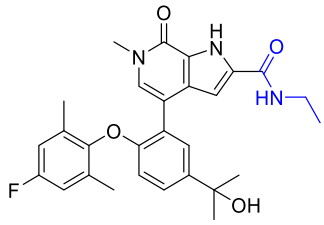

ABBV-744
2
BRD4 BD1 K_i = 520 nM
BRD4 BD2 K_i = 1.6 nM
BRD4 BD2 selectivity (fold) = 325
(ITC)

Figure 1. Structures of BD2-biased inhibitor RVX-208 and BD2-selective inhibitor ABBV-744 and their reported affinities to the BD1 and BD2 bromodomain of BRD4. Related amide substituent to those in Table 1 is shown in blue.

Table 1. Structure and Profile of 3 (GSK046), Pyridyl 4 (GSK941), and 5 (GSK620)[a]

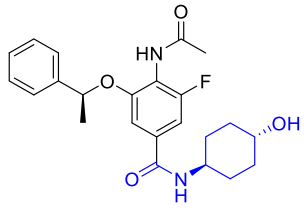

3

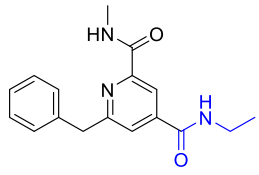

4

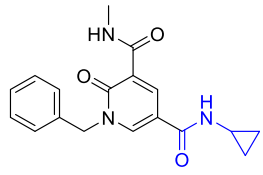

5

compound	3 (GSK046)	4 (GSK941)	5 (GSK620)
BRD4 BD1/BD2 pIC_{50} (n)	4.2 (10)/7.3 (14)	<4.3 (3)[b]/6.8 (4)	4.8 (14)/7.1 (16)
BRD4 BD2 selectivity (fold)	1000	315	200
BRD4 BD2 LE/LLE_{AT}[c]	0.33/0.38	0.42/0.37	0.41/0.51
clogP/MW	1.3/414	2.5/297	0.1/325
chromLog$D_{7.4}$/PFI	2.8/4.8	3.7/5.7	3.1/5.1
CLND[d] (μg/mL)/FaSSIF[e] (μg/mL)	91/996	≥102/310	≥154/25
$AMP_{pH=7.4}$[f] permeability (nm/s)	17	390	200

[a]Related amide substituents are shown in blue. Compounds **3** and **5** are now available from the Structural Genomic Consortium (SGC), visit: https://www.sgc-ffm.uni-frankfurt.de/. [b]Also tested 4.9 (n = 1). [c]Ligand lipophilicity index.[66] [d]CLND = chemiluminescent nitrogen detection measured at pH = 7.4. [e]FaSSIF = fasted-state simulated solubility measured at pH = 6.5. [f]AMP = artificial membrane permeability measured at pH = 7.4.

to the two bromodomains of any given BET protein, these inhibitors show some degree of selectivity either for the four BD1 or four BD2 domains. The first generation of pan-BD1,[43−48] BRD4 BD1,[49,50] and pan-BD2[51−53] inhibitors, including the clinical asset RVX-208 (**1**, Figure 1) showed limited degrees of selectivity (<100 fold) and it is only recently that molecules with a high degree of BD1[54−56] or BD2[57] selectivity have been identified, as exemplified with the highly BD2-selective inhibitor ABBV-744[58,59] (**2**, Figure 1) currently in phase I oncology trials.

We have previously reported our own effort toward the identification of drug-like BD2-selective inhibitors[60,61] and, in particular, the identification of **3**,[62] **4**,[63] and **5**[64] (GSK046, GSK941, and GSK620, respectively, Table 1). In a similar way to ABBV-744, they all contain related amide substituents (blue substructures in Figure 1 and Table 1). This functionality contributes to selectivity for the BD2 bromodomains over the BD1s by virtue of its interactions with a histidine residue in the BD2s (H433 in BRD2), which is replaced by aspartic acid in the BD1s.[58,59,62−64] Throughout this report, BRD4 potency is used as a representative of BET potency—some BRD2, 3, and T data can be found in Table 8. Inhibitor **3** showed the highest potency and selectivity for BRD4 BD2 among our inhibitors and has favorable physicochemical properties, with a chromLogD of 2.8, a property forecast index (PFI) of 4.8,[65] and reasonable solubility as measured by kinetic solubility (chemiluminescent nitrogen detection, CLND), with a value slightly below the acceptable benchmark of 100 μg/mL, but high solubility in the more relevant fasted-state simulated intestinal fluid (FaSSIF) solubility, with FaSSIF solubility above the acceptable benchmark value of 100 μg/mL. Its permeability measured by an artificial membrane permeability (AMP) was below the acceptable benchmark value of 50 nm/s, likely due to the presence of three hydrogen-bond donors. Compound **3** also contained an embedded aniline which ultimately halted its progression due to the associated genotoxic risk.

Herein, we describe our approach to mitigating this genotoxic risk through a template-hopping and hybridization approach: first, an isosteric replacement of the acetamide-acetylated lysine (AcK) mimetic of **3** with a heterocycle was sought, and second, the learnings from a second BD2-selective series were incorporated to guide the required redesign of the core.

https://dx.doi.org/10.1021/acs.jmedchem.0c02156
J. Med. Chem. 2021, 64, 3249−3281

Table 2. Comparison of Different Five-Membered Heterocycles (6−10) against Original Acetamide 11

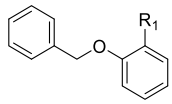

Compound	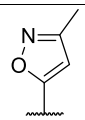 **6**	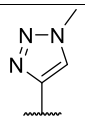 **7**	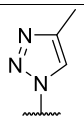 **8**	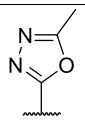 **9**	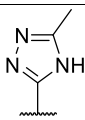 **10**	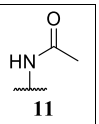 **11**
BRD4 BD2 / BD1 pIC_{50} (n)	5.4 (4) / 5.0 (2)[a]	5.4 (2) / 4.7 (2)	4.8 (5) / 4.5 (4)	4.9 (6) / <4.3 (3)[b]	5.1 (4) / <4.3 (3)[c]	4.6 (3) / <4.3 (3)
Selectivity (fold)	3	5	2	4	6	2
BD2 LE / LLE_{AT}	0.37 / 0.22	0.37 / 0.29	0.33 / 0.18	0.34 / 0.29	0.35 / 0.27	0.35 / 0.27
cLogP / $ChromLogD_{7.4}$	3.7 / 7.2	2.8 / 5.2	4.0 / 5.4	2.2 / 5.1	3.3 / 4.0	2.4 / 4.9
CLND (μg/mL)	1	87	96	≥252	≥70	≥113

[a]Also tested <4.3 (n = 1) and <4.8 (n = 1). [b]Also tested 4.4 (n = 1). [c]Also tested 5.0 (n = 1).

Table 3. Structure and Profile of Initial Leads 13 and 14

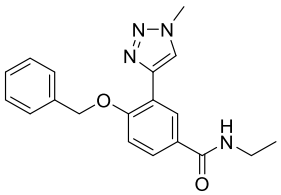

13

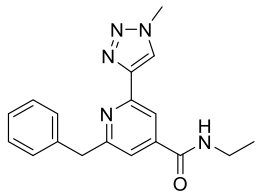

14

compound	13	14
BRD4 BD1/BD2 pIC50 (n)	4.9 (5)/6.9 (5)	4.7 (6)/7.0 (6)
selectivity (fold)	100	170
BD2 LE/LLE_{AT}	0.38/0.36	0.40/0.36
$cLogP/ChromLogD_{7.4}$	2.3/4.1	2.5/3.7
CLND (μg/mL)	46	≥157

For the latter, the starting point was pyridyl amide **4** (Table 1), whose amide AcK mimetic is reversed in direction compared to that of **3**.[63] Compound **4** was an early second-generation lead originating from the selective probes that have been previously introduced (e.g., **5**, GSK620,[64] Table 1), showing reasonable potency and selectivity for BD2 alongside acceptable physicochemical properties with a chromLogD of 3.7 and high solubility and permeability.

RESULTS AND DISCUSSION

Prior to consideration of the pyridyl core, attention was focused on a suitable heterocyclic replacement for the acetamide of **3**. Previous research on BET inhibitors has shown that a number of heterocycles can be used as suitable AcK mimetics,[67−69] not least iBET762 and (+)-JQ1.[6,70] By comparison of the published crystal structures in BRD4 BD1 of (+)-JQ1 and in BRD2 BD2 of **3** (Figure 2a), it was observed that the carbonyl oxygen of **3** and one of the triazole N atoms overlaid closely, each making similar interactions with the conserved asparagine side chain. A movement of the core was anticipated following the introduction of the heteroaryl AcK mimetics that would likely result in a need to reoptimize the core to enable more distant interactions with the bromodomain to be sustained.

A range of five-membered heterocycles (**6−10**), which contained the appropriate methyl group and ortho-heteroatom arrangement inferred from Figure 2a, were investigated and evaluated by their biochemical and physicochemical data (Table 2). All heterocycles showed an increase in BD2 potency compared with acetamide fragment **11**. The ligand efficiency of **8−10** was comparable to that of the acetamide; however, the isoxazole (**6**) and the C-linked 1,2,3-triazole (**7**) showed ligand efficiencies greater than that of the acetamide. The cyclohexanol amide of compound **3** was omitted in order to identify the best AcK mimetic before investigating substituents, so it was unsurprising that these compounds show little selectivity over BD1. The 1,2,3-triazole AcK mimetic was selected for further exploration over the isoxazole due to more favorable lipophilicity (chromLogD measurement of 5.2 compared with 7.2 for the isoxazole), which was reflected in the superior kinetic solubility shown for **7**.

A crystal structure of BRD2 BD2 bound to 1,2,4-triazole **10** was obtained and overlaid with that of **3**, as shown in Figure 2b. Despite a specific *NH* interaction with the protein, we hoped that triazole **10** was a fair representation of how the other, preferred 1,2,3-triazole **7** would bind. This structure confirmed the excellent overlay of the AcK mimetics of the two compounds with N1 of the triazole making the key hydrogen bond to N429. The core phenyl group of **10** is pushed further from the AcK binding pocket by the larger heteroaryl AcK mimetic. Despite this change, the benzyloxy group maintains a similar interaction with the WPF region of the shelf to **3**. This is an important region where positioning a lipophilic substituent close to W370 can lead to increased small molecule potency (Figure 2b).

Previous work on the series which led to compound **3** showed that incorporation of the cyclohexanol amide in the para-position led to an increase in potency and selectivity, due to a key, water-bridged hydrogen bond between the amide *NH* and N429 (BRD2 BD2 numbering).[62] This is in slight contrast with the series' which led to compounds **5** (GSK620) and **12**

https://dx.doi.org/10.1021/acs.jmedchem.0c02156
J. Med. Chem. 2021, 64, 3249−3281

Table 4. Structure and Profile of Initial Leads 13 and 14 Compared with α-Methyl Analogues 17 and 18

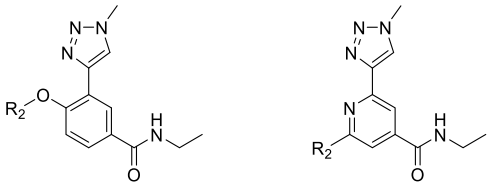

R2	Benzyloxy series, **13**, **17**			Pyridyl series, **14**, **18**		
	BRD4 BD2 pIC_{50} (n)	BRD4 BD1 pIC_{50} (n)	Selectivity (fold)	BRD4 BD2 (n)	BRD4 BD1 (n)	Selectivity (fold)
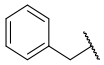 **13-14**	6.9 (5)	4.9 (5)	100	7.0 (6)	4.7 (6)	200
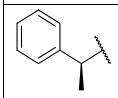 **17-18**	7.4 (5)	5.4 (5)	100	7.0 (5)[a]	4.9 (5)[a]	125

[a]Racemic material.

where the amide *NH* forms a direct hydrogen bond with N429 (Figure 2c).[63,64] From the crystal structure of **10**, it was clear that a para-amide substituent would not be able to engage N429. However, it suggested that moving the amide to the meta-position on the heterocycle-containing molecule could provide a viable vector for obtaining this interaction.

As has been mentioned previously, the 1,2,3-triazole **7** was selected for further exploration due to its favorable lipophilicity and BD2 potency (Table 2). Incorporation of a simple amide group onto fragment **7** gave ethyl amide **13** and led to a significant increase in BD2 potency and selectivity over BD1 (Table 3). This also resulted in a drop in clogP (2.8−2.3) and chromLogD (5.2−3.9) but did not lead to an increase in solubility (Table 3).

Before embarking on the optimization of this promising starting point, we decided to also evaluate the potential of utilizing the alternative core and substitution pattern of pyridyl **4** (Table 1) to maximize the opportunity to identify drug-like inhibitors bearing a heteroaryl AcK mimetic. In Figure 2c, an overlay of a representative example of this series for which we had a crystal structure, pyridyl **12**, with triazole **10** is shown. The core phenyl ring of **10** and the core pyridine ring of **12** overlay approximately. This suggested that it could be possible to replace the core of **10** with those of **12** and retain the favorable interactions made by its substituents. Hence, the pyridyl series and 1,2,3-triazole template were "hybridized" to give **14** (Table 3).

Compound **14** showed comparable potency and selectivity with **13** but had increased ligand efficiency, although ligand efficiencies were high for both compounds. The two compounds had similar lipophilicity, although **14** had higher solubility.

The binding mode of the two templates once functionalized with an amide is shown in Figure 3, using phenyl derivative **15** and pyridyl **16** for which we managed to obtain crystal structures in BRD2 BD2. If these two compounds have specific WPF shelf and amide substituents, their binding modes are representative of those of these two series of inhibitors. A good overlay is achieved in the AcK mimetic-core region, and a very similar access to the amide vector region is seen for both templates. However, the access to the WPF shelf is dissimilar, with the aromatic rings sitting in different orientations that do not overlay. Both aromatic rings form aromatic interactions with W370 and H433; in the case of the benzyloxy series analogue **15**, both of these interactions are edge-to-face, while pyridyl series analogue **16** shows an edge-to-face interaction with H433 but an offset stacking interaction with W370. This can be explained by the differences in the vectors of the linkers between the cores and WPF shelf groups, which cause the rings to sit in different orientations. Therefore, we thought that this may lead to differences in structure−activity relationship (SAR) between the two series in the WPF shelf region. These differences are exemplified below.

In the original pyridyl and acetamide series (**4** and **3** as representative examples, Figure 1), adding an α-methyl to the benzylic position gave an increase in potency, often around threefold, due to the methyl group making an extra lipophilic interaction in the ZA channel region, as exemplified by **3**.[62,63] This vacant region is also shown in Figure 3a and it seemed reasonable to investigate if productive interactions could be made with these heteroaryl series.

Incorporation of the methyl group gave contrasting results (Table 4). For the benzyloxy derivatives, we saw the expected boost in potency with **17** being ∼threefold more potent than **13**. However, for the pyridyl series, no increase in potency was observed. The protein crystallography offers a possible rationale for these findings, in that the benzylic vector in the unsubstituted pyridyl template is not directed toward the ZA channel (Figure 3a). As a result, the inhibitor is shown to subtly change conformation with the addition of a methyl group (**18**, Figure 4), which causes the amide vector to adopt a less-preferred conformation. This is not the case for benzyloxy

https://dx.doi.org/10.1021/acs.jmedchem.0c02156
J. Med. Chem. 2021, 64, 3249−3281

Table 5. WPF Shelf SAR Exploration for Benzyloxy Series

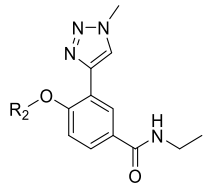

Entry	R_2	BRD4 BD2 pIC_{50} (n)	BRD4 BD1 pIC_{50} (n)	Selectivity (fold)	LE / LLE_{AT}	cLogP / Chrom $LogD_{7.4}$	CLND (μg/mL) / $AMP_{pH=7.4}$ (nm/s)
13		6.9 (5)	4.9 (5)	100	0.38 / 0.36	2.3 / 4.1	46 / 430
19	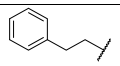	5.6 (5)	<4.3 (3)[a]	20	0.29 / 0.26	2.6 / 4.3	95 / 490
20		5.0 (4)	4.5 (2)[b]	30	0.27 / 0.34	0.8 / 2.5	≥208 / 110
17	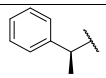	7.4 (5)	5.4 (5)	100	0.39 / 0.36	2.6 / 4.4	105 / 420
21	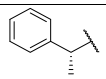	5.8 (6)	4.4 (1)	25	0.31 / 0.28	2.6 / 4.5	119 / 420
15		6.5 (4)	4.4 (3)[c]	125	0.36 / 0.42	0.8 / 2.6	114 / 140
22	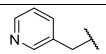	6.0 (5)	<4.3 (5)	50	0.33 / 0.40	0.8 / 1.9	103 / 180
23	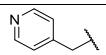	6.0 (4)	4.9 (3)	15	0.33 / 0.40	0.8 / 1.8	≥115 / 300
24		5.8 (5)	<4.3 (3)[d]	30	0.32 / 0.44	-0.2 / 2.0	≥103 / 37
25		6.9 (4)	4.7 (3)	160	0.35 / 0.35	2.2 / 4.4	≥162 / 480
26	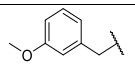	6.6 (3)	4.7 (3)	80	0.34 / 0.33	2.2 / 3.9	≥139 / 420
27	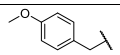	6.5 (3)	4.7 (3)	65	0.33 / 0.33	2.2 / 3.9	≥142 / 390
28	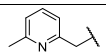	6.6 (5)	4.3 (3)	200	0.35 / 0.39	1.3 / 2.7	≥137 / 470
29		7.1 (5)	5.1 (5)	100	0.37 / 0.42	1.1 / 3.0	≥127 / 150

[a]Also tested 4.3 (n = 1) and 4.8 (n = 1). [b]Also tested <4.3 (n = 2). [c]Also tested <4.3 (n = 1). [d]Also tested 4.4 (n = 1) and 5.3 (n = 1).

17 (Figure 4) and hence the increase in potency is only observed for this template.

Following this initial work, further investigation was carried out into the WPF shelf SAR on the two templates. These data were divergent given the different trajectories, the templates accessed the WPF shelf and the data will be discussed independently.

For the benzyloxy series, incorporation of heteroatoms into the phenyl ring, as well as small additional substituents, was evaluated (Table 5). Compound **19** was synthesized to investigate the optimal linker length between the WPF shelf group and the phenyl core. The biochemical data showed that while this extended linker was tolerated, it led to a >10-fold drop in potency; hence, all other analogues were made with the identical length of **13**.

The opposite enantiomer of the original α-Me benzyl analogue **17** was synthesized to give **21**. Protein crystallography of **17** suggested that the (*S*)-enantiomer would be preferred over the (*R*)-enantiomer because it projected toward the ZA channel (Figure 4). This was reflected in the BRD4 data where (*S*)-compound **17** showed significantly higher potency and selectivity for BD2 than the (*R*)-analogue **21**. In

https://dx.doi.org/10.1021/acs.jmedchem.0c02156
J. Med. Chem. 2021, 64, 3249−3281

Table 6. WPF Shelf SAR Exploration for Pyridyl Series

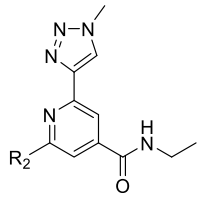

Entry	R_2	BRD4 BD2 pIC_{50} (n)	BRD4 BD1 pIC_{50} (n)	Selectivity (fold)	LE / LLE_{AT}	cLogP / Chrom $LogD_{7.4}$	CLND (μg/mL) / $AMP_{pH=7.4}$ (nm/s)
14		7.0 (6)	4.7 (6)	200	0.40 / 0.36	2.5 / 3.7	≥157 / 325
30		6.7 (4)	4.4 (4)	200	0.36 / 0.33	2.4 / 3.8	62 / 370
31	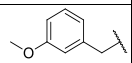	6.2 (4)	<4.3 (4)	80	0.33 / 0.30	2.4 / 3.8	≥45 / 470
32	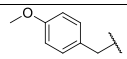	6.1 (5)	<4.3 (5)	65	0.32 / 0.30	2.4 / 3.6	53 / 320
33		6.7 (4)	4.7 (4)	100	0.37 / 0.33	2.7 / 3.8	66 / 300
34	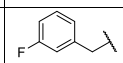	6.6 (4)	4.8 (4)	65	0.36 / 0.32	2.7 / 3.9	73 / 410
35	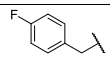	6.6 (4)	4.7 (4)	80	0.36 / 0.33	2.7 / 3.8	75 / 330
36	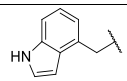	7.5 (4)	5.0 (4)	315	0.38 / 0.36	2.5 / 3.1	≥148 / 300

addition, the incorporation of the α-Me group in **17** led to an increase in kinetic solubility in comparison with the parent analogue **13**.

Next, saturation of the ring was investigated using a THP group (**20**), which led to an almost 100-fold drop in potency in comparison with the parent phenyl (**13**). Therefore, efforts were focused on investigating SAR through other aromatic ring replacements.

Nitrogen-containing heterocycle-based analogues were synthesized, and all pyridine isomers (**15**, **22**−**23**) and a pyrimidine (**24**) showed measurable potencies, with the 2-pyridine **15** offering the best potency and selectivity. This was contrary to other BD2-selective series where a pyridine on the WPF shelf led to a significant loss of potency;[63,64] however, it was clear from protein crystallography that this template occupied the WPF shelf differently to other series. The 2-pyridine **15** also had comparable ligand efficiency with parent **13** and showed an increase in LLE_{AT} by comparison. As expected, these compounds were less lipophilic than the parent phenyl and also had higher solubility. The drop in lipophilicity may also explain the decreases observed in membrane permeability, although the pyrimidine had much lower AMP than the pyridines despite having a similar $chromLogD_{7.4}$.

Based on previous SAR on the acetamide template, electron-donating methoxy-substituted phenyls **25**−**27** were also tested: the *ortho*-methoxy analogue **25** showed the highest potency and selectivity of the three analogues, although it showed no advantage over the parent phenyl **13**. All three methoxy-substituted compounds showed comparable permeabilities with **13** but large increases in solubility despite comparable chromLogD values. Finally, the 2-pyridine and α-Me were combined to give **29** which gave a good balance of key properties: high potency, selectivity, and ligand efficiencies with a reasonable chromLogD, solubility, and permeability. This group was therefore selected to explore the SAR for the amide vector (*vide infra*).

A similar approach to SAR exploration of the WPF shelf was taken with the pyridyl template (Table 6). Unlike the benzyloxy analogues, pyridine isomers were not synthesized in this template due to previous data from the parent series showing that they were not tolerated.[63] Since the WPF shelf groups of this template, such as **4** as a representative example, and compounds such as **16** overlaid well, this was considered a reasonable approach.

On this template, electron-rich and electron-poor aromatic rings were investigated using methoxy- and fluoro-substituted phenyls (**30**−**35**, Table 6). Similar to the benzyloxy series, the *ortho*-methoxy **30** gave the best potency and selectivity relative to the meta- and para-substituted analogues **31** and **32**, while the three fluoro-substituted rings (**33**−**35**) were equipotent and selective; however, none of these six compounds offered a potency or selectivity advantage over the parent phenyl **14**. With the exception of the *meta*-methoxy analogue **31**, both of these strategies led to compounds with decreased solubility in

https://dx.doi.org/10.1021/acs.jmedchem.0c02156
J. Med. Chem. 2021, 64, 3249−3281

Table 7. Amide SAR Exploration for Benzyloxy and Pyridyl Series

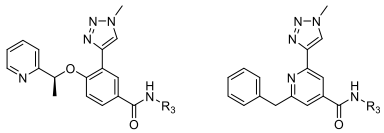

Entry	R_3	Series	BRD4 BD2 pIC50 (n)	BRD4 BD1 pIC50 (n)	Selectivity (fold)	LE / LLE_{AT}	cLogP / Chrom $LogD_{7.4}$	CLND (μg/mL) / $AMP_{pH\ 7.4}$ (nm/s)
37	H	Benzyloxy	6.6 (4)	5.2 (4)	25	0.38 / 0.47	0.3 / 1.8	131 / 47
38	Me	Benzyloxy	6.9 (3)	5.0 (3)	80	0.38 / 0.45	0.6 / 2.2	≥138 / 70
29	Et	Benzyloxy	7.1 (3)	5.1 (3)	100	0.37 / 0.42	1.1 / 3.0	≥127 / 150
39	cPr	Benzyloxy	7.3 (3)	5.3 (3)	100	0.37 / 0.42	1.1 / 3.1	145 / 150
40		Benzyloxy	7.6 (5)	5.8 (5)	65	0.35 / 0.43	1.0 / 2.5	≥169 / 42
41		Benzyloxy	6.9 (3)	4.8 (3)	100	0.31 / 0.41	0.2 / 2.9	≥194 / 59
42		Benzyloxy	6.3 (3)	4.5 (3)	65	0.28 / 0.35	0.8 / 3.1	≥192 / 55
43		Benzyloxy	6.4 (4)[a]	5.1 (4)[a]	20	0.29 / 0.37	0.5 / 2.5	≥188 / 13
44		Benzyloxy	7.6 (3)	5.2 (3)	250	0.32 / 0.41	0.5 / 1.7	≥177 / <3
45		Benzyloxy	7.2 (4)	5.1 (4)	125	0.31 / 0.40	0.5 / 1.5	≥182 / <3
46		Benzyloxy	8.0 (3)	5.4 (3)	400	0.32 / 0.36	1.7 / 1.8	≥193 / 5.3
47	H	Pyridyl	6.6 (4)	4.9 (4)	50	0.41 / 0.41	1.7 / 2.6	40 / 140
14	Et	Pyridyl	7.0 (6)	4.7 (6)	200	0.40 / 0.36	2.5 / 3.7	≥157 / 325
16	cPr	Pyridyl	6.9 (4)	4.8 (4)	125	0.38 / 0.35	2.6 / 4.0	≥76 / 360
48		Pyridyl	7.3 (3)	5.3 (3)	100	0.36 / 0.37	1.9 / 3.5	≥145 / 240
49		Pyridyl	6.9 (4)	4.7 (4)	160	0.34 / 0.37	1.6 / 3.5	≥141 / 270
50		Pyridyl	6.5 (4)	<4.3 (3)[b]	160	0.31 / 0.31	2.2 / 3.7	≥142 / 220
51		Pyridyl	7.5 (2)	4.9 (2)	400	0.34 / 0.36	1.9 / 2.2	≥138 / 18
52		Pyridyl	7.2 (3)	4.8 (3)	250	0.33 / 0.35	1.9 / 2.1	≥189 / 48
53		Pyridyl	7.6 (5)	5.2 (5)	250	0.34 / 0.32	2.7 / 2.1	≥181 / 19
54		Pyridyl	7.6 (5)	5.0 (5)	400	0.34 / 0.30	3.3 / 2.2	≥134 / <3
55		Pyridyl	8.0 (5)	5.3 (5)	500	0.34 / 0.32	3.1 / 2.3	≥172 / 23

[a]Trans diastereomer. [b]Also tested 4.4 (n = 1).

comparison with the parent phenyl analogue, with little change to the lipophilicity. Additionally, this strategy offered no advantage for potency and selectivity in comparison with parent compound **14**, and the six compounds (**30**−**35**) were disadvantageous for ligand efficiency so were not investigated further.

Finally, a bicyclic ring was investigated in the form of indole **36**. This group had led to significant increases in potency and selectivity in the original pyridone series.[64] Here, a ∼threefold increase in potency was observed (comparing **36** with **14**). Indole **36** also helped to lower the chromLogD in comparison with the parent phenyl **14**, while maintaining the high permeability and solubility. This indole compound was also the most selective and potent compound across the two templates, up to this point.

The SAR for the amide vector of the two templates was explored side-by-side due to the similar overlay in the crystallography of this portion of the molecules. For the benzyloxy series, the optimum α-Me 2-pyridyl group was used, while in the pyridyl template, the phenyl was selected over the indole due to synthetic challenges at the time.

In general, the amide SAR between the two templates was comparable and tracked with that of the previous series.[62−64] The primary amides (**37** and **47**) caused a drop in potency and selectivity in comparison with the ethyl amides. While the methyl amide was not made in the pyridyl template, incorporation of this group into the benzyloxy series to afford **38** led to comparable potency and selectivity with the ethyl amide but decreased lipophilicity which in turn reduced permeability. The cyclopropyl amides **39** and **16** offered no advantage over the ethyl amides in terms of potency or physicochemical properties, which is counter to the previous pyridyl and pyridone templates in which incorporation of this group led to a boost in potency and selectivity.[63,64]

A selection of substituents in this area was made based on SAR from historical templates. Hence, the oxygen-containing bicycle (**40** and **48**) was investigated, giving an increase in potency, particularly for the benzyloxy series, but this came without an increase in selectivity. Other saturated heterocycles were also synthesized: the directly linked THPs **41** and **49** appeared to be comparable to the ethyl amide with very similar biochemical and physicochemical data, while the homologated THPs **42** and **50** were not as well-tolerated. The cyclohexanol amide that was used in the acetamide lead compound **3** (Table 1—GSK046) was synthesized in the benzyloxy series (**43**) and showed reasonable potency but low selectivity for BRD4 BD2, thus highlighting the differences between the two series.

Finally, a range of extended six-membered ring amines were installed to provide further highly soluble compounds and possibly crystalline derivatives, either as the piperidine **54** or as morpholines **44**−**45** and **51**−**52**, and fluoro-piperidines **46**, **53**, and **55** to modulate the pK_a of the basic center. This strategy not only produced compounds with very high potencies and selectivities and lower lipophilicities but also led to appreciable drops in permeability in comparison with the ethyl amide. In both templates, high kinetic solubility was maintained with the incorporation of these amides as the measured values were at the upper limit of the assay for the benzyloxy analogues **44**−**46** and for the pyridyl analogues **51**−**55**. Nevertheless, fluoropiperidine amides **46** and **55** had the highest potencies and selectivities observed in these two templates, and given that the upper limit of the BRD4 assay was pIC_{50} ∼8, it is possible that these compounds were more potent, and therefore selective, than quoted here.

Chemistry. The SAR for the benzyloxy template was investigated *via* synthesis of intermediate **57** (MOM protected ester), which was prepared from the commercially available

https://dx.doi.org/10.1021/acs.jmedchem.0c02156
J. Med. Chem. 2021, 64, 3249−3281

Table 8. Profile of Lead Compounds 28 (GSK452), 39 (GSK737), and 36 (GSK217)

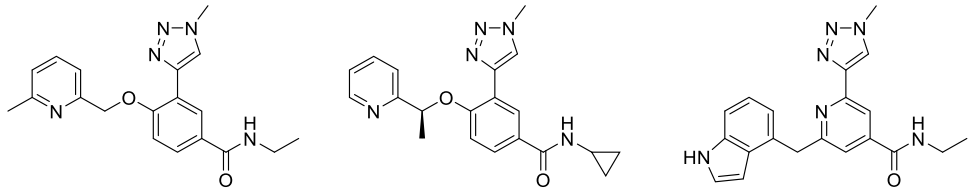

28 39 36

compound	GSK452, **28**	GSK737, **39**	GSK217, **36**
BRD4 BD2/BD1 pIC_{50} (n)	6.6 (5)/4.3 (3)[a]	7.3 (3)/5.3 (3)	7.5 (4)/5.0 (4)
BRD2 BD2/BD1 pIC_{50} (n)	5.8 (3)/<4.3 (4)	6.6 (2)/4.4 (2)	7.3 (2)/4.6 (2)
BRD3 BD2/BD1 pIC_{50} (n)	6.5 (4)/<4.3 (4)	7.1 (2)/4.9 (2)	7.5 (2)/4.5 (2)
BRDT BD2/BD1 pIC_{50} (n)	6.4 (4)/<4.3 (4)	ND	7.3 (2)/4.6 (2)
BRD4 BD2 selectivity (fold)	200	100	300
BRD4 BD2 LE/LLE_{AT}	0.35/0.39	0.37/0.42	0.38/0.36
PBMC/hWB pIC_{50} (n) (MCP-1)	6.6 (2)/5.6 (2)	7.8 (2)/6.7 (2)	7.6 (2)/6.4 (2)
cLogP/$ChromLogD_{7.4}$	1.3/2.7	1.1/3.1	2.5/3.1
$AMP_{pH=7.4}$ (nm/s)	470	150	300
CLND (μg/mL)/FaSSIF (μg/mL)	137/702	145/603	148/297
hERG pIC_{50} (n)/has	<4.3 (3)/84%	4.4 (1)[b]/84%	4.5 (1)[b]/90%
hepatocyte cli (rat/hu) (mL/min/g tissue)	1.09/1.18	<0.80/<0.45	1.98/<0.45
rat ivPK (1 mg/kg): CL_b ($CL_{b,ub}$) (mL/min/kg), $t_{1/2}$ (h); AUC (ng h/mL), V_{ss} (L/kg), f_{ub}	19 (102), 0.45; 873, 0.7, 0.19	14 (19), 1.65; 1175, 1.8, 0.76	21 (205[c]), 0.87, 778; 1.1, nd
rat poPK[d] (3 mg/kg): C_{max}, t_{max}; AUC/D (min kg/L), F (%)	634, 0.28; 30, 59	281, 0.25; 23, 32	366, 0.25; 15, 31

[a]Also tested <4.3 (n = 2). [b]Also tested <4.3 (n = 2). [c]Calculated using HSA. [d]Values are based on n = 3 mean apart from t_{max} which is n = 3 median.

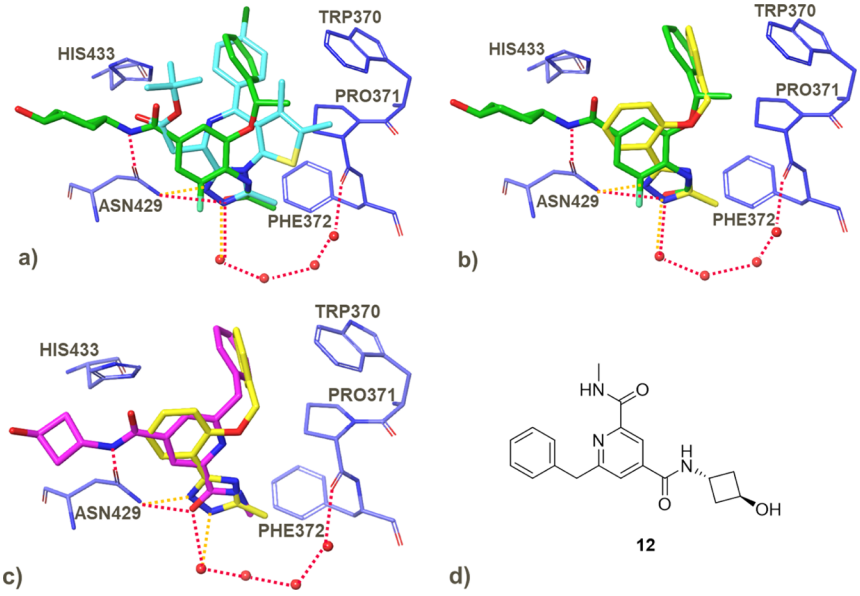

Figure 2. X-ray crystal structures (a) (+)-[JQ1] (cyan, PDB: 3MXF[6]) in BRD4 BD1 overlaid with **3** (GSK046, green, PDB: 6SWP[62]) in BRD2 BD2; (b) **3** (GSK046, green) and **10** (yellow, PDB: 7NQ5) in BRD2 BD2; (c) **10** (yellow) overlaid with **12** (magenta, PDB: 7NQ9); and (d) structure of **12**.

bromo methylester phenol **56** (Scheme 1). The phenol was first protected with an MOM group to give intermediate **63**. This underwent Sonogashira cross-coupling with trimethylsilane (TMS)-protected acetylene, giving alkyne **64**, and subsequent 1,3-dipolar cycloaddition with sodium azide and *in situ* methylation with methyl iodide gave 1,2,3-triazole **57**.[71] Route flexibility here allowed either amide or WPF shelf SAR investigation. For amide SAR evaluation, triazole **57** was first subjected to acidic conditions to remove the MOM-protecting group to afford **65**. The phenol could then undergo a Mitsunobu coupling to install the WPF shelf group **59**, giving inversion of stereochemistry as expected. From here, the intermediate was hydrolyzed to give acid **66**. Finally, HATU-mediated amide coupling gave the fully elaborated final compounds **13** and **37**−**43**. Where applicable, a Boc deprotection was then carried out using trifluoroacetic acid (TFA) to give the free amine final compounds **44**−**46**. Similarly, for WPF shelf SAR exploration, 1,2,3-triazole

https://dx.doi.org/10.1021/acs.jmedchem.0c02156
J. Med. Chem. 2021, 64, 3249−3281

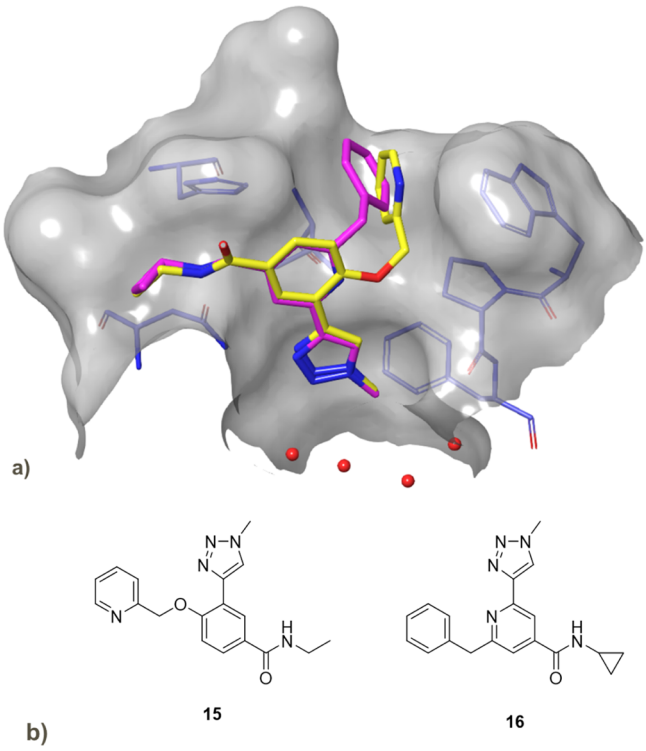

Figure 3. (a) X-ray crystal structure of **15** (yellow, PDB: 7NQ8) and **16** (magenta, PDB: 7NQI) in the BRD2 BD2 protein and the shape complementarity in the binding site; (b) structures of **15** and **16**.

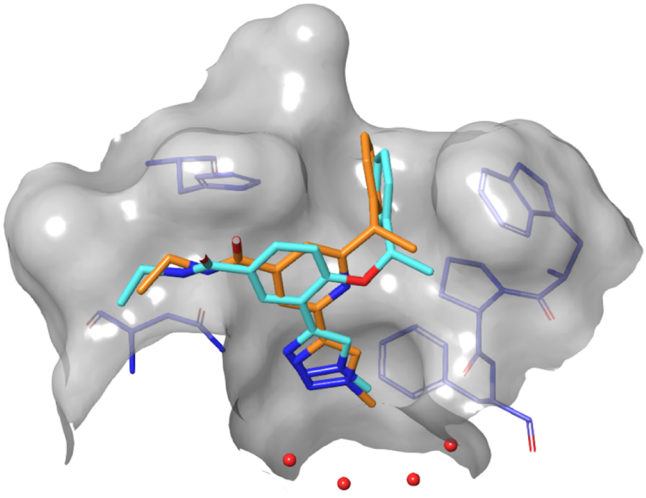

Figure 4. X-ray crystal structure of **17** (cyan, PDB: 7NQ7) and **18** (orange, PDB: 7NQJ) in the BRD2 BD2 protein, showing the shape complementarity to their binding site.

intermediate **57** underwent ester hydrolysis and subsequent HATU-mediated amide coupling to give **58**. Following MOM deprotection, this was then subjected to either Mitsunobu coupling with the relevant alcohol or nucleophilic substitution with the relevant bromide to give the final compounds **13**, **15**, **17**, and **19**−**29**.

For the pyridyl series, SAR investigation was enabled using similar chemistry to the benzyloxy derivatives *via* key intermediate **67** or **68**. First, the 1,2,3-triazole was installed from the commercially available dichloro *tert*-butyl ester pyridine or dibromo methyl ester pyridine which was subjected to Sonogashira cross-coupling conditions using $Pd(PPh_3)_4$ to afford **80** or **81**. This reaction was not high-yielding due to the formation of a byproduct *via* bis-substitution of the acetylene unit in a 1:1 ratio with **80**−**81**. Following this, alkyne **80** or **81** was subjected to a 1,3-dipolar cycloaddition using the same conditions, as in Scheme 1, to give 1,2,3-triazole **69** or **70**.[71] As with the previous template, the order of steps could be switched at this point to allow for SAR investigation of the two vectors, amide and WPF shelf. For investigation of amide SAR, the WPF shelf group was installed *via* a Negishi cross-coupling to afford **73** or **74**. The compound was then hydrolyzed with TFA or LiOH to give acid **82**, which could then undergo HATU-mediated amide coupling to give the desired final compounds **14**, **16**, and **48**−**50**. Where a Boc-protected amine had been installed into the molecule, this was then removed using TFA to give final compounds **51**−**55**. Carrying out the ester hydrolysis and subsequent amide coupling first on intermediate **69** or **70** allowed for efficient exploration of WPF shelf SAR from the late-stage intermediate **71** or **72**. This intermediate then underwent Negishi cross-coupling using either $Pd(PPh_3)_4$ or $(PPh_3)_2PdCl_2$, depending on the pyridyl halide being used, to give final compounds **14** and **30**−**35**.

For the preparation of indole **36**, a different synthetic route was employed (Scheme 3). Starting with bromomethyl methyl ester pyridine **83**, the Sonogashira cross-coupling and 1,3-dipolar cycloaddition reactions were carried out using the same conditions outlined in Scheme 2 to give intermediate **84**.[71] This was then subjected to oxidation conditions using mCPBA to give *N*-oxide species **85**, which was converted to an alcohol *via* Boekelheide rearrangement with TFAA. A chlorination with thionyl chloride then gave chloro intermediate **86**, which was used as a handle for an sp^2-sp^3 Suzuki cross-coupling with an indole boronic acid using XPhos Pd G1 to give **87**.[72] This reaction was low-yielding at 10%; however, optimization was not carried out as this was considered good enough to provide the small amount of compound required. Following this, the methyl ester was hydrolyzed with LiOH to give an acid that then underwent HATU-mediated amide coupling to give the fully elaborated compound **36**.

As one of the most selective and drug-like compounds made in the first iteration, **28** (GSK452, Table 5) was progressed into rat PK studies to provide a benchmark (Table 8). Following this, the two compounds with the best balance of potency, selectivity, lipophilicity, and solubility were identified and further profiled: **36** (GSK217, Table 6) and **39** (GSK737, Table 7). The three compounds showed the expected pan-BET BD2 selectivity, with largely equivalent potencies and selectivities for the BRD2, BRD3, and BRDT BD2 domains over the BD1 domains as was seen in the BRD4 assay. Here, analogue **36** (GSK217) particularly maintained high potency and high selectivity across the four BET bromodomains. The selectivity profile of this molecule was followed up in the DiscoverX BromoScan platform of the wider bromodomain family, and selectivity for the BET BD2 domains was confirmed (Figure 5).

The three compounds were also evaluated in cellular assays: an LPS-stimulated human whole blood (hWB) assay and an LPS-stimulated peripheral blood mononuclear cell (PBMC) assay.[62−64] These assays measure monocyte chemoattractant protein 1 (MCP-1/CCL2) levels, which is a chemokine that recruits monocytes, memory T-cells, and dendritic cells to sites of inflammation. In the PBMC assay, retention of potency from the biochemical BRD4 BD2 data was observed. In the hWB assay, we observed a drop-off versus biochemical potency

https://dx.doi.org/10.1021/acs.jmedchem.0c02156
J. Med. Chem. 2021, 64, 3249−3281

Scheme 1. Alternative Routes for the Preparation of Benzyloxy Analogues[a]

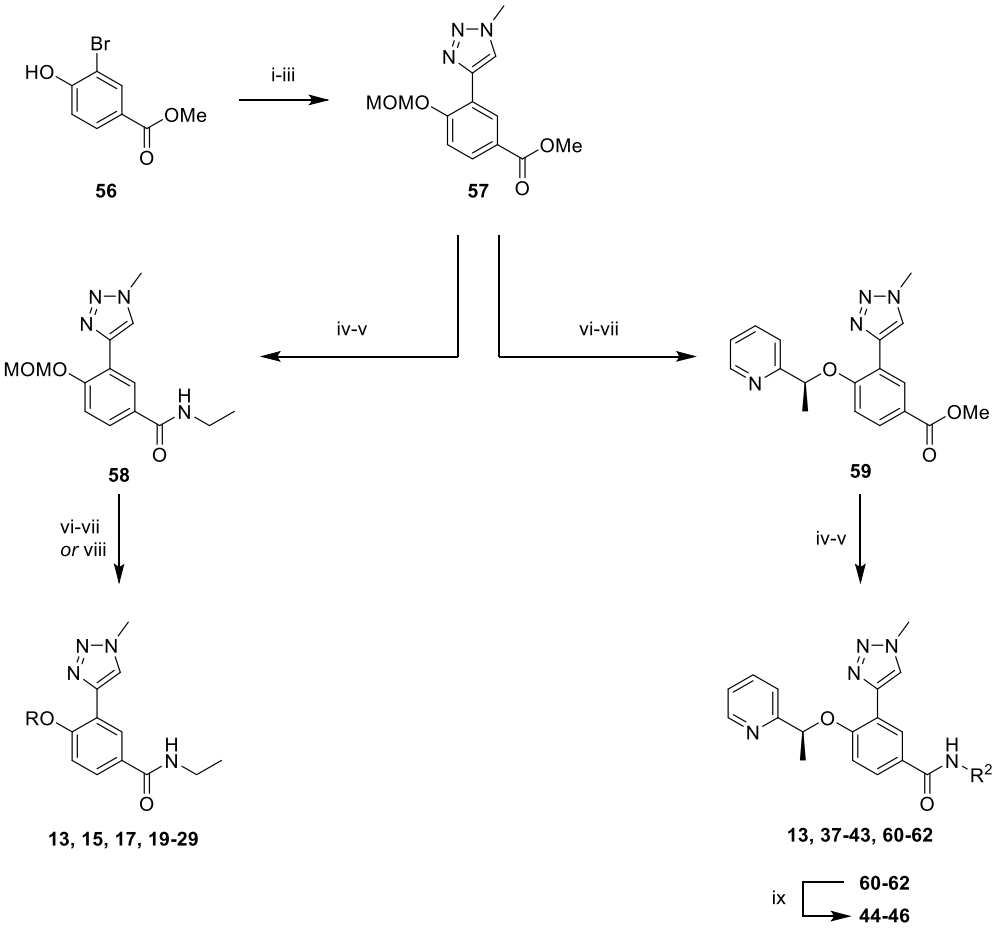

[a]Reagents and conditions: (i) MOMCl, Cs_2CO_3, DMF, 0 °C—rt, 16 h (quant.); (ii) TMS acetylene, Et_3N, Cu(I)I (10 mol %), $(PPh_3)_2Pd(II)Cl_2$ (1 mol %), 50 °C, 6 h (76%); (iii) NaN_3, MeI, pyridine, K_2CO_3, vitamin C (40 mol %), $Cu(II)SO_4$ (20 mol %), H_2O/MeOH (1:1), rt, 48 h (79%); (iv) NaOH or LiOH, THF/H_2O (1:1), rt—50 °C, 3–4 h (60–79%); (v) R^2NH_2, HATU, DIPEA, DMF, rt, 3–16 h; (vi) HCl, MeOH, rt—50 °C, 3–35 h (80–98%); (vii) ROH, CMBP, DMF, 170 °C, 2–3 h; (viii) RBr, K_2CO_3, acetone or DMF, rt—50 °C, 25–67 h; (ix) TFA, $CHCl_3$, rt, 1–3 h (14–75%).

for the three compounds, most likely due to protein binding and the need to permeate into the cell; however, the ranking of activities between compounds remained the same in both assays.

All three compounds were in a reasonable lipophilicity space, and **28** had a slightly lower chromLogD than **39** and **36**. Despite this, **28** had the highest permeability in the AMP assay, perhaps owing to the fact that the *NH* of the indole in **36** may hinder permeation through the lipophilic membrane. Additionally, the more-relevant FaSSIF solubility was determined, showing that all three compounds had high FaSSIF solubility >100 μg/mL. **28**, **36**, and **39** were tested for off-target toxicity in the hERG assay, and all three compounds showed no measurable activity.

To understand the pharmacokinetic properties of these compounds, they were first evaluated in an *in vitro* clearance assay, using rat and human hepatocytes. All three compounds showed moderate-to-high *in vitro* stability, with **39** having clearance below the lower limit of quantification (LLQ) in both rat and human hepatocyte assays. **36** showed high *in vitro* stability in human hepatocytes but higher clearance in rats, while **28** showed moderate rat stability. As these values offered the possibility of promising in vivo pharmacokinetics, all three compounds were profiled further *in vivo* in rats.

As predicted from *in vitro* measurements, the three compounds all had low measured Cl_b values. Although the values are similar, the rank order follows the same pattern as the *in vitro* clearance in that **39** had the lowest measured clearance, followed by **28** with **36** having the highest recorded value of the three compounds. A more appropriate comparison of unbound clearance reflects the in vitro data more starkly as **39** has a much higher fraction unbound than the other two compounds and therefore a significantly lower unbound clearance.

All three compounds show moderate oral bioavailability in the rat: **28** has the highest value of the three at 59%. The reason for the reduced oral bioavailability of **39** and **36** is unclear, given they have low clearance and good solubility and permeability but was not investigated further given that these pharmacokinetic data were sufficient to recommend these tools for *in vivo* use.

CONCLUSIONS

In conclusion, we were able to replace the embedded aniline AcK mimetic of **3** (GSK046) with a 1,2,3-triazole motif by altering the attachment point of the key amide substituent from the para- to meta-position. This motif was incorporated

https://dx.doi.org/10.1021/acs.jmedchem.0c02156
J. Med. Chem. 2021, 64, 3249–3281

Scheme 2. Alternative Routes for the Preparation of Pyridyl Analogues[a]

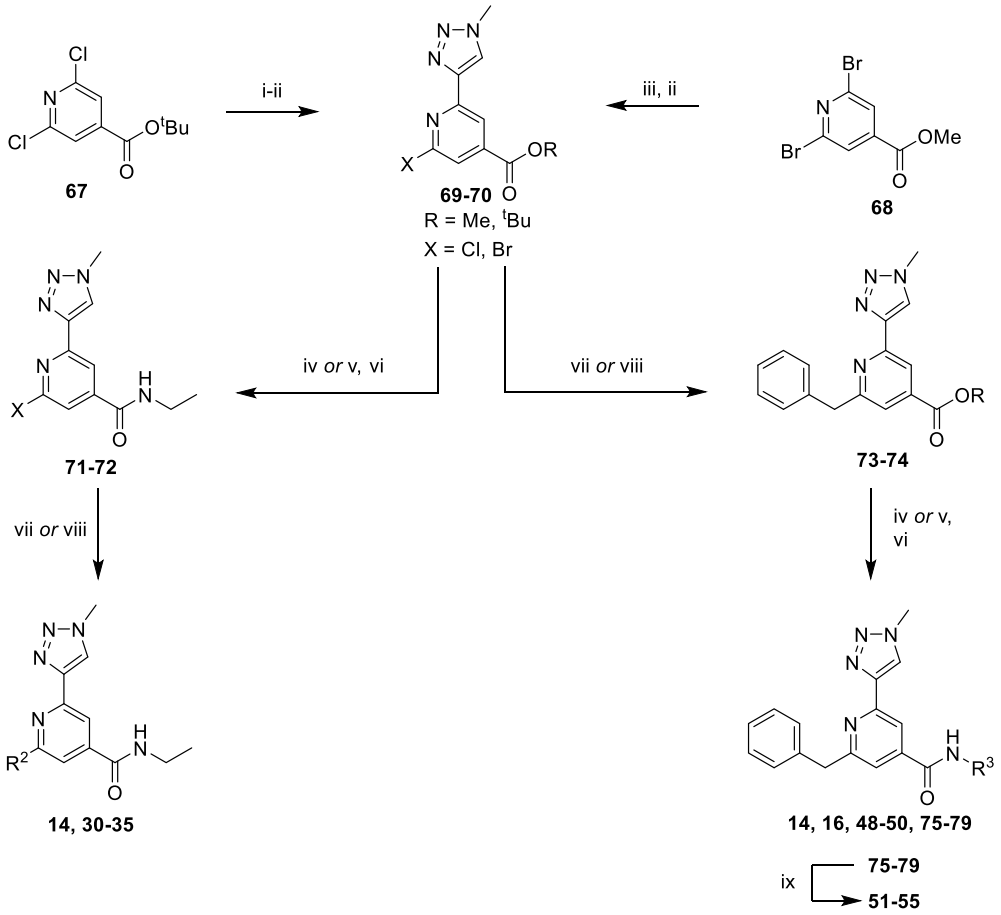

[a]Reagents and conditions: (i) TMS acetylene, Et_3N, Cu(I)I (4 mol %), $Pd(PPh_3)_4$ (4 mol %), PPh_3 (15 mol %), toluene, 80 °C, 3 h (37%); (ii) NaN_3, MeI, pyridine, K_2CO_3, vitamin C (40 mol %), $Cu(II)SO_4{\cdot}5H_2O$ (20 mol %), H_2O/MeOH/THF (1:1:1), rt, 18−48 h (19−89%); (iii) TMS acetylene, $^iPr_2NH$, Cu(I)I (4 mol %), $Pd(PPh_3)_4$ (2 mol %), THF, rt, 90 min (32%); (iv) (R = Me) LiOH, H_2O/THF (1:1), 50 °C, 1 h (98%); (v) (R = ^{t}Bu) TFA, $CHCl_3$, rt, 6−22 h (42−95%); (vi) R^3NH_2, HATU or EDC, DIPEA, DMF, rt, 1−16 h; (vii) (X = Br) R^2ZnBr or R^2ZnCl, $Pd(PPh_3)_4$ (5 mol %), THF, rt, 6.5 h; (viii) (X = Cl) R^2ZnBr or R^2ZnCl, $(PPh_3)_2Pd(II)Cl_2$ (10 mol %), THF, 100−110 °C, 30 min to 2 h; (ix) TFA, $CHCl_3$, rt, 5−21 h (34−66%).

with both an *ortho*-benzyloxy and *meta*-benzyl WPF shelf group. SAR exploration in the two templates delivered key analogues with comparable potencies and selectivities to previously reported series and provided an insight into the ability to gain further potency (or not) from the ZA channel using a methyl group. This work culminated with the identification of three compounds **28** (GSK452), **39** (GSK737), and **36** (GSK217), which had desirable cell potencies, solubilities, and rat pharmacokinetics. Overall, this work highlights selective pan-BD2 inhibitors that are structurally differentiated from the other literature tool molecules. These inhibitors also provide further structural insights into strategies to obtain second bromodomain selectivity.

EXPERIMENTAL SECTION

General Experiment. Unless otherwise stated, all reactions were carried out under an atmosphere of nitrogen in heat- or oven-dried glassware and anhydrous solvent. Solvents and reagents were purchased from commercial suppliers and used as received. Reactions were monitored by thin layer chromatography (TLC) or liquid chromatography−mass spectrometry (LC−MS). TLC was carried out on glass or aluminum-backed 60 silica plates coated with a UV_{254} fluorescent indicator. Spots were visualized using UV light (254 or 365 nm) or alkaline $KMnO_4$ solution, followed by gentle heating. LC−MS analysis was carried out on a Waters Acquity UPLC instrument equipped with a CSH C18 column (50 mm × 2.1 mm, 1.7 μm packing diameter) and Waters micromass ZQ MS using alternate-scan positive and negative electrospray. Analytes were detected as a summed UV wavelength of 210−350 nm. Three liquid-phase methods were used: formic—40 °C, 1 mL/min flow rate. Gradient elution with the mobile phases as (A) H_2O containing 0.1% volume/volume (v/v) formic acid and (B) acetonitrile containing 0.1% (v/v) formic acid. High pH—40 °C, 1 mL/min flow rate. Gradient elution with the mobile phases as (A) 10 mM aqueous ammonium bicarbonate solution, adjusted to pH 10 with 0.88 M aqueous ammonia and (B) acetonitrile. TFA—40 °C, 1 mL/min flow rate. Gradient elution with the mobile phases as (A) 0.1% v/v aqueous TFA solution and (B) 0.1% v/v TFA solution in acetonitrile. Flash column chromatography was carried out using Biotage SP4 or Isolera One apparatus with SNAP silica cartridges. Mass-directed automatic purification (MDAP) was carried out using a Waters ZQ MS using alternate-scan positive and negative electrospray and a summed UV wavelength of 210−350 nm. Two liquid-phase methods were used: formic—Sunfire C18 column (100 mm × 19 mm, 5 μm packing diameter, 20 mL/min flow rate) or Sunfire C18 column (150 mm × 30 mm, 5 μm packing diameter, 40 mL/min flow rate). Gradient elution at ambient temperature with the mobile phases as (A) H_2O containing 0.1% volume/volume (v/v) formic acid and (B) acetonitrile containing 0.1% (v/v) formic acid. High pH—Xbridge

https://dx.doi.org/10.1021/acs.jmedchem.0c02156
J. Med. Chem. 2021, 64, 3249−3281

Scheme 3. Route for the Preparation of the Pyridyl Indole Compound 36[a]

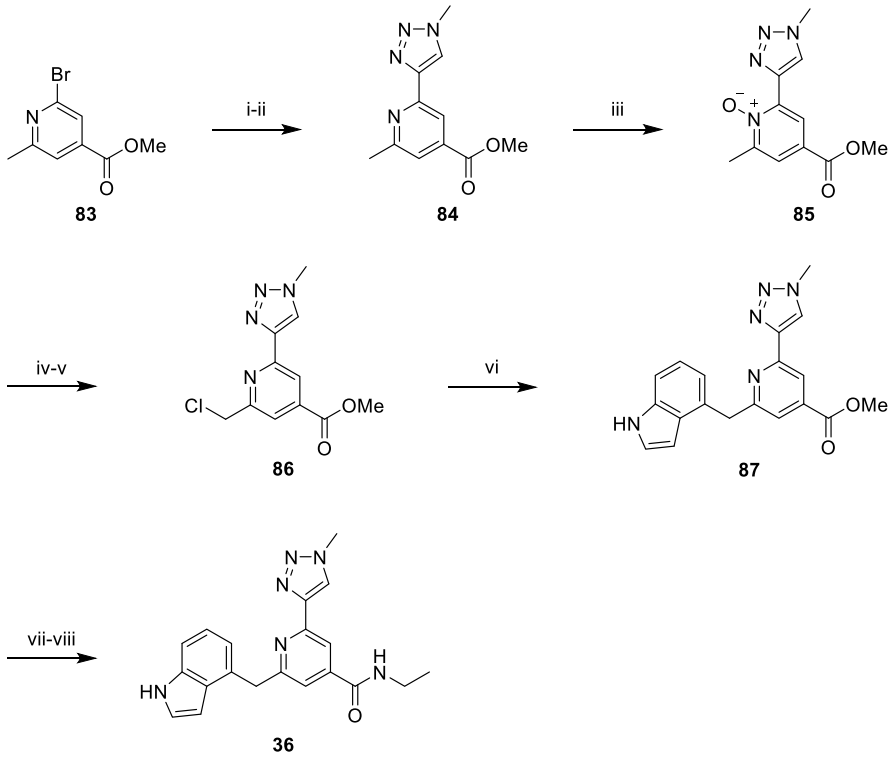

[a]Reagents and conditions: (i) TMS acetylene, Et_3N, Cu(I)I (10 mol %), $Pd(PPh_3)_4$ (5 mol %), 90 °C, 3 h (72%); (ii) NaN_3, MeI, pyridine, K_2CO_3, vitamin C (50 mol %), Cu(II)SO_4 (20 mol %), H_2O/MeOH (1:1), rt, 18−48 h (80%); (iii) mCPBA, $CHCl_3$, rt, 18 h (98%); (iv) TFAA, 50 °C, 12 h (86%); (v) $SOCl_2$, 90 °C, 25 min (65%); (vi) (1*H*-indol-4-yl)boronic acid, K_2CO_3, XPhos Pd G1 (5 mol %), XPhos (8 mol %), toluene/EtOH (9:1), 90 °C, 23 h (10%); (vii) LiOH, H_2O/THF (1:1), 50 °C, 90 min (57%); (viii) $EtNH_2$, HATU, DIPEA, DMF, rt, 17 h (39%).

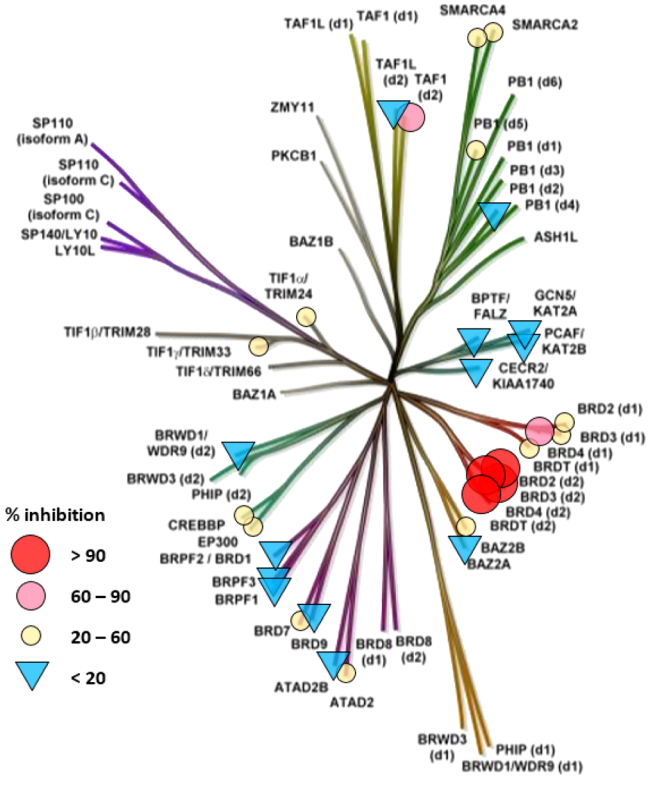

Figure 5. BromoScan profile of **36** at 10 μM concentration.

C18 column (100 mm × 19 mm, 5 μm packing diameter, 20 mL/min flow rate) or Xbridge C18 column (150 mm × 30 mm, 5 μm packing diameter, 40 mL/min flow rate). Gradient elution at ambient temperature with the mobile phases as (A) 10 mM aqueous ammonium bicarbonate solution, adjusted to pH 10 with 0.88 M aqueous ammonia and (B) acetonitrile. NMR spectra were recorded at ambient temperature (unless otherwise stated) using standard pulse methods on any of the following spectrometers and signal frequencies: Bruker AV-400 (^{1}H = 400 MHz, ^{13}C = 101 MHz), Bruker AV-600 (^{1}H = 600 MHz, ^{13}C = 150 MHz) or Bruker AV4 700 MHz spectrometer (^{1}H = 700 MHz, ^{13}C = 176 MHz). Chemical shifts are referenced to TMS or the residual solvent peak and are reported in ppm. Coupling constants are quoted to the nearest 0.1 Hz and multiplicities are given by the following abbreviations and combinations thereof: s (singlet), δ (doublet), t (triplet), q (quartet), quin (quintet), sxt (sextet), m (multiplet), and br (broad). Liquid chromatography high-resolution mass spectra (HRMS) were recorded on a Waters XEVO G2-XS Q-Tof mass spectrometer with the positive electrospray ionisation mode over a scan rate of 100−200 amu, with analytes separated on an Acquity UPLC CSH C18 column (100 mm × 2.1 mm, 1.7 μm packing diameter) at 50 °C. The purity of the synthesized compounds was determined by LC−MS analysis. All compounds for biological testing were >95% pure.

Synthetic Procedures. *1-(Benzyloxy)-2-bromobenzene (**88**).* 2-Bromophenol (0.123 mL, 1.156 mmol), benzyl bromide (0.151 mL, 1.272 mmol), and potassium carbonate (320 mg, 2.312 mmol) were added to acetone (10 mL), and the reaction mixture was heated at 50 °C for 2 days. The dry residue was dissolved into water and extracted into EtOAc, which was washed with brine. Brine (20 mL) was added to the remaining aqueous layer and the compound was extracted into EtOAc (30 mL). The combined organic layers were dried using a hydrophobic frit and concentrated *in vacuo*. The crude product was then purified by silica chromatography, eluting with 0−15% EtOAc/cyclohexane. The pure fractions were evaporated *in vacuo* to give 1-

https://dx.doi.org/10.1021/acs.jmedchem.0c02156
J. Med. Chem. 2021, 64, 3249−3281

(benzyloxy)-2-bromobenzene (**88**, 210 mg, 0.798 mmol, 69.0% yield) as a clear oil. LC−MS (formic, ES$^+$) t_R = 1.37 min; m/z = nd; ^{1}H NMR (400 MHz, $CDCl_3$-d): δ ppm 7.59 (dd, J = 7.8, 1.5 Hz, 1H) 7.50 (m, 2H) 7.38−7.45 (m, 2H) 7.31−7.38 (m, 1H) 7.25 (td, J = 8.3, 1.0 Hz, 1H) 6.96 (dd, J = 8.3, 1.5 Hz, 1H) 6.87 (td, J = 7.6, 1.5 Hz, 1H) 5.19 (br s, 2H) 1.56 (br s, 1H) 1.45 (s, 1H).

*5-(2-(Benzyloxy)phenyl)-3-methylisoxazole (**6**).* 3-Methyl-5-(4,4,5,5-tetramethyl-1,3,2-dioxaborolan-2-yl)isoxazole (230 mg, 1.100 mmol), 1-(benzyloxy)-2-bromobenzene (**88**, 210 mg, 0.798 mmol), $PdCl_2$(dppf)-CH_2Cl_2 adduct (80 mg, 0.098 mmol), and sodium carbonate (254 mg, 2.394 mmol) were dissolved in 1,4-dioxane (10 mL) and water (1 mL). The resulting mixture was stirred at 70 °C for 1.5 h. A further 3-methyl-5-(4,4,5,5-tetramethyl-1,3,2-dioxaborolan-2-yl)isoxazole (60 mg, 0.287 mmol), sodium carbonate (169 mg, 1.596 mmol), and $PdCl_2$(dppf)-CH_2Cl_2 adduct (80 mg, 0.098 mmol) were added, and the reaction mixture was heated to 170 °C overnight. The reaction was diluted with water and extracted with EtOAc, including a brine wash. The combined organic fractions were concentrated *in vacuo* giving a golden gum. The product was purified by silica chromatography, eluting with 0−20% EtOAc/cyclohexane. The fractions were evaporated *in vacuo* giving a yellowish oil, which was further purified by formic MDAP. The pure fractions were concentrated *in vacuo*, redissolved in MeOH, passed through an NH_2 ion-exchange column, and concentrated *in vacuo* to give 5-(2-(benzyloxy)phenyl)-3-methylisoxazole (**6**, 17 mg, 0.064 mmol, 8% yield) as a white solid. LC−MS (formic, ES$^+$) t_R = 1.32 min; m/z = 266.0; (100% pure) ^{1}H NMR (400 MHz, MeOD-d_4): δ ppm 7.90 (dd, J = 7.8, 1.5 Hz, 1H) 7.48−7.53 (m, 2H) 7.34−7.46 (m, 4H) 7.21−7.26 (m, 1H) 7.10 (td, J = 7.6, 1.0 Hz, 1H) 6.65 (s, 1H) 5.28 (s, 3H) 2.25−2.31 (m, 3H).

*((2-(Benzyloxy)phenyl)ethynyl)trimethylsilane (**89**).* 1-(Benzyloxy)-2-bromobenzene (**88**, 0.717 mL, 3.80 mmol), trimethylsilylacetylene (2.133 mL, 15.20 mmol), bis(triphenylphosphine)palladium(II) chloride (0.267 g, 0.380 mmol), copper(I) iodide (0.072 g, 0.380 mmol), and triethylamine (10 mL, 71.7 mmol) were stirred at 50 °C for 16 h. Trimethylsilylacetylene (2.133 mL, 15.20 mmol) and bis(triphenylphosphine)palladium(II) chloride (0.267 g, 0.380 mmol) were added, and the reaction mixture was stirred for 2 h. The reaction mixture was cooled to room temperature, filtered through a pad of celite, and concentrated *in vacuo*. The residue was purified by silica chromatography, eluting with 0−10% EtOAc/cyclohexane. The relevant fractions were concentrated *in vacuo* to give ((2-(benzyloxy)-phenyl)ethynyl)trimethylsilane (**89**, 660 mg, 2.353 mmol, 62% yield) as an orange oil. LC−MS (formic, ES$^+$) t_R = 1.56 min; m/z = 281.1; ^{1}H NMR (400 MHz, MeOD-d_4): δ ppm 7.54 (d, J = 7.3 Hz, 2H) 7.28−7.42 (m, 5H) 7.06 (d, J = 7.8 Hz, 1H) 6.93 (td, J = 7.3, 1.0 Hz, 1H) 5.17 (s, 2H) 0.23 (br s, 9H).

*1-(Benzyloxy)-2-ethynylbenzene (**90**).* ((2-(Benzyloxy)phenyl)-ethynyl)trimethylsilane (**89**, 514 mg, 1.833 mmol) and potassium carbonate (380 mg, 2.75 mmol) were stirred in methanol (10 mL) for 1.5 h. The reaction mixture was concentrated *in vacuo*, diluted with water, and extracted into EtOAc. The organic layers were combined, dried *via* a hydrophobic frit, and concentrated *in vacuo*. The compound was isolated by silica chromatography, eluting with 0−15% EtOAc/cyclohexane. The pure fractions were evaporated *in vacuo* to give 1-(benzyloxy)-2-ethynylbenzene (**90**, 410 mg, 1.969 mmol, 89% yield). LC−MS (formic, ES$^+$) t_R = 1.26 min; m/z = 209.2; ^{1}H NMR (400 MHz, MeOD-d_4): δ ppm 7.50 (d, J = 7.3 Hz, 2H) 7.43 (dd, J = 7.6, 1.7 Hz, 1H) 7.35−7.41 (m, 2H) 7.31 (td, J = 7.3, 2.4 Hz, 2H) 7.05 (d, J = 8.3 Hz, 1H) 6.93 (td, J = 6.8, 2.4 Hz, 1H) 5.18 (br s, 2H) 3.61 (s, 1H).

*4-(2-(Benzyloxy)phenyl)-1-methyl-1H-1,2,3-triazole (**7**).* 1-(Benzyloxy)-2-ethynylbenzene (**90**, 120 mg, 0.576 mmol), sodium azide (74.9 mg, 1.152 mmol), copper(II) sulfate (18.39 mg, 0.115 mmol), iodomethane (72.1 μL, 1.152 mmol), and copper powder (36.6 mg, 0.576 mmol) were irradiated at 125 °C in a Biotage microwave at high absorption for 2 h. Sodium azide (74.9 mg, 1.152 mmol) and iodomethane (72.1 μL, 1.152 mmol) were added, and the vial was irradiated at 125 °C in a Biotage microwave at high absorption; however, due to machine malfunction, the majority of the reaction mixture was lost. The residue was dissolved in 0.9 mL of dimethyl sulfoxide (DMSO)/MeOH 1:1 and purified by formic MDAP, and the relevant fractions were concentrated *in vacuo* to give 4-(2-(benzyloxy)phenyl)-1-methyl-1*H*-1,2,3-triazole (**7**, 1 mg, 3.77 μmol, 1% yield) as a pale yellow solid. LC−MS (formic, ES$^+$) t_R = 1.09 min; m/z = 266.1; (97% pure) ^{1}H NMR (400 MHz, MeOD-d_4): δ ppm 8.15 (br s, 1H) 8.11 (dd, J = 7.8, 1.5 Hz, 1H) 7.47 (d, J = 6.8 Hz, 2H) 7.39−7.44 (m, 2H) 7.35−7.39 (m, 1H) 7.31 (td, J = 7.9, 1.7 Hz, 1H) 7.16 (d, J = 8.3 Hz, 1H) 7.06 (td, J = 7.8, 1.0 Hz, 1H) 5.26 (s, 2H) 4.09 (br s, 3H).

*(E)-N′-(1,1-Dichloropropan-2-ylidene)-4-methylbenzenesulfonohydrazide (**91**).* 1,1-Dichloropropan-2-one (0.420 mL, 4.33 mmol) and *para*-toluenesulfonhydrazide (0.733 g, 3.94 mmol) were stirred in propionic acid (5 mL) at room temperature for 4 h, after which the solid was removed by filtration, washed with cyclohexane, and dried in a vacuum oven to give (*E*)-*N*′-(1,1-dichloropropan-2-ylidene)-4-methylbenzenesulfonohydrazide (**91**, 900 mg, 3.05 mmol, 77% yield) as a white solid. LC−MS (formic, ES$^+$) t_R = 0.88 min; m/z = 296.1; ^{1}H NMR (400 MHz, DMSO-d_6): δ ppm 11.82 (br s, 1H) 9.19 (s, 1H) 7.80 (dt, J = 8.3, 2.0 Hz, 2H) 7.43 (d, J = 7.8 Hz, 2H) 2.39 (br s, 3H) 1.83 (s, 3H).

*1-(2-(Benzyloxy)phenyl)-4-methyl-1H-1,2,3-triazole (**8**).* 2-(Benzyloxy)aniline (50 mg, 0.251 mmol) in ethanol (3 mL) was cooled to 0 °C and stirred for 10 min, after which (*E*)-*N*′-(1,1-dichloropropan-2-ylidene)-4-methylbenzenesulfonohydrazide (**91**, 96 mg, 0.326 mmol) in acetonitrile (2 mL) was added dropwise, and the reaction mixture was allowed to warm to room temperature and stirred for 16 h. The reaction mixture was concentrated *in vacuo*, taken up into 0.9 mL of 1:1 DMSO/MeOH, and purified by formic MDAP. The relevant fractions were combined and concentrated *in vacuo* to give 1-(2-(benzyloxy)phenyl)-4-methyl-1*H*-1,2,3-triazole (**8**, 43 mg, 0.162 mmol, 65% yield) as an orange oil. LC−MS (formic, ES$^+$) t_R = 1.09 min; m/z = 266.2; (100% pure) ^{1}H NMR (400 MHz, MeOD-d_4): δ ppm 8.03 (br s, 1H) 7.63 (dd, J = 7.8, 1.5 Hz, 1H) 7.47 (td, J = 7.3, 2.0 Hz, 1H) 7.27−7.37 (m, 6H) 7.14 (td, J = 7.7, 1.2 Hz, 1H) 5.20 (s, 2H) 2.37 (s, 3H).

*Methyl 2-(Benzyloxy)benzoate (**92**).* (Bromomethyl)benzene (1.093 mL, 9.20 mmol), methyl 2-hydroxybenzoate (0.855 mL, 6.57 mmol), and potassium carbonate (1.272 g, 9.20 mmol) were stirred in acetone (20 mL) at 50 °C for 24 h. The reaction mixture was concentrated *in vacuo* and partitioned between water and EtOAc; the organic phase was washed with brine, dried using a hydrophobic frit, and concentrated *in vacuo* to give methyl 2-(benzyloxy)benzoate (**92**, 1.641 g, 6.77 mmol, 76% yield) as a white solid. LC−MS (formic, ES$^+$) t_R = 1.18 min; m/z = 243.2; ^{1}H NMR (400 MHz, DMSO-d_6): δ ppm 7.69 (dd, J = 7.6, 1.7 Hz, 1H) 7.30−7.54 (m, 6H) 7.23 (d, J = 8.8 Hz, 1H) 7.04 (td, J = 6.8, 1.0 Hz, 1H) 5.21 (br s, 2H) 3.81 (s, 3H).

*2-(Benzyloxy)benzoic Acid (**93**).* Methyl 2-(benzyloxy)benzoate (**92**, 1.6 g, 6.60 mmol) and lithium hydroxide (0.237 g, 9.91 mmol) were stirred in tetrahydrofuran (THF) (10 mL)/water (10 mL) at 50 °C for 16 h and then at 18 °C for 5 h. The reaction mixture was concentrated *in vacuo* to remove the THF and was then acidified to pH 1 with 2 N HCl (aq), a fine precipitate formed, this was extracted into EtOAc; the organic layer was washed with brine, dried using a hydrophobic frit, and concentrated *in vacuo* to give 2-(benzyloxy)-benzoic acid (**93**, 1.297 g, 5.68 mmol, 86% yield) as a cream viscous oil. LC−MS (formic, ES$^+$) t_R = 1.00 min; m/z 229.1; ^{1}H NMR (400 MHz, DMSO-d_6): δ ppm 12.63 (br s, 1H) 7.67 (dd, J = 7.6, 1.7 Hz, 1H) 7.30−7.54 (m, 6H) 7.19 (d, J = 8.3 Hz, 1H) 7.02 (td, J = 7.3, 1.0 Hz, 1H) 5.20 (s, 2H).

*N′-Acetyl-2-(benzyloxy)benzohydrazide (**94**).* 2-(Benzyloxy)-benzoic acid (**93**, 370 mg, 1.621 mmol), HATU (678 mg, 1.783 mmol), and DIPEA (0.849 mL, 4.86 mmol) were stirred in dimethylformamide (DMF) (10 mL) at rt for 5 min, acetohydrazide (160 mg, 1.945 mmol) was added, and the reaction mixture was stirred at rt for 16 h. The reaction mixture was diluted with water and extracted with EtOAc; the organic phase was washed with 10% LiCl (aq), dried using a hydrophobic frit, and concentrated to give a yellow oil. This oil was purified by silica chromatography eluting with 20−

https://dx.doi.org/10.1021/acs.jmedchem.0c02156
J. Med. Chem. 2021, 64, 3249−3281

80% EtOAc/cyclohexane. The pure fractions were concentrated *in vacuo* to give *N*′-acetyl-2-(benzyloxy)benzohydrazide (**94**, 301 mg, 1.059 mmol, 65% yield) as a pale yellow oil. LC−MS (formic, ES$^+$) t_R = 0.83 min; *m*/*z* 285.1; ^{1}H NMR (400 MHz, DMSO-d_6): δ ppm 10.10 (br s, 1H) 9.94 (br s, 1H) 7.69 (dd, *J* = 7.8, 2.0 Hz, 1H) 7.27−7.61 (m, 6H) 7.22 (d, *J* = 7.8 Hz, 1H) 7.01−7.11 (m, 1H) 5.29 (s, 2H) 1.91 (s, 3H).

*2-(2-(Benzyloxy)phenyl)-5-methyl-1,3,4-oxadiazole (**9**).* *N*′-Acetyl-2-(benzyloxy)benzohydrazide (**94**, 301 mg, 1.059 mmol) and $POCl_3$ (5 mL, 53.6 mmol) were stirred at 110 °C for 1 h. $POCl_3$ was removed *in vacuo* azeotroping with toluene (×2); the resulting yellow oil was purified using silica chromatography eluting with a gradient of 0−100% EtOAc/cyclohexane. The relevant fractions were concentrated *in vacuo* and the material was further purified using formic MDAP. The pure fractions were concentrated *in vacuo* to give 2-(2-(benzyloxy)phenyl)-5-methyl-1,3,4-oxadiazole (**9**, 51 mg, 0.192 mmol, 18% yield) as a light green oil. LC−MS (formic, ES$^+$) t_R = 1.06 min; *m*/*z* = 267.1; (100% pure) ^{1}H NMR (400 MHz, DMSO-d_6): δ ppm 7.84 (dd, *J* = 7.6, 1.7 Hz, 1H) 7.49−7.62 (m, 3H) 7.37−7.45 (m, 2H) 7.30−7.37 (m, 2H) 7.14 (td, *J* = 7.6, 1.0 Hz, 1H) 5.30 (s, 2H) 2.57 (s, 3H).

*2-(5-Methyl-1H-1,2,4-triazol-3-yl)phenol (**95**).* A mixture of 2-(benzyloxy) benzonitrile (0.5 g, 2.38 mmol), acetohydrazide (176.3 mg, 2.38 mmol), and potassium carbonate (98 mg, 0.714 mmol) in ^{n}BuOH (4 mL) was heated to 150 °C for 6 h under microwave conditions. The reaction mixture was concentrated under reduced pressure; crude residue was diluted with water (20 mL) and extracted with EtOAc (2 × 30 mL). The organic layer was dried over anhydrous Na_2SO_4, filtered, concentrated, and dried to get 500 mg of the crude compound. The crude compound was purified by silica chromatography eluting with 0−30% EtOAc in pet ether. The pure fractions were collected, concentrated, and dried to give 2-(5-methyl-1*H*-1,2,4-triazol-3-yl)phenol (**95**, 120 mg, 0.616 mmol, 26% yield) as an off-white solid. LC−MS (high pH, ES$^+$) t_R = 3.38 min; *m*/*z* = 176.0; ^{1}H NMR (400 MHz, $CDCl_3$-*d*): δ ppm 11.01 (br s, 1H) 7.88 (br d, *J* = 7.0 Hz, 1H) 7.32 (td, *J* = 7.0, 1.5 Hz, 1H) 7.04 (d, *J* = 7.7 Hz, 1H) 6.92 (td, *J* = 7.2, 1.0 Hz, 1H) 2.55 (s, 3H).

*3-(2-(Benzyloxy)phenyl)-5-methyl-1H-1,2,4-triazole (**10**).* 2-(5-Methyl-1*H*-1,2,4-triazol-3-yl)phenol (**95**, 70 mg, 0.400 mmol), potassium carbonate (66.3 mg, 0.479 mmol), and benzyl bromide (0.048 mL, 0.400 mmol) were dissolved in acetone (8 mL) at rt, and the reaction mixture was stirred at 20 °C for 4 h. Then, the reaction mixture was heated to 40 °C for 4 h. The reaction mixture was quenched with ice-cold water (20 mL) and extracted with EtOAc (2 × 30 mL). The organic layer was dried over anhydrous Na_2SO_4, filtered, and concentrated to get 70 mg of the crude compound. This crude compound was purified by combining with the crude compound to get 120 mg of the crude compound. The crude compound was purified by silica chromatography eluting with 0−30% EtOAc in pet ether. The relevant fractions were collected, concentrated, and dried to get an impure material. This was further purified by formic MDAP. The pure fraction was lyophilized and dried to get 3-(2-(benzyloxy)phenyl)-5-methyl-1*H*-1,2,4-triazole (**10**, 10 mg, 0.038 mmol, 10% yield) as a white solid. LC−MS (formic, ES$^+$) t_R = 4.30 min; *m*/*z* = 266.3; (100% pure) ^{1}H NMR (400 MHz, $CDCl_3$-*d*): δ ppm 11.31 (br s, 1H) 8.33 (dd, *J* = 8.1, 1.5 Hz, 1H) 7.37−7.51 (m, 6H) 7.09−7.18 (m, 2H) 5.24 (s, 2H) 2.45 (s, 3H).

*N-(2-(Benzyloxy)phenyl)acetamide (**11**).* A mixture of acetamidophenol (154.17 g, 1.0 mol), potassium carbonate (138.2 g, 1.00 mol), sodium iodide (14.9 g, 0.1 mol), and benzyl bromide (125 mL, 1.05 mol) was combined in acetone (1 L) under nitrogen and heated to reflux for 4 h. The solvent was reduced to half volume by distillation at atmospheric pressure, and the cooled reaction mixture was partitioned between EtOAc (3 L) and water (500 mL). The organic layer was washed with 1:1 brine: water (500 mL) and then the solvent was removed by distillation at atmospheric pressure to give a brown solid. The solid was triturated with cyclohexane (450 mL) and collected by filtration. The filter cake was washed with cyclohexane (3 × 100 mL) and then dried under vacuum at room temperature to give *N*-(2-(benzyloxy)phenyl)acetamide (216.2 g, 0.9 mol, 89.6% yield). A small portion (78 mg, 0.323 mmol) was purified by formic MDAP. The appropriate fractions were concentrated under a stream of nitrogen to give *N*-(2-(benzyloxy)phenyl)acetamide (**11**, 59 mg, 0.244 mol, 76% yield) as a white solid. LC−MS (formic, ES$^+$) t_R = 0.96 min; *m*/*z* = 242; (100% pure) ^{1}H NMR (400 MHz, DMSO-d_6): δ ppm 9.10 (br s, 1H), 7.84 (br d, *J* = 7.8 Hz, 1H), 7.50 (d, *J* = 7.3 Hz, 2H), 7.29−7.44 (m, 3H), 6.97−7.11 (m, 2H), 6.89 (t, *J* = 7.5 Hz, 1H), 5.20 (s, 2H), 2.09 (s, 3H).

*Methyl 3-Bromo-4-(methoxymethoxy)benzoate (**63**).* Methyl 3-bromo-4-hydroxybenzoate (20 g, 87 mmol), MOM-Cl (9.86 mL, 130 mmol), and cesium carbonate (36.7 g, 113 mmol) were stirred in DMF (200 mL) at rt for 6 h. The reaction mixture was partitioned between water and EtOAc, and the organic layer was washed with 1 N NaOH, water, and 10% LiCl (aq), then eluted through a hydrophobic frit, and concentrated *in vacuo* to give methyl 3-bromo-4-(methoxymethoxy)benzoate (**63**, 23.649 g, 86 mmol, 99% yield) as a white solid. LC−MS (formic, ES$^+$) t_R = 1.12 min; *m*/*z* = 276.9; ^{1}H NMR (400 MHz, DMSO-d_6, 295 K): δ ppm 8.11 (d, *J* = 2.0 Hz, 1H), 7.94 (dd, *J* = 8.6, 2.2 Hz, 1H), 7.32 (d, *J* = 8.8 Hz, 1H), 5.40 (s, 2H), 3.84 (s, 3H), 3.42 (s, 3H).

*Methyl 4-(Methoxymethoxy)-3-((trimethylsilyl)ethynyl)benzoate (**64**).* Methyl 3-bromo-4-(methoxymethoxy)benzoate (**63**, 23 g, 84 mmol), ethynyltrimethylsilane (60 mL, 425 mmol), Et_3N (100 mL, 717 mmol), $PdCl_2(PPh_3)_2$ (2.93 g, 4.18 mmol), and copper iodide (1.592 g, 8.36 mmol) were combined under nitrogen, and the mixture was heated at 60 °C for 24 h. The reaction mixture was diluted with EtOAc (200 mL) and filtered, and the filtrate was then washed with water (2 × 200 mL), dried with sodium sulfate, and concentrated *in vacuo*. The resulting dark brown oil was purified by silica chromatography eluting with 0−25% EtOAc/cyclohexane. The product-containing fractions were concentrated *in vacuo* to give methyl 4-(methoxymethoxy)-3-((trimethylsilyl)ethynyl)benzoate (**64**, 22.3 g, 76 mmol, 91% yield) as a brown oil. LC−MS (formic, ES$^+$) t_R = 1.41 min; *m*/*z* = 293; ^{1}H NMR (400 MHz, $CDCl_3$-*d*, 295 K): δ ppm 8.15 (d, *J* = 2.4 Hz, 1H), 7.93−7.98 (dd, *J* = 8.8, 2.4 Hz, 1H), 7.13 (d, *J* = 8.8 Hz, 1H), 5.31 (s, 2H), 3.91 (s, 3H), 3.51−3.56 (m, 3H), 0.24−0.32 (m, 9H).

General Procedure A. *Methyl 4-(Methoxymethoxy)-3-(1-methyl-1H-1,2,3-triazol-4-yl)benzoate (**57**).* Sodium azide (6.67 g, 103 mmol), ascorbic acid (4.82 g, 27.4 mmol), potassium carbonate (17.02 g, 123 mmol), and copper(II) sulfate (2.183 g, 13.68 mmol) were combined and then water (160 mL) and methanol (160 mL) were added. The mixture was stirred at room temperature. Methyl 4-(methoxymethoxy)-3-((trimethylsilyl)ethynyl)benzoate (**64**, 20 g, 68.4 mmol), MeI (12.83 mL, 205 mmol), and pyridine (27.7 mL, 342 mmol) were added, and the mixture was stirred at room temperature over 60 h. The mixture was evaporated to approximately half volume and then extracted with dichloromethane (DCM) (3 × 200 mL), and the combined organics were washed with brine, then dried, and evaporated *in vacuo* to give a dark brown oil. The crude product was dissolved in DCM and purified by silica chromatography eluting with 0−100% EtOAc/cyclohexane, and the product-containing fractions were evaporated *in vacuo* to give methyl 4-(methoxymethoxy)-3-(1-methyl-1*H*-1,2,3-triazol-4-yl)benzoate (**57**, 15 g, 54.1 mmol, 79% yield). LC−MS (formic, ES$^+$) t_R = 0.86 min; *m*/*z* = 278.2; ^{1}H NMR (400 MHz, $CDCl_3$-*d*): δ ppm 9.03 (d, *J* = 2.0 Hz, 1H) 7.98−8.04 (m, 2H) 7.24 (d, *J* = 8.8 Hz, 1H) 5.39 (s, 2H) 4.19 (s, 3H) 3.94 (s, 3H) 3.52 (s, 3H).

*4-(Methoxymethoxy)-3-(1-methyl-1H-1,2,3-triazol-4-yl)benzoic Acid (**96**).* A suspension of methyl 4-(methoxymethoxy)-3-(1-methyl-1*H*-1,2,3-triazol-4-yl)benzoate (**57**, 11 g, 39.7 mmol) in THF (40 mL), water (40 mL), and NaOH (39.7 mL, 79 mmol) was stirred at rt for 4 h. The reaction mixture was concentrated and taken up into water. Acetic acid was added until pH 5, precipitating a gray solid, which was isolated by vacuum filtration through a sinter funnel. The filter cake was washed with water and dried in a vacuum oven to give 4-(methoxymethoxy)-3-(1-methyl-1*H*-1,2,3-triazol-4-yl)benzoic acid (**96**, 8.26 g, 31.4 mmol, 79% yield). LC−MS (formic, ES$^+$) t_R = 0.69 min; *m*/*z* = 264.1.

https://dx.doi.org/10.1021/acs.jmedchem.0c02156
J. Med. Chem. 2021, 64, 3249−3281

4-Hydroxy-3-(1-methyl-1H-1,2,3-triazol-4-yl)benzoic Acid (97). 4-(Methoxymethoxy)-3-(1-methyl-1*H*-1,2,3-triazol-4-yl)benzoic acid (**96**, 2 g, 7.60 mmol) and conc HCl (1 mL, 32.9 mmol) were stirred at 50 °C for 16 h. A precipitate had formed in the reaction, this was removed by filtration and dried to give 4-hydroxy-3-(1-methyl-1*H*-1,2,3-triazol-4-yl)benzoic acid (**97**, 1.432 g, 6.53 mmol, 86% yield) as a cream solid. LC−MS (formic, ES^+) t_R = 0.65 min; m/z = 220.1; ^{1}H NMR (400 MHz, DMSO-d_6): δ ppm 12.53 (br s, 1H) 10.97 (s, 1H) 8.66 (d, J = 2.4 Hz, 1H) 8.43 (s, 1H) 7.72−7.79 (m, 1H) 7.03 (d, J = 8.8 Hz, 1H) 4.11 (s, 3H).

Methyl 4-(Benzyloxy)-3-(1-methyl-1H-1,2,3-triazol-4-yl)benzoate (98). 4-Hydroxy-3-(1-methyl-1*H*-1,2,3-triazol-4-yl)benzoic acid (**97**, 2.498 g, 11.40 mmol), benzyl bromide (2.710 mL, 22.79 mmol), and potassium carbonate (4.730 g, 34.20 mmol) were stirred at rt in acetone (20 mL) for 16 h. The reaction mixture was concentrated *in vacuo*, and the residue was partitioned between water (25 mL) and EtOAc (25 mL). The organic layer was washed with brine (25 mL), dried using a hydrophobic frit, and concentrated to give benzyl 4-(benzyloxy)-3-(1-methyl-1*H*-1,2,3-triazol-4-yl)benzoate (**98**, 4.230 g, 10.59 mmol, 93% yield) as a beige solid. LC−MS (formic, ES^+) t_R = 1.32 min; m/z = 400.

4-(Benzyloxy)-3-(1-methyl-1H-1,2,3-triazol-4-yl)benzoic Acid (99). Benzyl 4-(benzyloxy)-3-(1-methyl-1*H*-1,2,3-triazol-4-yl)-benzoate (**98**, 4.23 g, 10.59 mmol) and lithium hydroxide (0.254 g, 10.59 mmol) were combined in THF (20 mL)/water (20 mL) and stirred at 50 °C for 16 h. The reaction mixture was concentrated *in vacuo* to remove the THF and was acidified to pH 2 with 2 N HCl (aq). The resulting precipitate was collected by filtration and dried to give 4-(benzyloxy)-3-(1-methyl-1*H*-1,2,3-triazol-4-yl)benzoic acid (**99**, 3.08 g, 9.96 mmol, 94% yield) as a cream solid. LC−MS (formic, ES^+) t_R = 0.94 min; m/z = 310; ^{1}H NMR (400 MHz, DMSO-d_6): δ ppm 12.73 (br s, 1H), 8.75 (d, J = 2.0 Hz, 1H), 8.31 (s, 1H), 7.87 (dd, J = 8.8, 2.4 Hz, 1H), 7.47−7.55 (m, 2H), 7.26−7.47 (m, 4H), 5.42 (s, 2H), 4.09 (s, 3H).

4-(Benzyloxy)-N-ethyl-3-(1-methyl-1H-1,2,3-triazol-4-yl)-benzamide (13). 4-(Benzyloxy)-3-(1-methyl-1*H*-1,2,3-triazol-4-yl)-benzoic acid (**99**, 2.6 g, 8.41 mmol) was taken up into DMF (65 mL). DIPEA (5.87 mL, 33.6 mmol) was added, and the mixture was left to stir for 10 s. HATU (4.79 g, 12.61 mmol) was then added, and the mixture was left to stir for 1 min. 2 M ethanamine in THF (5.04 mL, 10.09 mmol) was added, and the reaction mixture was stirred at room temperature for 2 h. The mixture was concentrated *in vacuo* to give a brown oil. The oil was partitioned between EtOAc and water (30 mL each), and the organic phase was washed with 2 M NaOH (60 mL), filtered through a hydrophobic frit, and concentrated *in vacuo* to give 4-(benzyloxy)-*N*-ethyl-3-(1-methyl-1*H*-1,2,3-triazol-4-yl)benzamide (**13**, 2.80 g, 8.32 mmol, 99% yield) as a pale yellow solid. LC−MS (formic, ES^+) t_R = 0.95 min; m/z = 337; (100% pure) ^{1}H NMR (400 MHz, MeOD-d_4): δ ppm 7.80 (dd, J = 9.3, 2.4 Hz, 1H), 7.34−7.51 (m, 5H), 7.23 (d, J = 8.8 Hz, 1H), 5.34 (s, 2H), 4.82−4.82 (m, 5H), 4.10 (s, 3H), 3.43 (q, J = 7.3 Hz, 2H), 3.34−3.38 (m, 1H), 2.94−3.09 (m, 1H), 1.25 (t, J = 6.4 Hz, 3H).

tert-Butyl 2-Chloro-6-((trimethylsilyl)ethynyl)isonicotinate (80). *tert*-Butyl 2,6-dichloroisonicotinate (2 g, 8.06 mmol), $Pd(PPh_3)_4$ (0.373 g, 0.322 mmol), triethylamine (5.2 mL, 37.3 mmol), triphenylphosphine (0.317 g, 1.209 mmol), and copper iodide (0.061 g, 0.322 mmol) were combined in toluene (13 mL) in a microwave vial, and the vial was vacuum-degassed and flushed with nitrogen. Ethynyltrimethylsilane (1.139 mL, 8.06 mmol) was added, and the vial was again degassed and flushed with nitrogen. The reaction mixture was heated to 80 °C for 6.5 h under microwave conditions and then left to stand in solution overnight. The reaction mixture was partitioned between ethyl acetate (100 mL) and water (40 mL). The organic layer was washed with water (40 mL) and brine (40 mL), then passed through a hydrophobic frit, and concentrated *in vacuo*. The resulting oil was suspended in cyclohexane and purified by silica gel chromatography using a gradient of 0−20% ethyl acetate/cyclohexane. The product-containing fractions were combined, and the solvent was removed *in vacuo* to give *tert*-butyl 2-chloro-6-((trimethylsilyl)ethynyl)isonicotinate (**80**, 6.574 g, 7.00 mmol, 87% yield) as an orange oil. LC−MS (formic, ES^+) t_R = 1.63 min; m/z = 310; ^{1}H NMR (400 MHz, $CDCl_3$-d): δ ppm 7.80−7.88 (m, 1H), 7.69−7.80 (m, 1H), 1.45 (s, 9H), 0.29 (s, 9H).

tert-Butyl 2-Chloro-6-(1-methyl-1H-1,2,3-triazol-4-yl)-isonicotinate (69). General procedure A was followed using the following amounts: methyl iodide (0.282 mL, 4.52 mmol), *tert*-butyl 2-chloro-6-((trimethylsilyl)ethynyl)isonicotinate (**80**, 1.166 g, 1.505 mmol), sodium azide (0.215 g, 3.31 mmol), vitamin C (0.106 g, 0.602 mmol), potassium carbonate (0.374 g, 2.71 mmol), pyridine (0.609 mL, 7.53 mmol), and copper sulfate pentahydrate (0.075 g, 0.301 mmol) in methanol (4 mL), THF (4.00 mL), and water (4.00 mL). This gave *tert*-butyl 2-chloro-6-(1-methyl-1*H*-1,2,3-triazol-4-yl)-isonicotinate (**69**, 211.5 mg, 0.718 mmol, 48% yield) as a cream solid. LC−MS (formic, ES^+) t_R = 1.19 min; m/z = 295.1; ^{1}H NMR (400 MHz, $CDCl_3$-d): δ ppm 8.55 (d, J = 1.0 Hz, 1H) 8.19 (s, 1H) 7.76 (d, J = 1.5 Hz, 1H) 4.19 (s, 3H) 1.64 (s, 9H).

2-Chloro-6-(1-methyl-1H-1,2,3-triazol-4-yl)isonicotinic Acid (100). TFA (0.971 mL, 12.61 mmol) was added to a solution of *tert*-butyl 2-chloro-6-(1-methyl-1*H*-1,2,3-triazol-4-yl)isonicotinate (**69**, 464.5 mg, 1.576 mmol) in DCM (7 mL), and the reaction mixture was stirred at room temperature under nitrogen for 3 h after which further TFA (0.971 mL, 12.61 mmol) was added. Stirring continued for 1 h after which further TFA (0.971 mL, 12.61 mmol) was added, and the reaction mixture was stirred for 2 h and left to stand at room temperature for 16 h. The reaction mixture was concentrated and the product was left to dry *in vacuo* at 40 °C for 3 h to give 2-chloro-6-(1-methyl-1*H*-1,2,3-triazol-4-yl)isonicotinic acid (**100**, 437 mg, 1.557 mmol, 99% yield) as a brown solid. LC−MS (formic, ES^+) t_R = 0.76 min; m/z = 239; ^{1}H NMR (400 MHz, DMSO-d_6, 303 K): δ ppm 8.72 (s, 1H), 8.37 (d, J = 1.5 Hz, 1H), 7.77 (d, J = 1.0 Hz, 1H), 4.13 (s, 3H) (carboxylic acid not visible in spectrum).

2-Chloro-N-ethyl-6-(1-methyl-1H-1,2,3-triazol-4-yl)-isonicotinamide (71). 2 M ethanamine in THF (0.758 mL, 1.516 mmol) was added to a solution of 2-chloro-6-(1-methyl-1*H*-1,2,3-triazol-4-yl)isonicotinic acid (**100**, 428 mg, 1.166 mmol), HATU (576 mg, 1.516 mmol), and DIPEA (0.407 mL, 2.332 mmol) in DMF (7 mL). The reaction mixture was stirred at room temperature under nitrogen for 2 h and left to stand in solution for 16 h. The reaction mixture was partitioned between ethyl acetate (30 mL) and water (20 mL), the organic layer was washed with water (10 mL) and 10% LiCl solution (10 mL) and then passed through a hydrophobic frit, and the solvent was removed *in vacuo*. The resulting oil was dissolved in DCM and purified by silica chromatography eluting with 0−70% ethyl acetate/cyclohexane. The product-containing fractions were combined, and the solvent was removed *in vacuo* to give 2-chloro-*N*-ethyl-6-(1-methyl-1*H*-1,2,3-triazol-4-yl)isonicotinamide (**71**, 251.5 mg, 0.852 mmol, 73% yield) as a pale yellow solid. LC−MS (formic, ES^+) t_R = 0.73 min; m/z = 266; ^{1}H NMR (400 MHz, $CDCl_3$-d): δ ppm 8.27 (d, J = 1.5 Hz, 1H), 8.21 (s, 1H), 7.73 (d, J = 1.5 Hz, 1H), 6.44 (br s, 1H), 4.20 (s, 3H), 3.48−3.62 (m, 3H), 1.30 (t, J = 6.9 Hz, 3H).

2-Benzyl-N-ethyl-6-(1-methyl-1H-1,2,3-triazol-4-yl)-isonicotinamide (14). $PdCl_2(PPh_3)_2$ (52.8 mg, 0.075 mmol) and 2-chloro-*N*-ethyl-6-(1-methyl-1*H*-1,2,3-triazol-4-yl)isonicotinamide (**71**, 100 mg, 0.376 mmol) were dissolved in THF (3 mL) in a microwave vial which was then sealed, and benzylzinc(II) bromide 0.5 M in THF (1.505 mL, 0.753 mmol) was added. The reaction mixture was heated to 110 °C for 1 h under microwave conditions. The reaction mixture was partitioned between ethyl acetate (30 mL) and water (10 mL), and the organic layer was washed with water (10 mL) and brine (10 mL). The organic layer was passed through a hydrophobic frit, and the solvent was removed *in vacuo*. The resulting solid was dissolved in DCM and purified by silica chromatography eluting with 0−80% ethyl acetate/cyclohexane followed by 0−4% ethyl acetate/ethanol. The product-containing fractions were combined, and the solvent was removed *in vacuo* to give a pale brown solid. The product was further purified by formic MDAP and the product-containing fraction was concentrated under a stream of nitrogen to give 2-benzyl-*N*-ethyl-6-(1-methyl-1*H*-1,2,3-triazol-4-yl)-

https://dx.doi.org/10.1021/acs.jmedchem.0c02156
J. Med. Chem. 2021, 64, 3249−3281

isonicotinamide (**14**, 6.6 mg, 0.021 mmol, 5.46% yield) as a white solid. LC−MS (formic, ES^+) t_R = 0.91 min; m/z = 322; (100% pure) ^{1}H NMR (400 MHz, $CDCl_3$-*d*): δ ppm 8.18 (s, 1H). 8.17 (d, J = 1.5 Hz, 1H), 7.56 (d, J = 1.5 Hz, 1H), 7.29−7.35 (m, 4H), 7.21−7.27 (m, 1H), 6.30 (br s, 1H), 4.23 (2H, s), 4.20 (s, 3H), 3.52 (qd, J = 7.3, 5.6 Hz, 3H), 1.28 (t, J = 7.3 Hz, 4H).

*Methyl 3-Ethynyl-4-(methoxymethoxy)benzoate (**101**).* Methyl 4-(methoxymethoxy)-3-((trimethylsilyl)ethynyl)benzoate (**64**, 2.61 g, 8.93 mmol) and potassium carbonate (2.96 g, 21.42 mmol) were stirred in methanol (20 mL) for 40 min. The reaction mixture was diluted with 2 M HCl and extracted into DCM, including a brine wash. The organic layers were then combined, dried *via* a hydrophobic frit, and concentrated *in vacuo*. The residue was taken up into DCM and purified by silica chromatography eluting with 20−70% EtOAc/cyclohexane, and the relevant fractions were concentrated to give methyl 3-ethynyl-4-(methoxymethoxy)benzoate (**101**, 600 mg, 2.72 mmol, 31% yield). LC−MS (formic, ES^+) t_R = 1.01 min; m/z = 221.1.

*N-Ethyl-4-(methoxymethoxy)-3-(1-methyl-1H-1,2,3-triazol-4-yl)-benzamide (**58**).* 4-(Methoxymethoxy)-3-(1-methyl-1*H*-1,2,3-triazol-4-yl)benzoic acid (**96**, 1.60 g, 6.08 mmol), HATU (2.54 g, 6.69 mmol) and DIPEA (2.123 mL, 12.16 mmol) were stirred in DMF (10 mL) at rt for 10 min, ethanamine (4.56 mL, 9.12 mmol) was added, and the reaction mixture was stirred at rt for 16 h. The reaction mixture was partitioned between water and EtOAc, the organic layer was washed with 10% LiCl (aq), dried using a hydrophobic frit, and concentrated to a cream solid. This solid was purified by silica chromatography eluting with 0−5% 2 M NH_3 in MeOH/DCM to give *N*-ethyl-4-(methoxymethoxy)-3-(1-methyl-1*H*-1,2,3-triazol-4-yl)-benzamide (**58**, 1.160 g, 4.00 mmol, 66% yield) as a cream solid. LC−MS (formic, ES^+) t_R = 0.69 min; m/z = 291.1; (98% pure).

*N-Ethyl-4-hydroxy-3-(1-methyl-1H-1,2,3-triazol-4-yl)benzamide (**102**).* *N*-Ethyl-4-(methoxymethoxy)-3-(1-methyl-1*H*-1,2,3-triazol-4-yl)benzamide (**58**, 85 mg, 0.293 mmol) and hydrochloric acid (1 mL, 12.00 mmol) were stirred in methanol (10 mL) at rt for 1 h. The reaction was warmed to 50 °C and stirred for 1.5 h. The reaction mixture was neutralized with NaOH and concentrated *in vacuo*. The residue was taken up into water and extracted into DCM, including a brine wash. The organic extracts were combined, dried *via* a hydrophobic frit, and concentrated *in vacuo*, giving *N*-ethyl-4-hydroxy-3-(1-methyl-1*H*-1,2,3-triazol-4-yl)benzamide (**102**, 71 mg, 0.288 mmol, 98% yield) as a white solid. LC−MS (formic, ES^+) t_R = 0.64 min; m/z = 247.1.

*N-Ethyl-3-(1-methyl-1H-1,2,3-triazol-4-yl)-4-(pyridin-2-ylmethoxy)benzamide (**15**).* *N*-Ethyl-4-hydroxy-3-(1-methyl-1*H*-1,2,3-triazol-4-yl)benzamide (**102**, 71 mg, 0.288 mmol), 2-(bromomethyl)pyridine, hydrobromide (80 mg, 0.317 mmol), and potassium carbonate (120 mg, 0.865 mmol) were stirred in acetone (10 mL) at rt for 67 h. The reaction mixture was concentrated *in vacuo*, partitioned between water and DCM, and extracted into DCM, including a brine wash. The organic extracts were combined, dried *via* a hydrophobic frit, and concentrated *in vacuo*. The residue was taken up into DCM and purified by silica chromatography eluting 0−5% MeOH/DCM and the relevant fractions were combined and concentrated *in vacuo* to give *N*-ethyl-3-(1-methyl-1*H*-1,2,3-triazol-4-yl)-4-(pyridin-2-ylmethoxy)benzamide (**15**, 78 mg, 0.231 mmol, 80% yield) as a white solid. LC−MS (formic, ES^+) t_R = 0.63 min; m/z = 338.2; (100% pure) ^{1}H NMR (400 MHz, MeOD-d_4): δ ppm 8.62 (m, J = 2.4 Hz, 2H) 8.38 (s, 1H) 7.88 (td, J = 7.7, 1.7 Hz, 1H) 7.80 (dd, J = 8.8, 2.4 Hz, 1H) 7.56 (d, J = 7.8 Hz, 1H) 7.38−7.44 (m, 1H) 7.21 (d, J = 8.3 Hz, 1H) 5.44 (s, 2H) 4.15 (s, 3H) 3.43 (q, J = 7.3 Hz, 2H) 1.25 (t, J = 7.3 Hz, 3H).

*Methyl 2-Bromo-6-((trimethylsilyl)ethynyl)isonicotinate (**81**).* Methyl 2,6-dibromoisonicotinate (5 g, 16.95 mmol), copper iodide (0.129 g, 0.678 mmol), diisopropylamine (14.50 mL, 102 mmol), and tetrakis (0.392 g, 0.339 mmol) in THF (35 mL) were stirred in a three-necked flask at rt and vacuum-degassed with N_2. Ethynyltrimethylsilane (2.156 mL, 15.26 mmol) was then added *via* syringe and stirring continued under nitrogen for 1 h. The reaction mixture was quenched with 2 M HCl and partitioned between EtOAc (75 mL) and water (75 mL). The organic layer was washed with water (50 mL) and brine (50 mL) and passed through a hydrophobic frit, and the solvent was removed *in vacuo*. The resulting oily solid was dissolved in DCM and loaded onto a 340 g Biotage SNAP silica column which was left to dry overnight. The product was eluted with a gradient of 0−20% cyclohexane/EtOAc, the product-containing fractions were combined, and the solvent was removed *in vacuo*. The product was left to dry *in vacuo* for 1 h to give methyl 2-bromo-6-((trimethylsilyl)ethynyl)isonicotinate (**81**, 3.5466 g, 5.68 mmol, 34% yield) as an orange oil. LC−MS (formic, ES^+) t_R = 1.47 min; m/z = 314.0; ^{1}H NMR (400 MHz, $CDCl_3$-*d*): δ 7.94 (d, J = 1.5 Hz, 1H) 7.91 (d, J = 1.5 Hz, 1H) 3.95 (s, 3H) 0.26 (s, 9H).

*Methyl 2-Bromo-6-(1-methyl-1H-1,2,3-triazol-4-yl)isonicotinate (**70**).* General procedure A was followed using the following amounts: pyridine (2.297 mL, 28.4 mmol), methyl 2-bromo-6-((trimethylsilyl)-ethynyl)isonicotinate (**81**, 3.5466 g, 5.68 mmol), sodium azide (0.812 g, 12.49 mmol), vitamin C (0.400 g, 2.272 mmol), methyl iodide (1.065 mL, 17.04 mmol), potassium carbonate (1.413 g, 10.22 mmol), and copper(II) sulphate pentahydrate (0.284 g, 1.136 mmol) in methanol (6 mL), THF (6 mL), and water (6 mL). This gave methyl 2-bromo-6-(1-methyl-1*H*-1,2,3-triazol-4-yl)isonicotinate (**70**, 615 mg, 1.656 mmol, 29% yield) as a pale yellow solid. LC−MS (formic, ES^+) t_R = 0.93 min; m/z = 299.0; ^{1}H NMR (400 MHz, $CDCl_3$-*d*): δ 8.67 (d, J = 1.5 Hz, 1H) 8.21 (s, 1H) 7.97 (d, J = 1.5 Hz, 1H) 4.20 (s, 3H) 4.00 (s, 3H).

*Methyl 2-Benzyl-6-(1-methyl-1H-1,2,3-triazol-4-yl)isonicotinate (**74**).* General procedure A was followed using the following amounts: iodomethane (1.015 mL, 16.23 mmol), potassium carbonate (1.346 g, 9.74 mmol), sodium azide (0.774 g, 11.90 mmol), methyl 2-benzyl-6-((trimethylsilyl)ethynyl)isonicotinate (**132**, 1.75 g, 5.41 mmol), L-ascorbic acid (0.381 g, 2.164 mmol), copper(II) sulfate pentahydrate (0.270 g, 1.082 mmol), and pyridine (2.188 mL, 27.1 mmol) in water (20 mL), methanol (20 mL), and THF (10 mL). This gave methyl 2-benzyl-6-(1-methyl-1*H*-1,2,3-triazol-4-yl)isonicotinate (**74**, 958 mg, 2.80 mmol, 52% yield) as a pale brown solid. LC−MS (TFA, ES^+) t_R = 1.01 min; m/z = 309.2; ^{1}H NMR (400 MHz, DMSO-d_6): δ 8.63 (s, 1H) 8.28 (d, J = 1.5 Hz, 1H) 7.64 (d, J = 1.5 Hz, 1H) 7.37−7.29 (m, 4H) 7.22 (tt, J = 6.8, 1.5 Hz, 1H) 4.23 (s, 2H) 4.13 (s, 3H) 3.91 (s, 3H).

*2-Benzyl-6-(1-methyl-1H-1,2,3-triazol-4-yl)isonicotinic Acid (**82**).* Lithium hydroxide (19.57 mg, 0.817 mmol) in water (3 mL) was added to a solution of methyl 2-benzyl-6-(1-methyl-1*H*-1,2,3-triazol-4-yl)isonicotinate (**74**, 420 mg, 0.409 mmol) in THF (3 mL). The reaction mixture was heated to 50 °C under nitrogen for 1 h. The reaction mixture was left to cool, passed through a hydrophobic frit, and THF was removed under reduced pressure. The remaining solution was acidified to pH 2 with 2 M HCl and a precipitate formed. The precipitate was collected by filtration and dried *in vacuo* to give 2-benzyl-6-(1-methyl-1*H*-1,2,3-triazol-4-yl)isonicotinic acid (**82**, 182 mg, 0.402 mmol, 98% yield) as an orange solid. LC−MS (formic, ES^+) t_R = 0.91 min; m/z 295.2; ^{1}H NMR (400 MHz, $CDCl_3$-*d*): δ ppm 8.66 (s, 1H) 8.20 (br d, J = 7.8 Hz, 1H) 7.66−7.75 (m, 1H) 7.17−7.35 (m, 5H) 4.23−4.29 (m, 2H) 4.18−4.22 (m, 3H).

*2-Benzyl-N-cyclopropyl-6-(1-methyl-1H-1,2,3-triazol-4-yl)-isonicotinamide (**16**).* DIPEA (0.031 mL, 0.177 mmol) was added to a solution of 2-benzyl-6-(1-methyl-1*H*-1,2,3-triazol-4-yl)isonicotinic acid (**82**, 40 mg, 0.088 mmol), cyclopropanamine (7.96 μL, 0.115 mmol), and HATU (43.7 mg, 0.115 mmol) in DMF (1 mL). The reaction mixture was stirred at room temperature under nitrogen for 1 h. The reaction mixture was purified by formic MDAP and the product-containing fraction was concentrated. The product was left to dry *in vacuo* for 2 days to give 2-benzyl-*N*-cyclopropyl-6-(1-methyl-1*H*-1,2,3-triazol-4-yl)isonicotinamide (**16**, 19.5 mg, 0.058 mmol, 66% yield) as a pale yellow solid. LC−MS (formic, ES^+) t_R = 0.92 min; m/z = 334.2; (100% pure) ^{1}H NMR (400 MHz, $CDCl_3$-*d*): δ ppm 8.42 (s, 1H) 8.23 (d, J = 1.0 Hz, 1H) 7.74 (s, 1H) 7.28−7.42 (m, 5H) 6.75 (br s, 1H) 4.33 (s, 2H) 4.21 (s, 3H) 2.93−3.01 (m, 1H) 0.86−0.96 (m, 2H) 0.69−0.78 (m, 2H).

*(S)-Methyl 3-Bromo-4-(1-phenylethoxy)benzoate (**103**).* Tri-*N*-butylphosphine (1.410 mL, 5.71 mmol), (*R*)-1-phenylethanol (0.690

https://dx.doi.org/10.1021/acs.jmedchem.0c02156
J. Med. Chem. 2021, 64, 3249−3281

mL, 5.71 mmol), and methyl 3-bromo-4-hydroxybenzoate (1.1 g, 4.76 mmol) were stirred in toluene (30 mL) under nitrogen. (*E*)-Diazene-1,2-diylbis(piperidin-1-ylmethanone) (1.442 g, 5.71 mmol) was added over 10 min, and the reaction mixture was stirred at rt for 17 h. The solvent was removed *in vacuo*, and the compound was dissolved in DCM and purified by silica chromatography eluting with 0−50% EtOAc/cyclohexane. The product-containing fractions were concentrated *in vacuo* to give (*S*)-methyl 3-bromo-4-(1-phenylethoxy)benzoate (**103**, 1.8 g, 5.37 mmol, 113% yield). LC−MS (formic, ES^+) t_R = 1.43 min; *m*/*z* = not seen; ^{1}H NMR (400 MHz, $CDCl_3$-*d*): δ ppm 8.24 (d, *J* = 2.0 Hz, 1H), 7.81 (dd, *J* = 8.6, 2.2 Hz, 1H), 7.27−7.42 (m, 5H), 6.77 (d, *J* = 8.3 Hz, 1H), 5.46 (q, *J* = 6.4 Hz, 1H), 3.87 (s, 3H), 1.74 (d, *J* = 6.4 Hz, 3H).

*(S)-Methyl 4-(1-Phenylethoxy)-3-((trimethylsilyl)ethynyl)-benzoate (**104**).* (*S*)-Methyl 3-bromo-4-(1-phenylethoxy)benzoate (**103**, 3 g, 8.95 mmol) was taken up into triethylamine (60 mL, 430 mmol), and the solution was degassed with nitrogen for 30 min. Copper(I) iodide (0.170 g, 0.895 mmol), trimethylsilylacetylene (16.33 mL, 116 mmol), and $Pd(PPh_3)_4$ (1.034 g, 0.895 mmol) were added, and the solution was stirred at 90 °C for 4 h. The reaction mixture was filtered through celite and the filtrate was concentrated *in vacuo*. The residue was partitioned between water and DCM (100 mL each). The organic layer was eluted through a hydrophobic frit and concentrated *in vacuo*. The resulting solid was purified by silica chromatography eluting with 0−20% EtOAc/cyclohexane to give (*S*)-methyl 4-(1-phenylethoxy)-3-((trimethylsilyl)ethynyl)benzoate (**104**, 3.75 g, 10.64 mmol, 119% yield). LC−MS (formic, ES^+) t_R = 1.61 min; *m*/*z* = 353; ^{1}H NMR (400 MHz, $CDCl_3$-*d*): δ ppm 8.12 (d, *J* = 2.4 Hz, 1H), 7.81−7.87 (m, 1H), 7.26−7.46 (m, 5H), 6.78 (d, *J* = 8.8 Hz, 1H), 5.48 (q, *J* = 6.4 Hz, 1H), 3.87 (s, 3H), 1.71 (d, *J* = 6.8 Hz, 3H), 0.25−0.33 (m, 9H).

*(S)-Methyl 3-Ethynyl-4-(1-phenylethoxy)benzoate (**105**).* (*S*)-Methyl 4-(1-phenylethoxy)-3-((trimethylsilyl)ethynyl)benzoate (**104**, 3.17 g, 8.99 mmol) was taken up into methanol (50 mL), and potassium carbonate (3.73 g, 27.0 mmol) was added. The reaction was stirred at room temperature for 1 h and then diluted with water (100 mL). The reaction mixture was extracted with DCM (3 × 50 mL). The combined organic phases were washed with 2 M aqueous HCl and then eluted through a hydrophobic frit and concentrated *in vacuo*. The resulting solid was purified by silica chromatography eluting with 0−30% EtOAc/cyclohexane. The product-containing fractions were concentrated *in vacuo* to give (*S*)-methyl 3-ethynyl-4-(1-phenylethoxy)benzoate (**105**, 1.76 g, 6.28 mmol, 70% yield). LC−MS (formic, ES^+) t_R = 1.30 min; *m*/*z* = 281; ^{1}H NMR (400 MHz, $CDCl_3$-*d*): δ ppm 8.15 (d, *J* = 2.0 Hz, 1H), 7.84 (dd, *J* = 8.8, 2.0 Hz, 1H), 7.26−7.48 (m, 5H), 6.77 (d, *J* = 8.8 Hz, 1H), 5.47 (q, *J* = 6.4 Hz, 1H), 3.87 (s, 3H), 1.73 (d, *J* = 6.4 Hz, 3H).

*(S)-Methyl 3-(1-Methyl-1H-1,2,3-triazol-4-yl)-4-(1-phenylethoxy)benzoate (**106**).* (*S*)-Methyl 3-ethynyl-4-(1-phenylethoxy)benzoate (**105**, 130 mg, 0.464 mmol), sodium azide (121 mg, 1.855 mmol), copper(II) sulfate (14.80 mg, 0.093 mmol), and copper powder (29.4 mg, 0.464 mmol) were dissolved in *tert*-butanol (1 mL) and water (1 mL). Iodomethane (116 μL, 1.855 mmol) was added, and the reaction mixture was heated in the microwave at 125 °C for 2.5 h. The reaction mixture was diluted with water (5 mL) and extracted with EtOAc (5 mL × 2). The organic layers were combined, eluted through a hydrophobic frit, and concentrated *in vacuo*. The resulting residue was purified by silica chromatography eluting with 0−70% EtOAc/cyclohexane. The product-containing fractions were concentrated *in vacuo* to give (*S*)-methyl 3-(1-methyl-1*H*-1,2,3-triazol-4-yl)-4-(1-phenylethoxy)-benzoate (**106**, 90 mg, 0.267 mmol, 58% yield) as a yellow solid. LC−MS (formic, ES^+) t_R = 1.14 min; *m*/*z* = 338.

*(S)-N-Ethyl-3-(1-methyl-1H-1,2,3-triazol-4-yl)-4-(1-phenylethoxy)benzamide (**17**).* (*S*)-Methyl 3-(1-methyl-1*H*-1,2,3-triazol-4-yl)-4-(1-phenylethoxy)benzoate (**106**, 40 mg, 0.119 mmol), DIBAL-Me_3 (24.31 mg, 0.095 mmol), and ethanamine (0.059 mL, 0.119 mmol) were dissolved in THF (2 mL) and heated in a microwave at 130 °C for 20 min. The reaction mixture was quenched with 1 M aqueous HCl (1 mL) and extracted into DCM (2 × 5 mL). The organic extracts were combined, eluted through a hydrophobic frit, and concentrated *in vacuo*. The residue was purified by formic MDAP, and the product-containing fractions were concentrated *in vacuo* to give (*S*)-*N*-ethyl-3-(1-methyl-1*H*-1,2,3-triazol-4-yl)-4-(1-phenylethoxy)benzamide (**17**, 35 mg, 0.100 mmol, 84% yield). LC−MS (formic, ES^+) t_R = 0.99 min; *m*/*z* = 351; (97% pure) ^{1}H NMR (400 MHz, MeOD-d_4): δ ppm 8.60 (d, *J* = 2.0 Hz, 1H), 8.38 (s, 1H), 7.61 (dd, *J* = 8.8, 2.4 Hz, 1H), 7.22−7.39 (m, 6H), 6.96 (d, *J* = 8.8 Hz, 1H), 5.64 (q, *J* = 6.4 Hz, 1H), 4.20 (s, 3H), 3.40 (q, *J* = 7.3 Hz, 2H), 1.76 (d, *J* = 6.4 Hz, 3H), 1.22 (t, *J* = 7.3 Hz, 3H).

*N-Ethyl-2-(1-methyl-1H-1,2,3-triazol-4-yl)-6-(1phenylethyl)-isonicotinamide (**18**).* (1-Phenylethyl)zinc(II) bromide 0.5 M in THF (0.514 mL, 0.257 mmol) was added to a sealed microwave vial containing 2-chloro-*N*-ethyl-6-(1-methyl-1*H*-1,2,3-triazol-4-yl)-isonicotinamide (**71**, 70 mg, 0.171 mmol) and $PdCl_2(PPh_3)_2$ (12.02 mg, 0.017 mmol) in THF (3 mL). The reaction mixture was heated to 110 °C for 60 min under microwave conditions after which further $PdCl_2(PPh_3)_2$ (12.02 mg, 0.017 mmol) and (1-phenylethyl)zinc(II) bromide 0.5 M in THF (0.514 mL, 0.257 mmol) were added. Heating continued for 35 min under microwave conditions after which further (1-phenylethyl)zinc(II) bromide 0.5 M in THF (0.514 mL, 0.257 mmol) and $PdCl_2(PPh_3)_2$ (12.02 mg, 0.017 mmol) were added. Heating continued for 30 min under microwave conditions. The reaction mixture was partitioned between ethyl acetate (30 mL) and water (20 mL), and the organic layer was washed with water (2 × 10 mL) and brine (10 mL). The organic layer was passed through a hydrophobic frit, and the solvent was removed *in vacuo*. The resulting solid was dissolved in DCM and purified by silica chromatography eluting with 30−100% ethyl acetate/heptane. The impure product-containing fractions were combined, and the solvent was removed *in vacuo*. The impure product was dissolved in 1:1 DMSO/methanol and purified by formic MDAP. The product-containing fraction was concentrated and left to dry *in vacuo* for 4 h to give *N*-ethyl-2-(1-methyl-1*H*-1,2,3-triazol-4-yl)-6-(1-phenylethyl)isonicotinamide (**18**, 11.7 mg, 0.035 mmol, 20% yield) as a white solid. LC−MS (formic, ES^+) t_R = 1.00 min; *m*/*z* = 336.2; (100% pure) ^{1}H NMR (400 MHz, DMSO-d_6): δ ppm 8.84 (br t, *J* = 5.4 Hz, 1H) 8.61 (s, 1H) 8.23 (d, *J* = 1.5 Hz, 1H) 7.58 (d, *J* = 1.5 Hz, 1H) 7.34−7.41 (m, 2H) 7.25−7.34 (m, 2H) 7.19 (tt, *J* = 6.8, 1.0 Hz, 1H) 4.36 (q, *J* = 7.0 Hz, 1H) 4.14 (s, 3H) 3.22−3.37 (m, 2H) 1.69 (d, *J* = 6.8 Hz, 3H) 1.14 (t, *J* = 7.1 Hz, 3H).

General Procedure B. *N-Ethyl-3-(1-methyl-1H-1,2,3-triazol-4-yl)-4-phenethoxybenzamide (**19**).* *N*-Ethyl-4-hydroxy-3-(1-methyl-1*H*-1,2,3-triazol-4-yl)benzamide (**102**, 210 mg, 0.853 mmol) was divided equally between 3 scintillation vials, to which DMF (2 mL) and (2-bromoethyl)benzene (55.2 mg, 0.298 mmol), (1-bromopropyl)benzene (59.4 mg, 0.298 mmol), and 4-(bromomethyl)tetrahydro-2*H*-pyran (53.4 mg, 0.298 mmol) were added. To each was added potassium carbonate (82 mg, 0.597 mmol), and the reaction mixture was stirred at 50 °C for 2 h. The temperature was increased to 50 °C for 3 h and then lowered to 50 °C, and the reaction mixture was stirred for 17 h. (2-Bromoethyl)-benzene (55.2 mg, 0.298 mmol), (1-bromopropyl)benzene (59.4 mg, 0.298 mmol), and 4-(bromomethyl)tetrahydro-2*H*-pyran (53.4 mg, 0.298 mmol) were added to their respective reaction mixtures and potassium carbonate (82 mg, 0.597 mmol) was added to each, the temperature increased to 50 °C, and the reaction mixture was stirred for 3 h, after which each was diluted with water and extracted into DCM. The organic extracts of each were washed with 10% LiCl, dried *via* a hydrophobic frit, and concentrated *in vacuo*. The residues were taken up into 50% MeOH/DMSO and purified by formic MDAP, and pure fractions were concentrated *in vacuo* to give *N*-ethyl-3-(1-methyl-1*H*-1,2,3-triazol-4-yl)-4-phenethoxybenzamide (**19**, 38 mg, 0.108 mmol, 38% yield). LC−MS (formic, ES^+) t_R = 0.99 min; *m*/*z* = 351.1; (100% pure) ^{1}H NMR (400 MHz, MeOD-d_4): δ ppm 8.55 (d, *J* = 2.4 Hz, 1H) 8.32 (br s, 1H) 7.82 (dd, *J* = 8.6, 2.2 Hz, 1H) 7.60 (s, 1H) 7.32−7.38 (m, 4H) 7.23−7.30 (m, 1H) 7.20 (d, *J* = 8.8 Hz, 1H) 4.51 (t, *J* = 6.6 Hz, 2H) 4.02 (s, 3H) 3.38−3.48 (m, 2H) 3.22 (t, *J* = 6.4 Hz, 2H) 1.25 (t, *J* = 7.3 Hz, 3H).

https://dx.doi.org/10.1021/acs.jmedchem.0c02156
J. Med. Chem. 2021, 64, 3249−3281

*N-Ethyl-3-(1-methyl-1H-1,2,3-triazol-4-yl)-4-((tetrahydro-2H-pyran-4-yl)methoxy)benzamide (**20**).* General procedure B was followed to give *N*-ethyl-3-(1-methyl-1*H*-1,2,3-triazol-4-yl)-4-((tetrahydro-2*H*-pyran-4-yl)methoxy)benzamide (**20**, 23 mg, 0.067 mmol, 23% yield). LC−MS (formic, ES$^+$) t_R = 0.77 min; m/z = 345.2; (100% pure) ^{1}H NMR (400 MHz, MeOD-d_4): δ ppm 8.57 (d, J = 2.4 Hz, 1H) 8.26−8.46 (m, 1H) 8.23 (s, 1H) 7.84 (dd, J = 8.8, 2.4 Hz, 1H) 7.20 (d, J = 8.8 Hz, 1H) 4.19 (s, 3H) 4.10 (d, J = 6.4 Hz, 2H) 4.01 (dd, J = 11.0, 3.2 Hz, 2H) 3.40−3.57 (m, 4H) 2.18−2.33 (m, 1H) 1.74−1.85 (m, 2H) 1.44−1.58 (m, 2H) 1.26 (t, J = 7.3 Hz, 3H).

*Methyl 4-Hydroxy-3-(1-methyl-1H-1,2,3-triazol-4-yl)benzoate, Hydrochloride (**65**).* Methyl 4-(methoxymethoxy)-3-(1-methyl-1*H*-1,2,3-triazol-4-yl)benzoate (**57**, 15.7 g, 56.6 mmol) was dissolved in DCM (10 mL) and 4 N HCl in 1,4-dioxane (70.8 mL, 283 mmol) was added. The mixture was stirred at room temperature over the weekend. The solvent was then evaporated *in vacuo*, and the residue was triturated with ether (100 mL). The solid was collected by filtration to give methyl 4-hydroxy-3-(1-methyl-1*H*-1,2,3-triazol-4-yl)benzoate, hydrochloride (**65**, 11.5 g, 42.6 mmol, 75% yield) as a pale yellow solid. LC−MS (formic, ES$^+$) t_R = 0.60 min; m/z = 234; ^{1}H NMR (400 MHz, DMSO-d_6, 303 K): δ ppm 11.20 (bs, 1H), 8.69 (d, J = 2.4 Hz, 1H), 8.44 (s, 1H), 7.79 (dd, J = 8.8, 2.4 Hz, 1H), 7.12 (d, J = 8.8 Hz, 1H), 4.12 (s, 3H), 3.84 (s, 3H).

*(R)-3-(1-Methyl-1H-1,2,3-triazol-4-yl)-4-(1-phenylethoxy)benzoic Acid (**108**).* NaOH (10 mL, 20.00 mmol) was added to a solution of (*S*)-methyl 3-(1-methyl-1*H*-1,2,3-triazol-4-yl)-4-(1-phenylethoxy)-benzoate (**106**, 1.5 g, 4.45 mmol) in methanol (20 mL) at room temperature and the solution was stirred for 3 h and then evaporated *in vacuo*. The residue was partitioned between water (20 mL) and ether (20 mL). The aqueous layer was acidified with 2 M aqueous HCl to pH 4 and stirred for 10 min. The resulting solid was collected by filtration and dried in a vacuum oven to give (*R*)-3-(1-methyl-1*H*-1,2,3-triazol-4-yl)-4-(1-phenylethoxy)benzoic acid (**108**, 0.75 g, 2.319 mmol, 52% yield) as a colorless solid. LC−MS (high pH, ES$^+$) t_R = 0.69 min; m/z = 324; ^{1}H NMR (400 MHz, DMSO-d_6): δ ppm 12.66 (br s, 1H), 8.75 (d, J = 2.4 Hz, 1H), 8.50 (s, 1H), 7.70 (dd, J = 8.8, 2.4 Hz, 1H), 7.40−7.50 (m, 2H), 7.24−7.38 (m, 3H), 7.07 (d, J = 8.8 Hz, 1H), 5.80 (q, J = 6.4 Hz, 1H), 4.19 (s, 3H), 1.74 (d, J = 6.4 Hz, 3H).

*(R)-N-Ethyl-3-(1-methyl-1H-1,2,3-triazol-4-yl)-4-(1-phenylethoxy)benzamide (**21**).* (*R*)-3-(1-Methyl-1*H*-1,2,3-triazol-4-yl)-4-(1-phenylethoxy)benzoic acid (**108**, 0.233 g, 0.72 mmol) and HATU (0.274 g, 0.72 mmol) were dissolved in DMF (4.2 mL). A total of 0.38 mL (2.16 mmol) of DIPEA was added to the solution and the mixture was left for 5 min. A total of 0.76 mL (0.12 mmol acid, 0.12 mmol HATU, 0.36 mmol DIPEA) of the mixture was added to ethylamine (0.005 g, 0.120 mmol). The reaction mixture was sealed and left stirring at 22 °C for 18 h. The reaction mixture was purified by high pH MDAP, and the product-containing fractions were concentrated under a stream of nitrogen to give (*R*)-*N*-ethyl-3-(1-methyl-1*H*-1,2,3-triazol-4-yl)-4-(1-phenylethoxy)benzamide (**21**, 30.1 mg, 0.086 mmol, 64% yield). LC−MS (formic, ES$^+$) t_R = 0.98 min; m/z = 351; (100% pure) ^{1}H NMR (600 MHz, DMSO-d_6): δ ppm 8.64 (d, J = 2.3 Hz, 1H), 8.49 (s, 1H), 8.38 (br t, J = 5.6 Hz, 1H), 7.62 (dd, J = 8.8, 2.4 Hz, 1H), 7.43 (d, J = 7.5 Hz, 2H), 7.34 (t, J = 7.7 Hz, 2H), 7.14−7.29 (m, 1H), 7.02 (d, J = 8.7 Hz, 1H), 5.76−5.81 (m, 1H), 4.19 (s, 3H), 3.25 (dt, J = 13.5, 6.6 Hz, 2H), 1.73 (d, J = 6.4 Hz, 3H), 1.10 (t, J = 7.2 Hz, 3H).

*N-Ethyl-3-(1-methyl-1H-1,2,3-triazol-4-yl)-4-(pyridin-3-ylmethoxy)benzamide (**22**).* General procedure B was followed to give *N*-ethyl-3-(1-methyl-1*H*-1,2,3-triazol-4-yl)-4-(pyridin-3-ylmethoxy)benzamide (**22**, 46 mg, 0.136 mmol, 48% yield). LC−MS (formic, ES$^+$) t_R = 0.49 min; m/z = 338.1; (100% pure) ^{1}H NMR (400 MHz, MeOD-d_4): δ ppm 8.69 (d, J = 2.0 Hz, 1H) 8.60 (d, J = 2.4 Hz, 1H) 8.55 (dd, J = 4.9, 1.5 Hz, 1H) 8.32−8.41 (m, 1H) 8.16 (s, 1H) 7.98 (dt, J = 7.8, 1.7 Hz, 1H) 7.82 (dd, J = 8.8, 2.4 Hz, 1H) 7.50 (dd, J = 7.8, 4.9 Hz, 1H) 7.27 (d, J = 8.8 Hz, 1H) 5.41 (s, 2H) 4.11 (s, 3H) 3.38−3.48 (m, 2H) 1.25 (t, J = 7.1 Hz, 3H).

*N-Ethyl-3-(1-methyl-1H-1,2,3-triazol-4-yl)-4-(pyridin-4-ylmethoxy)benzamide (**23**).* *N*-Ethyl-4-hydroxy-3-(1-methyl-1*H*-1,2,3-triazol-4-yl)benzamide (**102**, 70 mg, 0.284 mmol), potassium carbonate (118 mg, 0.853 mmol), and 4-(chloromethyl)pyridine, hydrochloride (51.3 mg, 0.313 mmol) were stirred in acetone (10 mL) at 50 °C for 16 h. The reaction mixture was taken up into DMF (5 mL) and 4-(chloromethyl)pyridine, hydrochloride (51.3 mg, 0.313 mmol) and potassium carbonate (118 mg, 0.853 mmol) were added, and the reaction mixture was stirred at 50 °C for 3 h. The reaction mixture was stirred at 50 °C for a further 3 h, after which stirring was stopped and the reaction mixture was left at rt for 72 h. The solvent was removed *in vacuo* and the residue was taken into water and extracted into DCM. The organic extracts were combined and dried *via* a hydrophobic frit and concentrated *in vacuo*. The residue was taken up into 50% DMSO/MeOH (0.9 mL) and purified by formic MDAP, and the relevant fractions were combined and concentrated to give *N*-ethyl-3-(1-methyl-1*H*-1,2,3-triazol-4-yl)-4-(pyridin-4-ylmethoxy)benzamide (**23**, 71 mg, 0.210 mmol, 74% yield). LC−MS (formic, ES$^+$) t_R = 0.45 min; m/z = 338.2; (100% pure) ^{1}H NMR (400 MHz, MeOD-d_4): δ ppm 8.54−8.63 (m, 3H) 8.29 (s, 1H) 8.11 (s, 1H) 7.79 (dd, J = 8.6, 2.2 Hz, 1H) 7.53 (d, J = 6.4 Hz, 2H) 7.16 (d, J = 8.3 Hz, 1H) 5.45 (s, 2H) 4.17 (s, 3H) 3.43 (q, J = 7.0 Hz, 2H) 1.25 (t, J = 7.3 Hz, 3H).

*N-Ethyl-3-(1-methyl-1H-1,2,3-triazol-4-yl)-4-(pyrimidin-2-ylmethoxy)benzamide (**24**).* *N*-Ethyl-4-hydroxy-3-(1-methyl-1*H*-1,2,3-triazol-4-yl)benzamide (**102**, 300 mg, 1.218 mmol) was sonicated and heated to 70 °C and stirred to create a homologous suspension. To a test tube, pyrimidin-2-ylmethanol (40.2 mg, 0.365 mmol) was added followed by tributylphosphine (0.122 mL, 0.487 mmol) and a quarter of the aforementioned suspension (5 mL). The reaction mixture was cooled to 0 °C and ADDP (215 mg, 0.853 mmol) was added to each. The reaction mixture was warmed to 50 °C and stirred for 17 h. The reaction mixture was concentrated *in vacuo*, diluted with water, and extracted into DCM. The organic extracts were combined, dried *via* a hydrophobic frit, and concentrated *in vacuo*. The residue was dissolved in DCM and purified by silica chromatography eluting 0−5% MeOH/DCM. The relevant fractions were combined and concentrated, and the residues were then taken up into 50% DMSO/MeOH (0.9 mL) and purified by formic MDAP and the relevant fractions were combined and concentrated to give *N*-ethyl-3-(1-methyl-1*H*-1,2,3-triazol-4-yl)-4-(pyrimidin-2-ylmethoxy)-benzamide (**24**, 35 mg, 0.103 mmol, 34% yield). LC−MS (formic, ES$^+$) t_R = 0.67 min; m/z = 339.1; (100% pure) ^{1}H NMR (400 MHz, MeOD-d_4): δ ppm 8.84−8.93 (m, 2H) 8.68 (d, J = 2.4 Hz, 1H) 8.36 (br s, 1H) 7.80 (dd, J = 8.6, 2.2 Hz, 1H) 7.47 (t, J = 4.9 Hz, 1H) 7.23 (d, J = 8.8 Hz, 1H) 5.53 (s, 2H) 4.19 (s, 3H) 3.39−3.49 (m, 2H) 1.26 (t, J = 7.3 Hz, 3H).

*N-Ethyl-4-((2-methoxybenzyl)oxy)-3-(1-methyl-1H-1,2,3-triazol-4-yl)benzamide (**25**).* A solution of *N*-ethyl-4-hydroxy-3-(1-methyl-1*H*-1,2,3-triazol-4-yl)benzamide (**102**, 25 mg, 0.102 mmol) was dissolved in DMF (0.5 mL) and added to 1-(chloromethyl)-2-methoxybenzene (24 mg, 0.152 mmol). Potassium carbonate (28.1 mg, 0.203 mmol) was added. A stirrer bar was added and vials were sealed and stood at room temperature for 18 h. More 1-(chloromethyl)-2-methoxybenzene (excess 50 μL) and potassium carbonate (28 mg) were added. The reaction vessels were sealed and reheated in Anton Parr using initial 600W to 70 °C for 15 min. They were reheated again in Anton Parr using initial 600W to 110 °C for 15 min. The sample was injected as is (filtered) and purified by high pH MDAP. The solvent was dried under a stream of nitrogen in the plate blowdown apparatus to give *N*-ethyl-4-((2-methoxybenzyl)oxy)-3-(1-methyl-1*H*-1,2,3-triazol-4-yl)benzamide (**25**, 6 mg, 0.016 mmol, 15% yield). LC−MS (formic, ES$^+$) t_R = 0.97 min; m/z = 367.0; (96% pure) ^{1}H NMR (400 MHz, DMSO-d_6): δ ppm 8.64 (d, J = 2.4 Hz, 1H) 8.44 (br t, J = 5.6 Hz, 1H) 8.23 (s, 1H) 7.78 (dd, J = 8.8, 2.4 Hz, 1H) 7.31−7.41 (m, 2H) 7.24 (d, J = 8.8 Hz, 1H) 7.09 (d, J = 9.3 Hz, 1H) 6.91−6.98 (m, 1H) 5.34 (s, 2H) 4.08 (s, 3H) 3.87 (s, 3H) 3.24−3.29 (m, 2H) 1.08−1.15 (m, 3H).

*N-Ethyl-4-((3-methoxybenzyl)oxy)-3-(1-methyl-1H-1,2,3-triazol-4yl)benzamide (**26**).* General procedure B was followed using silica chromatography eluting with EtOAc to give *N*-ethyl-4-((3-methoxybenzyl)oxy)-3-(1-methyl-1*H*-1,2,3-triazol-4-yl)benzamide

https://dx.doi.org/10.1021/acs.jmedchem.0c02156
J. Med. Chem. 2021, 64, 3249−3281

(**26**, 142 mg, 0.388 mmol, 77% yield) as a colorless oil. LC−MS (formic, ES^+) t_R = 0.95; m/z = 367.1; (100% pure) ^{1}H NMR (400 MHz, MeOD-d_4): δ ppm 8.61 (d, J = 2.4 Hz, 1H) 8.19 (s, 1H) 7.79 (dd, J = 8.8, 2.4 Hz, 1H) 7.32 (t, J = 8.1 Hz, 1H) 7.21 (d, J = 8.3 Hz, 1H) 7.01−7.07 (m, 2H) 6.88−6.95 (m, 1H) 5.30 (s, 2H) 4.81 (s, 3H) 4.11 (s, 3H) 3.43 (q, J = 7.3 Hz, 2H) 1.25 (t, J = 7.1 Hz, 3H).

*N-Ethyl-4-((4-methoxybenzyl)oxy)-3-(1-methyl-1H-1,2,3-triazol-4-yl)benzamide (**27**).* General procedure B was followed using silica chromatography eluting with EtOAc to give *N*-ethyl-4-((4-methoxybenzyl)oxy)-3-(1-methyl-1*H*-1,2,3-triazol-4-yl)benzamide (**27**, 121 mg, 0.330 mmol, 66% yield) as a white solid. LC−MS (formic, ES^+) t_R = 0.94 min; m/z = 367.1; (100% pure) ^{1}H NMR (400 MHz, MeOD-d_4): δ ppm 8.62 (d, J = 2.4 Hz, 1H) 8.10 (s, 1H) 7.77−7.83 (m, 1H) 7.37−7.45 (m, 2H) 7.24 (d, J = 8.8 Hz, 1H) 6.94−7.00 (m, 2H) 5.24 (s, 2H) 4.82 (s, 3H) 4.08 (s, 3H) 3.43 (q, J = 7.3 Hz, 2H) 1.25 (t, J = 7.3 Hz, 3H).

*N-Ethyl-3-(1-methyl-1H-1,2,3-triazol-4-yl)-4-((6-methylpyridin-2-yl)methoxy)benzamide (**28**).* General procedure B was followed to give *N*-ethyl-3-(1-methyl-1*H*-1,2,3-triazol-4-yl)-4-((6-methylpyridin-2-yl)methoxy)benzamide (**28**, 51 mg, 0.145 mmol, 60% yield). LC−MS (formic, ES^+) t_R = 0.58 min; m/z = 352.1; (94% pure) ^{1}H NMR (400 MHz, MeOD-d_4): δ ppm 8.63 (d, J = 2.4 Hz, 1H) 8.41 (s, 1H) 8.33−8.38 (m, 1H) 7.80 (dd, J = 8.8, 2.4 Hz, 1H) 7.75 (t, J = 7.8 Hz, 1H) 7.34 (d, J = 7.8 Hz, 1H) 7.28 (d, J = 7.3 Hz, 1H) 7.20 (d, J = 8.8 Hz, 1H) 5.39 (s, 2H) 4.15 (s, 3H) 3.39−3.48 (m, 2H) 2.60 (s, 3H) 1.25 (t, J = 7.1 Hz, 3H).

*Ethyl 4-Hydroxy-3-(1-methyl-1H-1,2,3-triazol-4-yl)benzoate (**108**).* 4-Hydroxy-3-(1-methyl-1*H*-1,2,3-triazol-4-yl)benzoic acid (**97**, 900 mg, 4.11 mmol), concn sulfuric acid (0.1 mL, 1.876 mmol), and ethanol (10 mL) were stirred at 50 °C for 16 h. The reaction mixture was stirred at 80 °C for 24 h. The reaction mixture was concentrated and dried to give ethyl 4-hydroxy-3-(1-methyl-1*H*-1,2,3-triazol-4-yl)benzoate (**108**, 890 mg, 3.60 mmol, 88% yield) as a cream solid. LC−MS (formic, ES^+) t_R = 0.91 min; m/z = 248.1; ^{1}H NMR (400 MHz, DMSO-d_6): δ ppm 11.06 (br s, 1H) 8.66−8.71 (m, 1H) 8.44 (s, 1H) 7.76−7.83 (m, 1H) 7.06 (d, J = 8.3 Hz, 1H) 4.12 (s, 3H) 3.75 (q, J = 7.0 Hz, 2H) 1.08−1.14 (m, 3H).

*Ethyl 3-(1-Methyl-1H-1,2,3-triazol-4-yl)-4-(1-(pyridin-2-yl)-ethoxy)benzoate (**109**).* General procedure B was followed with heating at 65 °C and using silica chromatography to give ethyl 3-(1-methyl-1*H*-1,2,3-triazol-4-yl)-4-(1-(pyridin-2-yl)ethoxy)benzoate (**109**, 1.36 g, 3.86 mmol, 81% yield). LC−MS (formic, ES^+) t_R = 0.95 min; m/z = 353.1.

*3-(1-Methyl-1H-1,2,3-triazol-4-yl)-4-(1-(pyridin-2-yl)ethoxy)-benzoic Acid (**110**).* Ethyl 3-(1-methyl-1*H*-1,2,3-triazol-4-yl)-4-(1-(pyridin-2-yl)ethoxy)benzoate (**109**, 1.36 g, 3.86 mmol) was stirred with LiOH (370 mg, 15.44 mmol) in THF (20 mL) and water (20 mL) at 50 °C for 16 h. Approximately, half the solvent was removed *in vacuo* and the mixture was acidified with 2 M HCl to pH 6, giving a white precipitate. This was isolated by filtration to give 3-(1-methyl-1*H*-1,2,3-triazol-4-yl)-4-(1-(pyridin-2-yl)ethoxy)benzoic acid (**110**, 1.07 g, 3.30 mmol, 85% yield) as a white solid. LC−MS (formic, ES^+) t_R = 0.71 min; m/z = 325.1; ^{1}H NMR (400 MHz, DMSO-d_6): δ ppm 12.69 (br s, 1H) 8.76 (d, J = 2.4 Hz, 1H) 8.57−8.62 (m, 1H) 8.55 (s, 1H) 7.71−7.82 (m, 2H) 7.36−7.44 (m, 1H) 7.25−7.36 (m, 1H) 7.03 (d, J = 9.3 Hz, 1H) 5.76 (q, J = 6.4 Hz, 1H) 4.17 (s, 3H) 1.76 (d, J = 6.4 Hz, 3H).

*Rel-(R)-Methyl 3-(1-methyl-1H-1,2,3-triazol-4-yl)-4-(1-(pyridin-2-yl)ethoxy)benzoate (**59**).* 3-(1-Methyl-1*H*-1,2,3-triazol-4-yl)-4-(1-(pyridin-2-yl)ethoxy)benzoic acid (**110**, 1.13 g, 3.48 mmol) was stirred in methanol (20 mL) and hydrochloric acid (0.106 mL, 3.48 mmol) at 100 °C for 2 h. Hydrochloric acid (0.212 mL, 6.97 mmol) was added, and the reaction mixture was stirred at 100 °C for 16 h. The reaction mixture was stirred at 100 °C for a further 24 h. Hydrochloric acid (1 mL) was added, and the reaction mixture was stirred at 100 °C for 24 h. Hydrochloric acid (1 mL) was added, and the reaction mixture was stirred at 100 °C for 24 h. The reaction mixture was concentrated *in vacuo*, partitioned between water and EtOAc, and extracted into EtOAc. The organic extracts were combined, dried *via* a hydrophobic frit, and concentrated *in vacuo*. The residue was taken into MeOH and passed through an Isolute NH_2 ion-exchange column. The eluent was concentrated *in vacuo*, and the residue was stirred in DCM, sonicated, and heated to reach complete dissolution. This was then purified by silica chromatography eluting with 0−5% MeOH/DCM. The relevant fractions were combined and concentrated to give *rac*-methyl 3-(1-methyl-1*H*-1,2,3-triazol-4-yl)-4-(1-(pyridin-2-yl)ethoxy)benzoate (900 mg, 2.66 mmol, 76% yield) as a white solid. The racemic mixture was dissolved in EtOH (9 mL) and injected onto the column (column: 30 mm × 25 cm Chiralpak AD-H, 5 μm), eluting with 25% EtOH/heptane, flow rate = 30 mL/min, detection wavelength 215.4 nm. The pure fractions from peak 1 were combined and concentrated *in vacuo* to give rel-(*R*)-methyl 3-(1-methyl-1*H*-1,2,3-triazol-4-yl)-4-(1-(pyridin-2-yl)ethoxy)-benzoate (**59**, 377 mg, 1.114 mmol, 32% yield). LC−MS (formic, ES^+) t_R = 0.86 min; m/z = 339.1; ^{1}H NMR (400 MHz, DMSO-d_6): δ ppm 8.78 (d, J = 2.4 Hz, 1H) 8.59−8.63 (m, 1H) 8.57 (s, 1H) 7.73−7.82 (m, 2H) 7.41 (d, J = 7.8 Hz, 1H) 7.32 (ddd, J = 7.5, 4.8, 1.0 Hz, 1H) 7.07 (d, J = 8.8 Hz, 1H) 5.79 (q, J = 6.4 Hz, 1H) 4.17 (s, 3H) 3.83 (s, 3H) 1.77 (d, J = 6.4 Hz, 3H).

*Rel-(R)-3-(1-Methyl-1H-1,2,3-triazol-4-yl)-4-(1-(pyridin-2-yl)-ethoxy)benzoic Acid (**66**).* LiOH (110 mg, 4.59 mmol) and rel-(*R*)-methyl 3-(1-methyl-1*H*-1,2,3-triazol-4-yl)-4-(1-(pyridin-2-yl)ethoxy)-benzoate (**59**, 377 mg, 1.114 mmol) were stirred in THF (5 mL) and water (5 mL) at 50 °C for 16 h. The reaction mixture was concentrated to about half volume *in vacuo* and 2 M HCl was added dropwise until a white precipitate formed. The suspension was then filtered through a sinter funnel; however, this did not successfully isolate the precipitate. The sinter funnel was washed with ethyl acetate, and the suspension was extracted with EtOAc (2 × 10 mL). The organics were combined, dried *via* a hydrophobic frit, and concentrated *in vacuo* to give a clear glassy residue. LC−MS of the aqueous phase suggested that the product remained and so 2 M HCl was added until the addition of a drop caused resolvation of the product (due to zwitterionic nature of product). A drop of 2 M NaOH was then added and the pH was tested as pH 2. The aqueous fraction was extracted again with EtOAc (2 × 10 mL), and the organics were combined, dried *via* a hydrophobic frit, combined with the previous residue, and concentrated *in vacuo* to give rel-(*R*)-3-(1-methyl-1*H*-1,2,3-triazol-4-yl)-4-(1-(pyridin-2-yl)ethoxy)benzoic acid (**66**, 254 mg, 0.783 mmol, 70% yield) as a white solid. LC−MS (formic, ES^+) t_R = 0.69 min; m/z = 325.1; ^{1}H NMR (400 MHz, DMSO-d_6): δ ppm 12.63 (br s, 1H) 8.76 (d, J = 2.4 Hz, 1H) 8.59−8.63 (m, 1H) 8.55 (s, 1H) 7.70−7.82 (m, 2H) 7.38−7.43 (m, 1H) 7.28−7.36 (m, 1H) 7.03 (d, J = 8.8 Hz, 1H) 5.77 (q, J = 6.4 Hz, 1H) 4.17 (s, 3H) 1.77 (d, J = 6.4 Hz, 3H).

General Procedure C. In four vials, HATU (164 mg, 0.431 mmol) was weighed in each. (*S*)-3-(1-Methyl-1*H*-1,2,3-triazol-4-yl)-4-(1-(pyridin-2-yl)ethoxy)benzoic acid (254 mg, 0.783 mmol) was dissolved in DMF (6 mL) and dispensed in portions (1.5 mL) to each vial. To each vial was added DIPEA (0.075 mL, 0.431 mmol), and the reaction mixtures were stirred for 15 min at rt. Amine (0.230 mmol) was then added. The reaction mixtures were stirred for 64 h. The reaction mixtures were diluted with water (5 mL) and saturated sodium bicarbonate solution (3 mL) and extracted into DCM (2 × 10 mL). The organics were washed with an equal volume of 10% LiCl aqueous solution, dried *via* a hydrophobic frit, and concentrated *in vacuo*. The residues were dissolved in 50% MeOH/DMSO (0.9 mL) and purified by MDAP (formic acid method), and the relevant fractions were combined to give the product.

*(S)-N-Ethyl-3-(1-methyl-1H-1,2,3-triazol-4-yl)-4-(1-(pyridin-2-yl)-ethoxy)benzamide (**29**).* General procedure C was followed to give (*S*)-*N*-ethyl-3-(1-methyl-1*H*-1,2,3-triazol-4-yl)-4-(1-(pyridin-2-yl)-ethoxy)benzamide (**29**, 50 mg, 0.142 mmol, 73% yield). LC−MS (formic, ES^+) t_R = 0.69 min; m/z = 352.1; (100% pure) ^{1}H NMR (400 MHz, MeOD-d_4): δ ppm 8.54−8.65 (m, 2H) 8.49 (s, 1H) 7.80 (td, J = 7.7, 1.7 Hz, 1H) 7.64 (dd, J = 8.8, 2.4 Hz, 1H) 7.45 (d, J = 7.8 Hz, 1H) 7.35 (ddd, J = 7.5, 5.0, 1.2 Hz, 1H) 6.94 (d, J = 8.8 Hz, 1H) 5.69 (q, J = 6.5 Hz, 1H) 4.22 (s, 3H) 3.40 (q, J = 7.3 Hz, 2H) 1.82 (d, J = 6.4 Hz, 3H) 1.22 (t, J = 7.3 Hz, 3H).

https://dx.doi.org/10.1021/acs.jmedchem.0c02156
J. Med. Chem. 2021, 64, 3249−3281

*tert-Butyl 2-Chloro-6-(1-methyl-1H-1,2,3-triazol-4-yl)-isonicotinate (**69**).* General procedure A was followed, purified by silica chromatography eluting with 0−70% EtOAc/cyclohexane, to give *tert*-butyl 2-chloro-6-(1-methyl-1*H*-1,2,3-triazol-4-yl)-isonicotinate (**69**, 1.8046 g, 6.12 mmol, 89% yield) as a pale orange solid. LC−MS (formic, ES^+) t_R = 1.18 min; m/z = 295.1; ^{1}H NMR (400 MHz, $CDCl_3$-*d*): δ ppm 8.55 (d, J = 1.5 Hz, 1H) 8.20 (s, 1H) 7.75−7.79 (m, 1H) 4.19 (s, 3H) 1.64 (s, 9H).

General Procedure D. 2-Chloro-*N*-ethyl-6-(1-methyl-1*H*-1,2,3-triazol-4-yl)isonicotinamide (**71**, 60 mg, 0.226 mmol) and $PdCl_2(PPh_3)_2$ (16 mg, 0.023 mmol) were dissolved in THF (2 mL) in a microwave vial. The vial was sealed and Negishi reagent (0.5 M in THF) (0.677 mL, 0.339 mmol) was added. The vial was heated to 110 °C for 1 h. The reaction mixture was blown down under a stream of nitrogen and the resulting solid was dissolved in 1:1 DMSO/methanol and purified by formic MDAP. The product-containing fractions were concentrated *in vacuo*, and the product was left to dry under a stream of nitrogen overnight to give the required products listed below.

*N-Ethyl-2-(2-methoxybenzyl)-6-(1-methyl-1H-1,2,3-triazol-4-yl)-isonicotinamide (**30**).* General procedure D was followed including an additional purification by silica chromatography eluting with 30−100% EtOAc/cyclohexane to give *N*-ethyl-2-(2-methoxybenzyl)-6-(1-methyl-1*H*-1,2,3-triazol-4-yl)isonicotinamide (**30**, 11.5 mg, 0.033 mmol, 14% yield). LC−MS (formic, ES^+) t_R = 0.92 min; m/z = 352.2; (100% pure) ^{1}H NMR (400 MHz, $CDCl_3$-*d*): δ ppm 8.16 (s, 1H) 8.13 (d, J = 2.0 Hz, 1H) 7.51 (d, J = 1.5 Hz, 1H) 7.24 (dt, J = 7.3, 1.5 Hz, 1H) 7.19 (dd, J = 8.1, 1.7 Hz, 1H) 6.87−6.93 (m, 2H) 6.30 (br s, 1H) 4.22 (s, 2H) 4.18 (s, 3H) 3.82 (s, 3H) 3.45−3.54 (m, 2H) 1.26 (t, J = 7.3 Hz, 3H).

*N-Ethyl-2-(3-methoxybenzyl)-6-(1-methyl-1H-1,2,3-triazol-4-yl)-isonicotinamide (**31**).* General procedure D was followed using the following amounts: 0.5 M (3-methoxybenzyl)zinc(II) chloride in THF (4.35 mL, 2.175 mmol), 2-chloro-*N*-ethyl-6-(1-methyl-1*H*-1,2,3-triazol-4-yl)isonicotinamide (**71**, 289 mg, 1.088 mmol) and $PdCl_2(PPh_3)_2$ (153 mg, 0.218 mmol) in THF (7 mL), and was purified by silica chromatography using a gradient of 33−100% ethyl acetate/cyclohexane. The product-containing fractions were combined, and the solvent was removed *in vacuo*. The product was left to dry *in vacuo* for 1 h to give *N*-ethyl-2-(3-methoxybenzyl)-6-(1-methyl-1*H*-1,2,3-triazol-4-yl)isonicotinamide (**31**, 171 mg, 0.487 mmol, 45% yield) as a pale brown solid. LC−MS (formic, ES^+) t_R = 0.90 min; m/z = 352; (100% pure) ^{1}H NMR (400 MHz, $CDCl_3$-*d*): δ ppm 8.18 (s, 1H), 8.17 (d, J = 1.5 Hz, 1H), 7.56 (d, J = 1.5 Hz, 1H), 7.21−7.26 (m, 1H), 6.88−6.92 (m, 1H), 6.85−6.87 (m, 1H), 6.77−6.81 (m, 1H), 6.25−6.33 (m, 1H), 4.18−4.21 (m, 5H), 3.80 (s, 3H), 3.47−3.56 (m, 3H), 1.28 (t, J = 7.3 Hz, 3H).

*N-Ethyl-2-(4-methoxybenzyl)-6-(1-methyl-1H-1,2,3-triazol-4-yl)-isonicotinamide (**32**).* General procedure D was followed including an additional purification by silica chromatography eluting with 30−100% EtOAc/cyclohexane to give *N*-ethyl-2-(4-methoxybenzyl)-6-(1-methyl-1*H*-1,2,3-triazol-4-yl)isonicotinamide (**32**, 15.7 mg, 0.045 mmol, 19% yield). LC−MS (formic, ES^+) t_R = 0.90 min; m/z = 352.2; (100% pure) ^{1}H NMR (400 MHz, $CDCl_3$-*d*): δ ppm 8.17 (s, 1H) 8.14 (d, J = 1.5 Hz, 1H) 7.52 (d, J = 1.5 Hz, 1H) 7.21 (qt, J = 8.3, 1.5 Hz, 2H) 6.85 (qt, J = 8.8, 2.9 Hz, 2H) 6.32 (br s, 1H) 4.19 (s, 3H) 4.15 (s, 2H) 3.79 (s, 3H) 3.45−3.55 (m, 2H) 1.26 (t, J = 7.1 Hz, 3H).

*N-Ethyl-2-(2-fluorobenzyl)-6-(1-methyl-1H-1,2,3-triazol-4-yl)-isonicotinamide (**33**).* General procedure D was followed to give *N*-ethyl-2-(2-fluorobenzyl)-6-(1-methyl-1*H*-1,2,3-triazol-4-yl)-isonicotinamide (**33**, 21 mg, 0.062 mmol, 26% yield). LC−MS (formic, ES^+) t_R = 0.92 min; m/z = 340.2; (100% pure) ^{1}H NMR (400 MHz, $CDCl_3$-*d*): δ ppm 8.12−8.21 (m, 2H) 7.55 (d, J = 1.5 Hz, 1H) 7.20−7.26 (m, 2H) 7.02−7.12 (m, 2H) 6.35 (br s, 2H) 4.25 (s, 2H) 4.18 (s, 3H) 3.46−3.55 (m, 2H) 1.27 (obs. t, J = 7.3 Hz, 3H).

*N-Ethyl-2-(3-fluorobenzyl)-6-(1-methyl-1H-1,2,3-triazol-4-yl)-isonicotinamide (**34**).* General procedure D was followed to give *N*-ethyl-2-(3-fluorobenzyl)-6-(1-methyl-1*H*-1,2,3-triazol-4-yl)-isonicotinamide (**34**, 35 mg, 0.103 mmol, 44% yield). LC−MS (formic, ES^+) t_R = 0.94 min; m/z = 340.2; (100% pure) ^{1}H NMR (400 MHz, $CDCl_3$-*d*): δ ppm 8.15−8.19 (m, 2H) 7.56 (d, J = 1.5 Hz, 1H) 7.22−7.30 (m, 1H) 7.07 (d, J = 7.3 Hz, 1H) 7.01 (dt, J = 10.0, 1.8 Hz, 1H) 6.92 (td, J = 8.4, 2.7 Hz, 1H) 6.35 (br s, 1H) 4.13−4.23 (m, 5H) 3.51 (qd, J = 7.3, 5.6 Hz, 2H) 1.27 (obs. t, J = 7.3 Hz, 3H).

*N-Ethyl-2-(4-fluorobenzyl)-6-(1-methyl-1H-1,2,3-triazol-4-yl)-isonicotinamide (**35**).* General procedure D was followed to give *N*-ethyl-2-(4-fluorobenzyl)-6-(1-methyl-1*H*-1,2,3-triazol-4-yl)-isonicotinamide (**35**, 46.9 mg, 0.138 mmol, 55% yield). LC−MS (formic, ES^+) t_R = 0.93 min; m/z = 340.2; (85% pure) ^{1}H NMR (400 MHz, $CDCl_3$-*d*): δ ppm 8.13−8.19 (m, 2H) 7.54 (d, J = 1.5 Hz, 1H) 7.22−7.30 (m, 4H) 6.94−7.03 (m, 2H) 6.36 (br s, 1H) 4.14−4.24 (m, 5H) 3.47−3.55 (m, 2H) 1.27 (t, J = 7.3 Hz, 3H).

*Methyl 2-Methyl-6-((trimethylsilyl)ethynyl)isonicotinate (**111**).* A solution of methyl 2-bromo-6-methylisonicotinate (30 g, 130 mmol) and Et_3N (182 mL, 1304 mmol) was degassed with nitrogen for 10 min followed by the addition of $Pd(Ph_3P)_4$ (7.53 g, 6.52 mmol), copper(I) iodide (2.484 g, 3.04 mmol), and ethynyltrimethylsilane (111 mL, 782 mmol) and again degassed with nitrogen for 5 min. The reaction mixture was heated at 90 °C for 3 h and then cooled and filtered. Water (200 mL) was added to the filtrate and it was extracted with ethyl acetate (200 mL × 2). The combined organic layers were dried with Na_2SO_4, filtered, and concentrated *in vacuo* to give methyl 2-methyl-6-((trimethylsilyl)ethynyl)isonicotinate (**111**, 38 g, 82 mmol, 72% yield). LC−MS (formic, ES^+) t_R = 2.00 min; m/z = 248; ^{1}H NMR (400 MHz, $CDCl_3$-*d*): δ ppm 7.82 (s, 1H) 7.64 (obs. s, 1H) 3.94 (s, 3H) 2.62 (s, 3H) 0.25−0.32 (m, 9H).

*Methyl 2-Methyl-6-(1-methyl-1H-1,2,3-triazol-4-yl)isonicotinate (**84**).* Methyl 2-methyl-6-((trimethylsilyl)ethynyl)isonicotinate (**111**, 30 g, 74.5 mmol), ascorbic acid (6.56 g, 37.3 mmol), sodium azide (10.17 g, 156 mmol), copper(II) sulfate (2.379 g, 14.90 mmol), and K_2CO_3 (15.45 g, 112 mmol) were combined in water (50 mL) and methanol (50.0 mL). The reaction mixture was stirred at room temperature. MeI (14.91 mL, 238 mmol) and pyridine (30.1 mL, 373 mmol) were added and the reaction mixture was stirred at room temperature until no starting material remained by TLC (30% EtOAc in pet ether). The reaction mixture was concentrated under reduced pressure to remove the methanol. The mixture was diluted with water (200 mL) and extracted with ethyl acetate (300 mL × 3). The combined organic extracts were dried over Na_2SO_4, filtered, and concentrated under reduced pressure. The residue was triturated with 10% ethyl acetate in pet ether (50 mL), and the resulting solid was dried to give methyl 2-methyl-6-(1-methyl-1*H*-1,2,3-triazol-4-yl)-isonicotinate (**84**, 20 g, 59.6 mmol, 80% yield). LC−MS (formic, ES^+) t_R = 1.97 min; m/z = 233; ^{1}H NMR (400 MHz, DMSO-d_6): δ ppm 8.64 (s, 1H) 8.25 (s, 1H) 7.68 (obs. s, 1H) 4.13 (s, 3H) 3.93 (s, 3H) 2.60 (s, 3H).

*4-(Methoxycarbonyl)-2-methyl-6-(1-methyl-1H-1,2,3-triazol-4-yl)pyridine-1-oxide (**85**).* To a solution of methyl 2-methyl-6-(1-methyl-1*H*-1,2,3-triazol-4-yl)isonicotinate (**84**, 15 g, 44.6 mmol) in DCM (100 mL) was added a solution of 3-chlorobenzoperoxoic acid (15.38 g, 89 mmol). The reaction mixture was stirred at room temperature for 18 h. The reaction mixture was concentrated under reduced pressure to remove the DCM. Water (100 mL) was added to the reaction mixture, and the reaction mixture was neutralized with aq saturated $NaHCO_3$. The mixture was extracted with ethyl acetate (3 × 200 mL). The combined organic extracts were dried over Na_2OSO_4, filtered, and concentrated under reduced pressure. The residue was triturated with diethyl ether (200 mL), and the resulting solid was collected by filtration to give 4-(methoxycarbonyl)-2-methyl-6-(1-methyl-1*H*-1,2,3-triazol-4-yl)pyridine 1-oxide (**85**, 12 g, 43.5 mmol, 98% yield). LC−MS (formic, ES^+) t_R = 1.84 min; m/z = 249; ^{1}H NMR (400 MHz, DMSO-d_6): δ ppm 9.12 (s, 1H) 8.71 (d, J = 2.4 Hz, 1H) 7.98 (d, J = 2.2 Hz, 1H) 4.17 (s, 3H) 3.92 (s, 3H) 3.30 (obs. s, 3H).

*Methyl 2-(Hydroxymethyl)-6-(1-methyl-1H-1,2,3-triazol-4-yl)-isonicotinate (**112**).* A solution of 4-(methoxycarbonyl)-2-methyl-6-(1-methyl-1*H*-1,2,3-triazol-4-yl)pyridine 1-oxide (**85**, 11.5 g, 41.7 mmol) in TFAA (17.67 mL, 125 mmol) was stirred at 50 °C for 12 h. The reaction mixture was quenched slowly with methanol and then

https://dx.doi.org/10.1021/acs.jmedchem.0c02156
J. Med. Chem. 2021, 64, 3249−3281

concentrated under reduced pressure. The crude compound was triturated with diethyl ether (50 mL), and the collected solid was triturated with MeOH (50 mL). The resulting solid was collected by filtration and dried to give methyl 2-(hydroxymethyl)-6-(1-methyl-1*H*-1,2,3-triazol-4-yl)isonicotinate (**112**, 7.4 g, 28.5 mmol, 68% yield). LC−MS (formic, ES$^+$) t_R = 1.36 min; m/z = 249; ^{1}H NMR (400 MHz, DMSO-d_6): δ ppm 8.60 (s, 1H) 8.31 (br s, 1H) 7.88 (br s, 1H) 4.67 (s, 2H) 4.12 (obs. s, 3H) 3.95 (obs. s, 3H).

*Methyl 2-(Chloromethyl)-6-(1-methyl-1H-1,2,3-triazol-4-yl)-isonicotinate (**86**).* Thionyl chloride (2 mL, 27.4 mmol) was added to methyl 2-(hydroxymethyl)-6-(1-methyl-1*H*-1,2,3-triazol-4-yl)-isonicotinate (**112**, 1.5 g, 6.04 mmol), and the reaction mixture was heated to 90 °C under nitrogen for 25 min and then cooled to room temperature. Ice (20 g) and sodium acetate (6 g) were added, and the aqueous layer was extracted with ethyl acetate (3 × 30 mL). The organic layer was filtered, and the filtrate was passed through a hydrophobic frit and then concentrated *in vacuo*. The resulting solid was purified by silica chromatography using a gradient of 20−80% ethyl acetate/cyclohexane. The product-containing fractions were combined, and the solvent was removed *in vacuo* to give methyl 2-(chloromethyl)-6-(1-methyl-1*H*-1,2,3-triazol-4-yl)isonicotinate (**86**, 1.051 g, 3.94 mmol, 65.2% yield) as a pale yellow solid. LC−MS (formic, ES$^+$) t_R = 0.86 min; m/z = 267; ^{1}H NMR (400 MHz, $CDCl_3$-d): δ ppm 8.65 (d, J = 1.5 Hz, 1H), 8.19 (s, 1H), 7.97 (d, J = 1.0 Hz, 1H), 4.74 (s, 2H), 4.13−4.27 (m, 3H), 3.98−4.04 (m, 3H).

*Methyl 2-((1H-Indol-4-yl)methyl)-6-(1-methyl-1H-1,2,3-triazol-4-yl)isonicotinate (**87**).* (1*H*-Indol-4-yl)boronic acid (543 mg, 3.37 mmol) was added to a solution of methyl 2-(chloromethyl)-6-(1-methyl-1*H*-1,2,3-triazol-4-yl)isonicotinate (**86**, 750 mg, 2.81 mmol), XPhos Pd G1 (104 mg, 0.141 mmol), and K_2CO_3 (800 mg, 5.79 mmol) in ethanol (2.222 mL) and toluene (20 mL). The reaction mixture was stirred at 90 °C for 1.5 h and then an additional 1 equiv. of XPhos PdG1 was added to the reaction mixture. The reaction mixture was stirred for a further 20 h and then cooled to room temperature. The reaction flask was degassed with nitrogen and an additional equivalent of XPhos Pd G1 was added. The reaction mixture was stirred for 2 h and Xphos (104 mg) was added. The reaction mixture was stirred for 1 h at 90 °C and then cooled to room temperature. The reaction mixture was partitioned between EtOAc (25 mL) and water (30 mL). The organic layer was washed (1× water 20 mL, 2× sat. aq $NaHCO_3$ 20 mL), passed through a hydrophobic frit, and concentrated *in vacuo*. The resulting solid was purified by column chromatography using a gradient of 50−100% EtOAc/cyclohexane. The product-containing fractions were combined, and the solvent was removed *in vacuo*. The sample was then dried under a stream of nitrogen for 1 h to give methyl 2-((1*H*-indol-4-yl)methyl)-6-(1-methyl-1*H*-1,2,3-triazol-4-yl)isonicotinate (**87**, 190 mg, 0.273 mmol, 10% yield) as a white/brown solid. LC−MS (formic, ES$^+$) t_R = 0.99 min; m/z = 348; ^{1}H NMR (400 MHz, DMSO-d_6): δ ppm 11.09 (br s, 1H), 8.67 (s, 1H), 8.17−8.35 (m, 2H), 7.48−7.60 (m, 1H), 7.20−7.41 (m, 3H), 7.05 (dd, J = 8.1, 7.1 Hz, 2H), 6.84−6.99 (m, 2H), 6.43−6.59 (m, 1H), 4.45 (s, 2H), 4.17 (s, 3H), 3.86 (s, 3H).

*2-((1H-Indol-4-yl)methyl)-6-(1-methyl-1H-1,2,3-triazol-4-yl)-isonicotinic Acid (**113**).* Methyl 2-((1*H*-indol-4-yl)methyl)-6-(1-methyl-1*H*-1,2,3-triazol-4-yl)isonicotinate (**87**, 203 mg, 0.292 mmol) and LiOH (28.0 mg, 1.169 mmol) were dissolved in water (3 mL) and THF (3.00 mL). The reaction mixture was stirred for 1.5 h at 50 °C under nitrogen. The reaction mixture was concentrated *in vacuo* to remove any THF. The aqueous solution remaining was acidified using 2 M HCl and then concentrated *in vacuo*. The resulting solid was purified by reverse-phase chromatography eluting with 5−95% MeCN/0.1% formic acid in water. The product-containing fractions were combined, and the solvent was removed *in vacuo*. The sample was then dried for 14 h under a stream of nitrogen to give 2-((1*H*-indol-4-yl)methyl)-6-(1-methyl-1*H*-1,2,3-triazol-4-yl)-isonicotinic acid (**113**, 62 mg, 0.167 mmol, 57% yield) as a green/gray solid. LC−MS (formic, ES$^+$) t_R = 0.56 min; m/z = 334; ^{1}H NMR (400 MHz, DMSO-d_6): δ ppm 11.10 (br s, 1H), 8.65 (s, 1H), 8.23 (d, J = 1.0 Hz, 1H), 7.52 (d, J = 1.5 Hz, 1H), 7.24−7.35 (m, 2H), 7.05 (t, J = 7.6 Hz, 1H), 6.75−7.00 (m, 2H), 6.45−6.59 (m, 1H), 4.43 (s, 2H), 4.14 (s, 3H).

*2-((1H-Indol-4-yl)methyl)-N-ethyl-6-(1-methyl-1H-1,2,3-triazol-4-yl)isonicotinamide (**36**).* General procedure C was followed using the following amounts: HATU (151 mg, 0.396 mmol), 2-((1*H*-indol-4-yl)methyl)-6-(1-methyl-1*H*-1,2,3-triazol-4-yl)isonicotinic acid (88 mg, 0.264 mmol), 2 M ethanamine in THF (0.172 mL, 0.343 mmol), DIPEA (0.092 mL, 0.528 mmol), and DMF (4 mL). The sample was purified using silica chromatography eluting with 50−80% EtOAc/cyclohexane. The product-containing fractions were combined, and the solvent was removed *in vacuo* to give 2-((1*H*-indol-4-yl)methyl)-*N*-ethyl-6-(1-methyl-1*H*-1,2,3-triazol-4-yl)isonicotinamide (**36**, 41 mg, 0.102 mmol, 39% yield) as a white solid. LC−MS (formic, ES$^+$) t_R = 0.85 min; m/z = 361; (100% pure) ^{1}H NMR (400 MHz, DMSO-d_6): δ ppm 11.08 (br s, 1H), 8.71−8.97 (m, 1H), 8.61 (s, 1H), 8.23 (d, J = 1.5 Hz, 1H), 7.51 (d, J = 1.5 Hz, 1H), 7.17−7.40 (m, 2H), 6.98−7.16 (m, 1H), 6.92 (d, J = 7.8 Hz, 1H), 6.36−6.63 (m, 1H), 4.40 (s, 2H), 4.14 (s, 3H), 3.17−3.28 (m, 2H), 1.05−1.22 (t, 3H).

*(S)-Methyl 3-(1-Methyl-1H-1,2,3-triazol-4-yl)-4-(1-(pyridin-2-yl)-ethoxy)benzoate (**59**).* To a mixture of (*R*)-1-(pyridin-2-yl)ethanol (2.8188 g, 22.89 mmol) and methyl 4-hydroxy-3-(1-methyl-1*H*-1,2,3-triazol-4-yl)benzoate (**114**, 4.8116 g, 20.63 mmol) in toluene (100 mL) in a 250 mL round-bottomed flask was added 2-(tributylphosphoranylidene)acetonitrile (16 mL, 61.1 mmol). The mixture was stirred at 95 °C for 45 min. The reaction mixture was then stirred at reflux for 4 h after which the reaction mixture was removed from heating and cooled overnight. The mixture was evaporated *in vacuo* and redissolved in DCM (10 mL). This solution was split equally between two 100 g silica columns and was purified by flash chromatography. Each column was eluted with a gradient of 30−90% EtOAc/cyclohexane, producing 2 collections for each column of varying purities of the product. The first collections for each column were combined, and the second collections for each column were combined. These 2 combined solutions were both separately concentrated *in vacuo*, before being dissolved in DCM (10 and 5 mL). Both solutions were repurified separately *via* normal-phase column chromatography, eluting with a gradient of 30−90% EtOAc/cyclohexane. All product-containing fractions were concentrated *in vacuo*, dissolved in DCM (10 mL), and combined. The combined material was concentrated *in vacuo* to give (*S*)-methyl 3-(1-methyl-1*H*-1,2,3-triazol-4-yl)-4-(1-(pyridin-2-yl)ethoxy)benzoate (**59**, 5.1842 g, 15.32 mmol, 74% yield) as a sticky brown solid. LC−MS (formic, ES$^+$) t_R = 0.86 min; m/z = 339.2; ^{1}H NMR (400 MHz, $CDCl_3$-d): δ 9.04 (d, J = 2.4 Hz, 1H) 8.64 (dt, J = 4.9, 1.0 Hz, 1H) 8.22 (s, 1H) 7.85 (dd, J = 8.8, 2.4 Hz, 1H) 7.63 (td, J = 7.8, 2.0 Hz, 1H) 7.26−7.20 (m, 2H) 6.85 (d, J = 8.8 Hz, 1H) 5.67 (q, J = 6.8 Hz, 1H) 4.21 (s, 3H) 3.90 (s, 3H) 1.84 (d, J = 6.4 Hz, 3H).

*(S)-3-(1-Methyl-1H-1,2,3-triazol-4-yl)-4-(1-(pyridin-2-yl)ethoxy)-benzoic Acid (**66**).* To a mixture of (*S*)-methyl 3-(1-methyl-1*H*-1,2,3-triazol-4-yl)-4-(1-(pyridin-2-yl)ethoxy)benzoate (**59**, 5.1788 g, 15.31 mmol) in water (60 mL) and THF (60 mL) in a 250 mL round-bottomed flask was added lithium hydroxide (1.8546 g, 77 mmol). This mixture was stirred at room temperature for 20.5 h. The reaction mixture was washed with diethyl ether (3 × 100 mL), and the aqueous layer was concentrated *in vacuo*. The mixture was acidified to pH 3 using 2 M HCl and left to precipitate out for 48 h to give a brown gum. The acidic mother liquor was decanted from the gum and the gum was washed with water (2 × 20 mL). The gum was dried *in vacuo*, triturated with diethyl ether (200 mL), and filtered. The solid was dried *in vacuo* to give (*S*)-3-(1-methyl-1*H*-1,2,3-triazol-4-yl)-4-(1-(pyridin-2-yl)ethoxy)benzoic acid (**66**, 3.2319 g, 9.96 mmol, 65% yield) as a brown powder. LC−MS (formic, ES$^+$) t_R = 0.69 min; m/z = 325.2; ^{1}H NMR (400 MHz, DMSO-d_6): δ 12.70 (br s, 1H) 8.76 (d, J = 2.0 Hz, 1H) 8.60 (d, J = 4.9 Hz, 1H) 8.56 (s, 1H), 7.81−7.74 (m, 2H) 7.41 (d, J = 7.8 Hz, 1H) 7.33 (ddd, J = 7.3, 4.9, 1.0 Hz, 1H) 7.03 (d, J = 8.8 Hz, 1H) 5.77 (q, J = 6.7 Hz, 1H) 4.18 (s, 3H), 1.77 (d, J = 6.4 Hz, 3H).

*3-(1-Methyl-1H-1,2,3-triazol-4-yl)-4-((S)-1-(pyridin-2-yl)ethoxy)-N-(2-(tetrahydro-2H-pyran-3-yl)ethyl)benzamide (**37**).* General pro-

https://dx.doi.org/10.1021/acs.jmedchem.0c02156
J. Med. Chem. 2021, 64, 3249−3281

cedure C was followed using the following amounts: (*S*)-3-(1-methyl-1*H*-1,2,3-triazol-4-yl)-4-(1-(pyridin-2-yl)ethoxy)benzoic acid (**66**, 90 mg, 0.277 mmol), DMF (2.5 mL), DIPEA (0.097 mL, 0.555 mmol), HATU (127 mg, 0.333 mmol), and 2-(tetrahydro-2*H*-pyran-3-yl)ethanamine (39.4 mg, 0.305 mmol). This gave 3-(1-methyl-1*H*-1,2,3-triazol-4-yl)-4-((*S*)-1-(pyridin-2-yl)ethoxy)-*N*-(2-(tetrahydro-2H-pyran-3-yl)ethyl)benzamide (**37**, 12.5 mg, 0.029 mmol, 10% yield). LC−MS (formic, ES$^+$) t_R = 0.87 min; m/z = 436; (100% pure) ^{1}H NMR (400 MHz, MeOD-d_4): δ ppm 8.85 (d, J = 4.9 Hz, 1H), 8.48 (s, 1H), 8.37−8.44 (m, 1H), 8.09 (s, 1H), 7.98 (d, J = 8.3 Hz, 1H), 7.87 (s, 1H), 7.60−7.83 (m, 1H), 7.18 (d, J = 8.8 Hz, 1H), 6.04 (d, J = 6.4 Hz, 1H), 4.25 (s, 3H), 3.91−4.04 (m, 1H), 3.40−3.55 (m, 4H), 1.90 (d, J = 6.4 Hz, 3H), 1.67−1.84 (m, 3H), 1.46−1.67 (m, 4H), 1.22−1.45 (m, 1H).

*(S)-N-Methyl-3-(1-methyl-1H-1,2,3-triazol-4-yl)-4-(1-(pyridin-2-yl)ethoxy)benzamide (**38**).* General procedure C was followed using the following amounts: (*S*)-3-(1-methyl-1*H*-1,2,3-triazol-4-yl)-4-(1-(pyridin-2-yl)ethoxy)benzoic acid (**66**, 0.311 g, 0.96 mmol), HATU (0.365 g, 0.96 mmol), DIPEA (0.504 mL, 2.88 mmol), and DMF (5.6 mL). A 0.76 mL aliquot of this solution was added to methylamine (0.120 mmol). The sample was purified by high pH MDAP, and the solvent was subsequently dried under a stream of nitrogen to give (*S*)-*N*-methyl-3-(1-methyl-1*H*-1,2,3-triazol-4-yl)-4-(1-(pyridin-2-yl)-ethoxy)benzamide (**38**, 24.6 mg, 0.073 mmol, 55% yield). LC−MS (formic, ES$^+$) t_R = 0.62 min; m/z = 338.3; (100% pure) ^{1}H NMR (600 MHz, DMSO-d_6): δ 8.66 (d, J = 2.3 Hz, 1H) 8.60 (br d, J = 4.9 Hz, 1H) 8.55 (s, 1H) 8.35 (q, J = 4.5 Hz, 1H) 7.77 (td, J = 7.9, 1.5 Hz, 1H) 7.64 (dd, J = 8.7, 2.3 Hz, 1H) 7.40 (d, J = 7.9 Hz, 1H) 7.31 (ddd, J = 7.5, 4.9, 1.1 Hz, 1H) 6.99 (d, J = 8.7 Hz, 1H) 5.74 (q, J = 6.0 Hz, 1H) 4.18 (s, 3H) 2.76 (d, J = 4.5 Hz, 3H) 1.76 (d, J = 6.4 Hz, 3H).

*(S)-N-Cyclopropyl-3-(1-methyl-1H-1,2,3-triazol-4-yl)-4-(1-(pyridin-2-yl)ethoxy)benzamide (**39**).* General procedure C was followed using the following amounts: HATU (41 mg, 0.108 mmol), (*S*)-3-(1-methyl-1*H*-1,2,3-triazol-4-yl)-4-(1-(pyridin-2-yl)ethoxy)benzoic acid (**66**, 64 mg, 0.196 mmol), DMF (1.5 mL), DIPEA (0.075 mL, 0.431 mmol), and cyclopropanamine (23 mg, 0.403 mmol). This gave (*S*)-*N*-cyclopropyl-3-(1-methyl-1*H*-1,2,3-triazol-4-yl)-4-(1-(pyridin-2-yl)ethoxy)benzamide (**39**, 27 mg, 0.074 mmol, 38% yield) as an orange solid. LC−MS (formic, ES$^+$) t_R = 0.71 min; m/z = 364.2; (100% pure) ^{1}H NMR (400 MHz, MeOD-d_4): δ 8.58 (d, J = 2.4 Hz, 1H) 8.57−8.56 (m, 1H) 8.49 (s, 1H) 8.37 (br s, 1H) 7.78 (td, J = 7.8, 2.0 Hz, 1H) 7.62 (dd, J = 8.3, 2.0 Hz, 1H) 7.46−7.41 (m, J = 7.8 Hz, 1H) 7.34 (ddd, J = 7.8, 4.9, 1.5 Hz, 1H) 6.93 (d, J = 8.8 Hz, 1H) 5.69 (q, J = 6.8 Hz, 1H) 4.22 (s, 3H) 2.88−2.80 (m, J = 3.9 Hz, 1H) 1.82 (d, J = 6.4 Hz, 3H) 0.83−0.76 (m, 2H), 0.66−0.60 (m, 2H).

*Methyl 4-Hydroxy-3-(1-methyl-1H-1,2,3-triazol-4-yl)benzoate (**114**).* To a mixture of methyl 4-(methoxymethoxy)-3-(1-methyl-1*H*-1,2,3-triazol-4-yl)benzoate (**57**, 25.3760 g, 92 mmol) in methanol (150 mL) in a 500 mL round-bottomed flask was added conc. HCl (20 mL, 658 mmol). The reaction mixture was stirred at 50 °C for 20 h. The solvent was evaporated from the reaction mixture *in vacuo*, and the residue was triturated in methanol (approx 150 mL) for 30 min. The solid was filtered and washed with further methanol (approx 100 mL) and diethyl ether (approx 100 mL). The solid was dried *in vacuo* to give methyl 4-hydroxy-3-(1-methyl-1*H*-1,2,3-triazol-4-yl)benzoate (**114**, 17.8 g, 76 mmol, 83% yield) as a pale yellow solid. LC−MS (formic, ES$^+$) t_R = 0.80 min; m/z = 234.3; ^{1}H NMR (400 MHz, DMSO-d_6): δ 11.14−11.06 (m, 1H) 8.69 (d, J = 2.4 Hz, 1H) 8.48−8.38 (m, 1H) 7.79 (dd, J = 8.3, 2.4 Hz, 1H) 7.07 (d, J = 8.8 Hz, 1H) 4.12 (s, 3H) 3.84 (s, 3H).

*(1R,5S,6r)-3-Oxabicyclo[3.1.0]hexane-6-carboxylic Acid (**115**).* (1*R*,5*S*,6*r*)-Ethyl 3-oxabicyclo[3.1.0]hexane-6-carboxylate (2.1 g, 13.45 mmol) was dissolved in ethanol (20 mL), then NaOH (20 mL, 40.0 mmol) was added, and the mixture was stirred for 2 h at rt and then evaporated to half volume *in vacuo*. The solution was washed with ether (20 mL), then acidified with 2 M HCl to pH 4, and extracted with DCM (4 × 20 mL) and 10% MeOH/DCM (2 × 20 mL). The combined organics were dried and evaporated *in vacuo* to give (1*R*,5*S*,6*r*)-3-oxabicyclo[3.1.0]hexane-6-carboxylic acid (**115**, 1.45 g, 11.32 mmol, 84% yield) as a colorless solid. ^{1}H NMR (400 MHz, $CDCl_3$-*d*): δ 3.97 (d, J = 8.8 Hz, 2H) 3.78 (d, J = 8.3 Hz, 2H) 2.28−2.20 (m, 2H) 1.64 (t, J = 3.4 Hz, 1H).

*tert-Butyl (1R,5S,6r)-3-Oxabicyclo[3.1.0]hexan-6-ylcarbamate (**116**).* (1*R*,5*S*,6*r*)-3-Oxabicyclo[3.1.0]hexane-6-carboxylic acid (**115**, 1.45 g, 11.32 mmol) was suspended in toluene (20 mL), triethylamine (5 mL, 35.9 mmol) and diphenyl phosphorazidate (3 mL, 13.95 mmol) were added, and the mixture was stirred for 20 min and then *tert*-butanol (10 mL, 105 mmol) was added and the solution was heated at reflux for 5 h. This was then diluted with EtOAc (50 mL) and washed with water (50 mL) and saturated sodium bicarbonate solution (50 mL). The organic layer was dried and evaporated *in vacuo* to give a beige crystalline solid. The crude product was purified by normal-phase chromatography on a 50 g silica column eluting with 0−100% EtOAc/cyclohexane to give *tert*-butyl (1*R*,5*S*,6*r*)-3-oxabicyclo[3.1.0]hexan-6-ylcarbamate (**116**, 1.65 g, 8.28 mmol, 73.2% yield) as a colorless solid. ^{1}H NMR (400 MHz, $CDCl_3$-*d*): δ 4.65 (br s, 1H) 3.97 (d, J = 8.8 Hz, 2H) 3.72 (d, J = 8.3 Hz, 2H) 2.42 (d, J = 1.5 Hz, 1H) 1.78 (s, 2H) 1.46 (s, 9H).

*(1R,5S,6r)-3-Oxabicyclo[3.1.0]hexan-6-amine, Hydrochloride (**117**).* *tert*-Butyl (1*R*,5*S*,6*r*)-3-oxabicyclo[3.1.0]hexan-6-ylcarbamate (**116**, 1.65 g, 8.28 mmol) was dissolved in DCM (10 mL), and HCl (10.35 mL, 41.4 mmol) was added. The mixture was stirred for 1 h at rt and then evaporated *in vacuo* to give (1*R*,5*S*,6*r*)-3-oxabicyclo-[3.1.0]hexan-6-amine, hydrochloride (**117**, 1.1 g, 8.11 mmol, 98% yield) as a colorless solid. LC−MS (formic, ES$^+$) t_R = 0.62 min; m/z = 424.4; ^{1}H NMR (400 MHz, DMSO-d_6): δ 8.48 (br s, 2H) 3.81 (d, J = 8.8 Hz, 2H) 3.60 (d, J = 8.8 Hz, 2H) 2.24 (br t, J = 2.4 Hz, 1H) 2.08 (br t, J = 2.4 Hz, 2H).

*N-((1R,5S,6r)-3-Oxabicyclo[3.1.0]hexan-6-yl)-3-(1-methyl-1H-1,2,3-triazol-4-yl)-4-((S)-1-(pyridin-2yl)ethoxy)benzamide (**40**).* General procedure C was followed using the following amounts: (*S*)-3-(1-methyl-1*H*-1,2,3-triazol-4-yl)-4-(1-(pyridin-2-yl)ethoxy)-benzoic acid (**66**, 50 mg, 0.154 mmol), HATU (70.3 mg, 0.185 mmol), DIPEA (0.081 mL, 0.462 mmol), DMF (5 mL), and (1*R*,5*S*,6*r*)-3-oxabicyclo[3.1.0]hexan-6-amine hydrochloride (**117**, 22.99 mg, 0.170 mmol). The sample was purified by MDAP (high pH method). The relevant fractions were combined and concentrated *in vacuo* to give *N*-((1*R*,5*S*,6*r*)-3-oxabicyclo[3.1.0]hexan-6-yl)-3-(1-methyl-1*H*-1,2,3-triazol-4-yl)-4-((*S*)-1-(pyridin-2-yl)ethoxy)-benzamide (**40**, 34 mg, 0.084 mmol, 54% yield) as an off-white solid. LC−MS (high pH, ES$^+$) t_R = 0.79 min; m/z = 406.4; (100% pure); ^{1}H NMR (400 MHz, MeOD-d_4): δ 8.59 (d, J = 2.4 Hz, 1H) 8.57 (dt, J = 4.4, 1.2 Hz, 1H) 8.48 (s, 1H), 7.78 (td, J = 7.5, 1.9 Hz, 1H) 7.62 (dd, J = 8.8, 2.0 Hz, 1H) 7.43 (d, J = 7.8 Hz, 1H) 7.33 (ddd, J = 7.3, 4.9, 1.5 Hz, 1H) 6.93 (d, J = 8.8 Hz, 1H), 5.68 (q, J = 6.4 Hz, 1H) 4.22 (s, 3H), 4.01 (d, J = 8.8 Hz, 2H) 3.74 (d, J = 8.3 Hz, 2H) 2.62 (t, J = 2.4 Hz, 1H) 1.93 (br t, J = 2.9 Hz, 2H) 1.81 (d, J = 6.8 Hz, 3H).

*(S)-3-(1-Methyl-1H-1,2,3-triazol-4-yl)-4-(1-(pyridin-2-yl)ethoxy)-N-(tetrahydro-2H-pyran-4-yl)benzamide (**41**).* General procedure C was followed using the following amounts: (*S*)-3-(1-methyl-1*H*-1,2,3-triazol-4-yl)-4-(1-(pyridin-2-yl)ethoxy)benzoic acid (**66**, 39 mg, 0.12 mmol), HATU (46 mg, 0.120 mmol), DIPEA (0.063 mL, 0.360 mmol), DMF (0.70 mL), and tetrahydro-2*H*-pyran-4-amine (0.120 mmol). The sample was purified by high pH MDAP. The solvent was dried under a stream of nitrogen in the Radleys blowdown apparatus to give (*S*)-3-(1-methyl-1*H*-1,2,3-triazol-4-yl)-4-(1-(pyridin-2-yl)-ethoxy)-*N*-(tetrahydro-2*H*-pyran-4-yl)benzamide (**41**, 22.6 mg, 0.055 mmol, 42% yield). LC−MS (formic, ES$^+$) t_R = 0.68 min; m/z = 408.2; (100% pure) ^{1}H NMR (600 MHz, DMSO-d_6): δ 8.66−8.65 (m, 1H) 8.60−8.58 (m, 1H) 8.56 (s, 1H) 8.28−8.25 (m, 1H) 7.78−7.75 (m, 1H) 7.67−7.64 (m, 1H) 7.40−7.37 (m, 1H) 7.32−7.29 (m, 1H) 7.00−6.98 (m, 1H) 5.75 (d, J = 6.8 Hz, 1H) 4.18 (s, 3H) 4.12−4.08 (m, 1H) 3.87 (br d, J = 9.8 Hz, 2H) 3.3 (obs, m, 2H) 1.77−1.75 (m, 3H) 1.75−1.70 (m, 2H) 1.62−1.53 (m, 2H).

*(S)-3-(1-Methyl-1H-1,2,3-triazol-4-yl)-4-(1-(pyridin-2-yl)ethoxy)-N-((tetrahydro-2H-pyran-4-yl)methyl)benzamide (**42**).* General procedure C was followed using the following amounts: (*S*)-3-(1-methyl-1*H*-1,2,3-triazol-4-yl)-4-(1-(pyridin-2-yl)ethoxy)benzoic acid (**66**, 39 mg, 0.12 mmol), HATU (46 mg, 0.120 mmol), DIPEA (0.063 mL,

https://dx.doi.org/10.1021/acs.jmedchem.0c02156
J. Med. Chem. 2021, 64, 3249−3281

0.360 mmol), DMF (0.70 mL), and (tetrahydro-2*H*-pyran-4-yl)-methanamine (0.120 mmol). The sample was purified by high pH MDAP. The solvent was dried under a stream of nitrogen in the Radleys blowdown apparatus to give (*S*)-3-(1-methyl-1*H*-1,2,3-triazol-4-yl)-4-(1-(pyridin-2-yl)ethoxy)-*N*-((tetrahydro-2*H*-pyran-4-yl)methyl)benzamide (**42**, 19.6 mg, 0.047 mmol, 35% yield). LC−MS (formic, ES$^+$) t_R = 0.71 min; m/z = 422.2; (100% pure) ^{1}H NMR (600 MHz, DMSO-d_6): δ 8.66 (d, J = 1.9 Hz, 1H) 8.59 (br d, J = 4.9 Hz, 1H) 8.56 (s, 1H) 8.43 (t, J = 5.6 Hz, 1H) 7.77 (td, J = 7.9, 1.5 Hz, 1H) 7.66 (dd, J = 8.7, 2.3 Hz, 1H) 7.39 (d, J = 7.9 Hz, 1H) 7.31 (ddd, J = 6.4, 4.9, 0.8 Hz, 1H) 6.99 (d, J = 9.0 Hz, 1H) 5.75 (q, J = 6.4 Hz, 1H) 4.18 (s, 3H) 3.83 (dd, J = 10.9, 2.6 Hz, 2H) 3.25 (t, J = 11.7 Hz, 2H) 3.13 (t, J = 6.4 Hz, 2H) 1.82−1.77 (m, J = 3.8 Hz, 1H) 1.76 (d, J = 6.4 Hz, 3H) 1.57 (br d, J = 12.4 Hz, 2H) 1.18 (qd, J = 12.4, 4.5 Hz, 2H).

*N-((trans)-4-Hydroxycyclohexyl)-3-(1-methyl-1H-1,2,3-triazol-4-yl)-4-((S)-1-(pyridin-2-yl)ethoxy)benzamide (**43**).* General procedure C was followed using the following amounts: (*S*)-3-(1-methyl-1*H*-1,2,3-triazol-4-yl)-4-(1-(pyridin-2-yl)ethoxy)benzoic acid (**66**, 39 mg, 0.12 mmol), HATU (46 mg, 0.120 mmol), DIPEA (0.063 mL, 0.360 mmol), DMF (0.70 mL), and (*trans*)-4-aminocyclohexan-1-ol (14 mg, 0.120 mmol). The sample was purified by high pH MDAP. The solvent was dried under a stream of nitrogen in the Radleys blowdown apparatus to give *N*-((*trans*)-4-hydroxycyclohexyl)-3-(1-methyl-1*H*-1,2,3-triazol-4-yl)-4-((*S*)-1-(pyridin-2-yl)ethoxy)benzamide (**43**, 18.5 mg, 0.044 mmol, 33% yield). LC−MS (formic, ES$^+$) t_R = 0.64 min; m/z = 408.2; (100% pure) ^{1}H NMR (600 MHz, DMSO-d_6): δ ppm 8.63 (d, J = 2.3 Hz, 1H) 8.57−8.60 (m, 1H) 8.53−8.56 (m, 1H) 8.12 (d, J = 7.9 Hz, 1H) 7.76 (td, J = 7.6, 1.7 Hz, 1H) 7.63 (dd, J = 8.7, 2.3 Hz, 1H) 7.38 (d, J = 7.9 Hz, 1H) 7.30 (dd, J = 7.0, 5.5 Hz, 1H) 6.97 (d, J = 9.0 Hz, 1H) 5.71−5.77 (obs. q, 1H) 4.55 (br s, 1H) 4.18 (obs. s, 3H) 4.06−4.14 (m, 1H) 3.64−3.75 (m, 1H) 1.84 (br d, J = 10.5 Hz, 2H) 1.72−1.81 (m, 4H) 1.31−1.42 (m, 2H) 1.19−1.28 (m, 2H).

*(S)-tert-Butyl 2-(((Methylsulfonyl)oxy)methyl)morpholine-4-carboxylate (**118**).* (*S*)-*tert*-Butyl 2-(hydroxymethyl)morpholine-4-carboxylate (3 g, 13.81 mmol) and triethylamine (3.85 mL, 27.6 mmol) were stirred in DCM (30 mL) at 0 °C, methanesulfonyl chloride (1.614 mL, 20.71 mmol) was added portionwise over 5 min, and the reaction mixture was stirred at rt for 4 h. The reaction mixture was diluted with further DCM and was washed with 1 N HCl (aq), $NaHCO_3$ (aq), and water, dried using a hydrophobic frit, and concentrated to give (*S*)-*tert*-butyl 2-(((methylsulfonyl)oxy)methyl)-morpholine-4-carboxylate (**118**, 4.242 g, 14.36 mmol, 104% yield) as a yellow oil. ^{1}H NMR (400 MHz, DMSO-d_6): δ 4.29−4.17 (m, J = 25.9, 10.8, 3.4 Hz, 2H) 3.88−3.80 (m, J = 11.2 Hz, 2H) 3.71 (d, J = 13.2 Hz, 1H) 3.66−3.59 (m, J = 3.4, 2.0 Hz, 1H) 3.43 (td, J = 11.7, 2.9 Hz, 1H) 3.20 (s, 3H) 2.94−2.80 (m, 1H) 2.78−2.63 (m, 1H) 1.42 (s, 9H).

*(R)-tert-Butyl 2-(Cyanomethyl)morpholine-4-carboxylate (**119**).* (*S*)-*tert*-Butyl 2-(((methylsulfonyl)oxy)methyl)morpholine-4-carboxylate (**118**, 4.2 g, 14.22 mmol), KCN (0.972 g, 14.93 mmol), and KI (3.54 g, 21.33 mmol) were stirred at 100 °C in DMSO (30 mL) for 4 h. The reaction mixture was diluted with water and was extracted with EtOAc, the organic layer was washed with water and brine, dried using a hydrophobic frit, and concentrated to a yellow oil. This oil was purified using silica chromatography eluting with a gradient of 0−50% EtOAc/cyclohexane to give (*R*)-*tert*-butyl 2-(cyanomethyl)-morpholine-4-carboxylate (**119**, 2.393 g, 10.58 mmol, 74% yield) as a white solid. ^{1}H NMR (400 MHz, DMSO-d_6): δ 3.89−3.82 (m, J = 11.7, 2.0 Hz, 2H) 3.70 (br d, J = 13.2 Hz, 1H) 3.63−3.55 (m, J = 2.9, 1.5 Hz, 1H) 3.45 (td, J = 11.2, 2.9 Hz, 1H) 2.85 (dd, J = 17.1, 4.4 Hz, 1H) 2.92−2.82 (m, 1H) 2.73 (dd, J = 17.1, 7.3 Hz, 1H) 2.77−2.60 (m, 1H) 1.41 (s, 9H).

*(R)-tert-Butyl 2-(2-Aminoethyl)morpholine-4-carboxylate (**120**).* (*R*)-*tert*-Butyl 2-(cyanomethyl)morpholine-4-carboxylate (**119**, 2.39 g, 10.56 mmol) was taken up into THF (20 mL) and stirred at rt, before the borane tetrahydrofuran complex (15.84 mL, 15.84 mmol) was added over 10 min, and the reaction mixture was stirred at rt for 2 h. The reaction was quenched by the careful addition of MeOH until all effervescence stopped. The reaction mixture was concentrated and diluted with MeOH and treated with 1 M NaOH (50 mL) and stirred at rt for 2 h, a precipitate resulted. The reaction mixture was concentrated to remove the MeOH and was diluted with water and extracted with EtOAc, and the combined organics were washed with water, dried using a hydrophobic frit, and concentrated to give a colorless oil. This oil was further purified using silica chromatography eluting with 0−8% 2 M NH_3 in MeOH/DCM to give (*R*)-*tert*-butyl 2-(2-aminoethyl)morpholine-4-carboxylate (**120**, 965 mg, 4.19 mmol, 40% yield) as a colorless oil. ^{1}H NMR (400 MHz, DMSO-d_6): δ 3.73 (dd, J = 35.2, 11.7 Hz, 3H) 3.35 (td, J = 11.7, 3.4 Hz, 1H) 3.42−3.30 (m, 1H) 3.07−2.73 (m, 1H) 3.07−2.73 (m, 1H) 2.61 (td, J = 6.8, 2.9 Hz, 2H) 1.53−1.44 (m, 2H) 1.41 (s, 9H).

*(R)-tert-Butyl 2-(2-(3-(1-Methyl-1H-1,2,3-triazol-4-yl)-4-((S)-1-(pyridin-2-yl)ethoxy)benzamido)ethyl)morpholine-4-carboxylate (**60**).* General procedure C was followed using the following amounts: (*S*)-3-(1-methyl-1*H*-1,2,3-triazol-4-yl)-4-(1-(pyridin-2-yl)ethoxy)-benzoic acid (**66**, 100 mg, 0.308 mmol), HATU (141 mg, 0.370 mmol), DIPEA (0.162 mL, 0.925 mmol), DMF (5 mL), and (*R*)-*tert*-butyl 2-(2-aminoethyl)morpholine-4-carboxylate (**120**, 71.0 mg, 0.308 mmol). The sample was purified by silica chromatography eluting with 0−25% 2 M NH_3 in 20:80 MeOH/DCM. The relevant fractions were combined and concentrated *in vacuo* to give (*R*)-*tert*-butyl 2-(2-(3-(1-methyl-1*H*-1,2,3-triazol-4-yl)-4((*S*)-1-(pyridin-2-yl)-ethoxy)benzamido)ethyl)morpholine-4-carboxylate (**60**, 146 mg, 0.272 mmol, 88% yield) as a yellow oil. LC−MS (formic, ES$^+$) t_R = 0.96 min; m/z = 537.2; ^{1}H NMR (400 MHz, MeOD-d_4): δ 8.61 (d, J = 2.0 Hz, 1H) 8.58−8.56 (m, 1H) 8.49 (s, 1H) 8.32 (t, J = 5.4 Hz, 1H) 7.78 (td, J = 7.3, 1.5 Hz, 1H) 7.64 (dd, J = 8.3, 2.0 Hz, 1H) 7.43 (d, J = 7.8 Hz, 1H) 7.33 (ddd, J = 7.8, 5.4, 1.5 Hz, 1H) 6.94 (d, J = 8.8 Hz, 1H) 5.69 (q, J = 6.8 Hz, 1H) 4.22 (s, 3H) 3.92−3.86 (m, 2H) 3.83 (dt, J = 13.2, 1.0 Hz, 1H) 3.54−3.44 (m, 4H) 2.98−2.89 (m, 1H) 2.75−2.59 (m, 1H) 1.82 (d, J = 6.8 Hz, 3H) 1.80−1.72 (m, 2H) 1.45 (s, 9H).

*3-(1-Methyl-1H-1,2,3-triazol-4-yl)-N-(2-((R)-morpholin-2-yl)-ethyl)-4-((S)-1-(pyridin-2yl)ethoxy)benzamide (**44**).* (*R*)-*tert*-Butyl 2-(2-(3-(1-methyl-1*H*-1,2,3-triazol-4-yl)-4-((*S*)-1-(pyridin-2-yl)-ethoxy)benzamido)ethyl)morpholine-4-carboxylate (**60**, 146 mg, 0.272 mmol) was dissolved in DCM (3 mL), and TFA (0.105 mL, 1.360 mmol) was added. The reaction mixture was stirred at rt for 2 h after which TFA (0.4 mL, 5.19 mmol) was added. The reaction mixture was stirred for 30 min. Sat. $NaHCO_3$ solution (10 mL) was added to quench the reaction, and the reaction mixture was left to stand for 4 days. The reaction mixture was diluted with water (5 mL) and extracted with DCM (3 × 30 mL). The organics were dried *via* a hydrophobic frit and concentrated *in vacuo*. The residue was taken up into DCM (3 mL) and purified by silica chromatography eluting with 0−25% 2 M NH_3 in 20:80 MeOH/DCM. The relevant fractions were combined and concentrated *in vacuo* to give the product 3-(1-methyl-1*H*-1,2,3-triazol-4-yl)-*N*-(2-((*R*)-morpholin-2-yl)ethyl)-4-((*S*)-1-(pyridin-2-yl)ethoxy)benzamide (**44**, 16.6 mg, 0.038 mmol, 14% yield) as an off-white solid. LC−MS (formic, ES$^+$) t_R = 0.48 min; m/z = 437.3; (100% pure) ^{1}H NMR (400 MHz, MeOD-d_4): δ 8.62−8.60 (m, 1H) 8.59−8.56 (m, 1H) 8.50 (s, 1H) 7.82−7.77 (m, 1H) 7.66−7.62 (m, 1H) 7.46−7.42 (m, 1H) 7.37−7.32 (m, 1H) 6.95 (d, J = 8.8 Hz, 1H) 5.70 (d, J = 6.4 Hz, 1H) 4.23 (s, 3H) 3.95−3.90 (m, 1H) 3.70−3.56 (m, 2H) 3.48 (t, J = 6.8 Hz, 2H) 2.98−2.93 (m, 1H) 2.87 (s, 2H) 2.62 (d, J = 10.3 Hz, 1H) 1.83 (d, J = 6.8 Hz, 3H) 1.78−1.69 (m, 2H).

*(R)-tert-Butyl 2-(((Methylsulfonyl)oxy)methyl)morpholine-4-carboxylate (**121**).* (*R*)-*tert*-Butyl 2-(hydroxymethyl)morpholine-4-carboxylate (3 g, 13.81 mmol) and triethylamine (2.89 mL, 20.71 mmol) were stirred in DCM (30 mL) at 0 °C, methanesulfonyl chloride (1.184 mL, 15.19 mmol) was added portionwise over 5 min, and the reaction mixture was stirred at rt for 1 h. The reaction mixture was treated with further methanesulfonyl chloride (1.076 mL, 13.81 mmol) and triethylamine (1.925 mL, 13.81 mmol) and stirred at rt for 1 h. The reaction mixture was diluted with further DCM and was washed with 1 M HCl (aq), $NaHCO_3$ (aq), and water, dried using a hydrophobic frit, and concentrated to give (*R*)-*tert*-butyl 2-(((methylsulfonyl)oxy)methyl)morpholine-4-carboxylate (**121**, 4.402

https://dx.doi.org/10.1021/acs.jmedchem.0c02156
J. Med. Chem. 2021, 64, 3249−3281

g, 14.90 mmol, 108% yield) as a yellow oil. ^{1}H NMR (400 MHz, DMSO-d_6): δ 4.29−4.17 (m, J = 10.8, 5.9, 3.4 Hz, 2H) 3.84 (d, J = 11.7 Hz, 2H) 3.70 (d, J = 13.2 Hz, 1H) 3.66−3.59 (m, 1H) 3.43 (td, J = 11.7, 2.9 Hz, 1H) 3.20−3.19 (m, 3H) 2.93−2.82 (m, 1H) 2.76−2.66 (m, 1H) 1.42 (s, 9H).

*(S)-tert-Butyl 2-(Cyanomethyl)morpholine-4-carboxylate (**122**).* (*R*)-*tert*-Butyl 2-(((methylsulfonyl)oxy)methyl)morpholine-4-carboxylate (**121**, 4 g, 13.54 mmol), KCN (0.926 g, 14.22 mmol), and KI (3.37 g, 20.31 mmol) were stirred at 80 °C in DMSO (30 mL) for 4 h and then at 100 °C for 3 h. The reaction mixture was diluted with water and was extracted with EtOAc. The organic layer was washed with water and brine, dried using a hydrophobic frit, and concentrated to a yellow oil. This oil was purified using silica chromatography, eluting with a gradient of 0−50% EtOAc/cyclohexane to give (*S*)-*tert*-butyl 2-(cyanomethyl)morpholine-4-carboxylate (**122**, 2.693 g, 11.90 mmol, 88% yield) as a white solid. ^{1}H NMR (400 MHz, DMSO-d_6): δ 3.90−3.81 (m, J = 11.7 Hz, 2H) 3.70 (d, J = 13.7 Hz, 1H) 3.63−3.55 (m, 1H) 3.45 (td, J = 11.7, 2.9 Hz, 1H) 2.85 (dd, J = 17.1, 4.4 Hz, 1H) 2.92−2.81 (m, 1H) 2.73 (dd, J = 17.6, 7.8 Hz, 1H) 2.77−2.57 (m, 1H) 1.42 (s, 9H).

*(S)-tert-Butyl 2-(2-Aminoethyl)morpholine-4-carboxylate (**123**).* (*S*)-*tert*-Butyl 2-(cyanomethyl)morpholine-4-carboxylate (**122**, 2.6 g, 11.49 mmol) was taken up into THF (20 mL) and stirred at rt. The borane tetrahydrofuran complex (17.24 mL, 17.24 mmol) was added over 10 min, and the reaction mixture was stirred at rt for 2 h. The reaction was quenched by the careful addition of MeOH until all effervescence stopped. The reaction mixture was concentrated and diluted with MeOH and treated with 1 M NaOH (50 mL) and stirred at rt for 2 h, a precipitate resulted. The reaction mixture was concentrated to remove the MeOH and was diluted with water and extracted with EtOAc. The combined organics were washed with water, dried using a hydrophobic frit, and concentrated to a colorless oil. The oil was again taken up into THF (20 mL), treated with the borane tetrahydrofuran complex (17.24 mL, 17.24 mmol), and stirred at 70 °C under reflux conditions for 4 h. The reaction was quenched by the careful addition of MeOH until all effervescence stopped. The reaction mixure was concentrated and diluted with MeOH and treated with 1 M NaOH (50 mL) and stirred at rt for 1 h, a precipitate resulted. The reaction mixture was concentrated to remove the MeOH and was diluted with water and extracted with EtOAc. The combined organics were washed with water, dried using a hydrophobic frit, and concentrated to give (*S*)-*tert*-butyl 2-(2-aminoethyl)-morpholine-4-carboxylate (**122**, 763 mg, 3.31 mmol, 29% yield) as a colorless viscous oil. ^{1}H NMR (400 MHz, DMSO-d_6): δ 3.80−3.65 (m, J = 34.2, 11.7 Hz, 3H) 3.35 (td, J = 11.7, 2.9 Hz, 1H) 3.41−3.27 (m, 1H) 3.41−3.27 (m, 1H) 2.89−2.79 (m, 1H) 2.62−2.57 (m, 2H) 1.52−1.42 (m, 2H) 1.41 (s, 9H).

*(S)-tert-Butyl 2-(2-(3-(1-Methyl-1H-1,2,3-triazol-4-yl)-4-((S)-1-(pyridin-2-yl)ethoxy)benzamido)ethyl)morpholine-4-carboxylate (**61**).* General procedure C was followed using the following amounts: (*S*)-3-(1-methyl-1*H*-1,2,3-triazol-4-yl)-4-(1-(pyridin-2-yl)ethoxy)-benzoic acid (**66**, 100 mg, 0.308 mmol), DIPEA (0.162 mL, 0.925 mmol), HATU (141 mg, 0.370 mmol), DMF (5.5 mL), and (*S*)-*tert*-butyl 2-(2-aminoethyl)morpholine-4-carboxylate (**123**, 78 mg, 0.339 mmol). The sample was purified by silica chromatography eluting with 0−5% MeOH/DCM. The relevant fractions were combined and concentrated *in vacuo* to give (*S*)-*tert*-butyl 2-(2-(3-(1-methyl-1*H*-1,2,3-triazol-4-yl)-4-((*S*)-1-(pyridin-2-yl)ethoxy)benzamido)ethyl)-morpholine-4-carboxylate (**61**, 142 mg, 0.265 mmol, 86% yield), a colorless oil. LC−MS (formic, ES$^+$) t_R = 0.96 min; m/z = 537.2; ^{1}H NMR (400 MHz, MeOD-d_4): δ 8.61 (d, J = 2.4 Hz, 1H) 8.57 (dt, J = 4.9, 1.0 Hz, 1H) 8.50−8.49 (m, 1H) 7.79 (d, J = 2.0 Hz, 1H) 7.64 (dd, J = 8.3, 2.0 Hz, 1H) 7.44 (dt, J = 7.8, 1.0 Hz, 1H) 7.34 (ddd, J = 7.3, 4.9, 1.0 Hz, 1H) 6.95 (d, J = 8.8 Hz, 1H) 5.69 (q, J = 6.8 Hz, 1H) 4.23 (s, 3H) 3.93−3.86 (m, 2H) 3.83 (dt, J = 13.7, 1.0 Hz, 1H) 3.52−3.47 (m, 4H) 2.99−2.90 (m, 1H) 2.74−2.63 (m, 1H) 1.82 (d, J = 6.8 Hz, 3H) 1.80−1.72 (m, 2H) 1.45 (s, 9H).

*3-(1-Methyl-1H-1,2,3-triazol-4-yl)-N-(2-((S)-morpholin-2-yl)-ethyl)-4-((S)-1-(pyridin-2-yl)ethoxy)benzamide (**45**).* (*S*)-*tert*-Butyl 2-(2-(3-(1-methyl-1*H*-1,2,3-triazol-4-yl)-4-((*S*)-1-(pyridin-2-yl)-ethoxy)benzamido)ethyl)morpholine-4-carboxylate (**61**, 142 mg, 0.265 mmol) was dissolved in DCM (5 mL), and TFA (0.041 mL, 0.529 mmol) was added. The reaction mixture was stirred at rt for 2 h after which TFA (0.5 mL, 6.49 mmol) and DCM (1 mL) were added. The reaction mixture was stirred at rt for 1 h. The reaction mixture was quenched with sat. $NaHCO_3$ solution (10 mL), diluted with water (5 mL), and extracted with DCM (3 × 30 mL). The organics were dried using a hydrophobic frit and concentrated *in vacuo* to give 3-(1-methyl-1*H*-1,2,3-triazol-4-yl)-*N*-(2-((*S*)-morpholin-2-yl)ethyl)-4-((*S*)-1-(pyridin-2-yl)ethoxy)benzamide (**45**, 87 mg, 0.199 mmol, 75% yield) as an off-white solid. LC−MS (formic, ES$^+$) t_R = 0.48 min; m/z = 219.3; (100% pure) ^{1}H NMR (400 MHz, MeOD-d_4): δ 8.61 (d, J = 2.4 Hz, 1H) 8.58 (dd, J = 4.9, 1.0 Hz, 1H) 8.50−8.49 (m, 1H) 7.79 (tt, J = 7.8, 1.5 Hz, 1H) 7.64 (ddd, J = 8.8, 2.4, 1.0 Hz, 1H) 7.44 (d, J = 7.8 Hz, 1H) 7.36−7.32 (m, 1H), 6.95 (dd, J = 8.8, 1.0 Hz, 1H) 5.70 (q, J = 6.4 Hz, 1H) 4.23 (s, 3H) 3.88 (d, J = 11.2 Hz, 1H) 3.65−3.52 (m, 2H) 3.47 (t, J = 6.8 Hz, 2H) 2.87 (d, J = 12.7 Hz, 1H) 2.81−2.76 (m, 2H), 2.53 (dd, J = 13.2, 9.8 Hz, 1H) 1.83 (d, J = 6.4 Hz, 3H) 1.75−1.67 (m, 2H).

*(R,E)-tert-Butyl 3-(3-Ethoxy-3-oxoprop-1-en-1-yl)-3-fluoropiperidine-1-carboxylate (**124**).* (*S*)-*tert*-Butyl 3-fluoro-3-(hydroxymethyl)-piperidine-1-carboxylate (10 g, 42.9 mmol) was dissolved in DCM (60 mL), and Dess−Martin periodinane (23.64 g, 55.7 mmol) was added. The mixture was stirred at rt for 18 h and then washed with water, and the organic layer was dried over sodium sulphate and decanted into a clean, dry flask. Ethyl 2-(triphenylphosphoranylidene)acetate (19.41 g, 55.7 mmol) was added, and the mixture was stirred overnight and then washed with water, and the organic layer was dried and evaporated *in vacuo*. The residue was purified by silica chromatography eluting with 0−50% EtOAc/cyclohexane, and product-containing fractions were evaporated *in vacuo* to give (*R,E*)-*tert*-butyl-3-(3-ethoxy-3-oxoprop-1-en-1-yl)-3-fluoropiperidine-1-carboxylate (**124**, 10.5 g, 34.8 mmol, 81% yield) as a colorless oil. ^{1}H NMR (400 MHz, $CDCl_3$-*d*): δ 6.90 (dd, J = 19.6, 15.7 Hz, 1H) 6.16 (d, J = 15.6 Hz, 1H) 4.23 (q, J = 6.8 Hz, 2H) 4.07−3.96 (m, 1H) 3.92 (d, J = 13.2 Hz, 1H) 3.24−3.03 (m, 1H) 3.01−2.92 (m, J = 11.7 Hz, 1H) 2.02−1.92 (m, 1H) 1.89−1.79 (m, 1H) 1.77−1.65 (m, 1H) 1.63−1.54 (m, 1H) 1.47 (s, 9H) 1.32 (t, J = 6.8 Hz, 3H).

*(R)-tert-Butyl 3-(3-Ethoxy-3-oxopropyl)-3-fluoropiperidine-1-carboxylate (**125**).* (*R,E*)-*tert*-Butyl 3-(3-ethoxy-3-oxoprop-1-en-1-yl)-3-fluoropiperidine-1-carboxylate (**124**, 10 g, 33.2 mmol) was dissolved in ethanol (100 mL) and added to Pd-C 5% (2 g, 18.79 mmol) under N_2. The mixture was then hydrogenated at atmospheric pressure for 6 h. The mixture was filtered through celite under nitrogen, and the filtrate was evaporated *in vacuo* to give (*R*)-*tert*-butyl 3-(3-ethoxy-3-oxopropyl)-3-fluoropiperidine-1-carboxylate (**125**, 9.5 g, 31.3 mmol, 94% yield) as a pale yellow oil. ^{1}H NMR (400 MHz, $CDCl_3$-*d*): δ 4.15 (q, J = 7.3 Hz, 2H) 3.96−3.82 (m, 1H) 3.76 (dt, J = 13.7, 4.4 Hz, 1H) 3.19−2.94 (m, 1H) 3.03 (br t, J = 9.8 Hz, 1H) 2.48 (t, J = 7.8 Hz, 2H) 2.01−1.87 (m, 3H) 1.85−1.73 (m, 1H) 1.64−1.50 (m, 2H) 1.47 (s, 9H) 1.27 (t, J = 6.8 Hz, 3H).

*(R)-tert-Butyl 3-Fluoro-3-(3-hydroxypropyl)piperidine-1-carboxylate (**126**).* $LiBH_4$ (2.046 g, 94 mmol) was added to a solution of (*R*)-*tert*-butyl 3-(3-ethoxy-3-oxopropyl)-3-fluoropiperidine-1-carboxylate (**125**, 9.5 g, 31.3 mmol) in THF (100 mL), and the mixture was stirred at rt under nitrogen for 48 h. The mixture was then cooled in an ice bath and quenched very cautiously, initially dropwise addition of ammonium chloride solution (100 mL). The mixture was then stirred for 20 min and diluted with EtOAc (100 mL), and the combined organics were separated, dried over sodium sulphate, and evaporated *in vacuo*. The crude material was dissolved in DCM and purified by silica chromatography eluting with 0−100% EtOAc/cyclohexane, and product-containing fractions were evaporated *in vacuo* to give (*R*)-*tert*-butyl 3-fluoro-3-(3-hydroxypropyl)piperidine-1-carboxylate (**126**, 6.0 g, 23.0 mmol, 73% yield). ^{1}H NMR (400 MHz, $CDCl_3$-*d*): δ 3.91−3.74 (m, 2H) 3.73−3.64 (m, 2H) 3.14−2.96 (m, J = 14.2 Hz, 2H) 2.00−1.90 (m, 1H) 1.86−1.58 (m, 7H) 1.47 (s, 9H).

*(R)-tert-Butyl 3-Fluoro-3-(3-((methylsulfonyl)oxy)propyl)-piperidine-1-carboxylate (**127**).* (*R*)-*tert*-Butyl 3-fluoro-3-(3-

https://dx.doi.org/10.1021/acs.jmedchem.0c02156
J. Med. Chem. 2021, 64, 3249−3281

hydroxypropyl)piperidine-1-carboxylate (**126**, 6 g, 22.96 mmol) was dissolved in DCM (100 mL). Et_3N (4.80 mL, 34.4 mmol) was added, and the mixture was cooled in an ice bath, then methanesulfonyl chloride (2.326 mL, 29.8 mmol) was added dropwise, and the mixture was stirred for 2 h, allowing it to warm to rt. The solution was washed with water (100 mL) and brine (100 mL), and the organic layer was dried and evaporated *in vacuo* to give (*R*)-*tert*-butyl 3-fluoro-3-(3((methylsulfonyl)oxy)propyl)piperidine-1-carboxylate (**127**, 7.2 g, 21.21 mmol, 92% yield) as a colorless oil. ^{1}H NMR (400 MHz, $CDCl_3$-*d*): δ 4.28 (td, *J* = 6.4, 2.9 Hz, 2H) 3.91−3.72 (m, 2H) 3.02 (s, 3H) 3.15−2.99 (m, 2H) 1.95 (quin, *J* = 7.3 Hz, 3H) 1.84−1.52 (m, 5H) 1.48 (s, 9H).

*(R)-tert-Butyl 3-(3-Azidopropyl)-3-fluoropiperidine-1-carboxylate (**128**).* Sodium azide (2.68 g, 41.2 mmol) was added to a solution of (*R*)-*tert*-butyl 3-fluoro-3-(3-((methylsulfonyl)oxy)propyl)-piperidine-1-carboxylate (**127**, 7 g, 20.62 mmol) in DMF (50 mL), and the mixture was heated at 70 °C for 2 h and then diluted with water (200 mL) and extracted with EtOAc (2 × 100 mL). The combined organics were washed with water (2 × 100 mL), dried, and evaporated *in vacuo*. The crude product was dissolved in DCM (10 mL) and purified by silica chromatography eluting with 0−50% EtOAc/cyclohexane, and product-containing fractions (visualized by ninhydrin) were evaporated *in vacuo* to give (*R*)-*tert*-butyl 3-(3-azidopropyl)-3-fluoropiperidine-1-carboxylate (**128**, 5.2 g, 18.16 mmol, 88% yield) as a colorless oil. ^{1}H NMR (400 MHz, $CDCl_3$-*d*): δ 3.77 (dt, *J* = 13.2, 4.4 Hz, 1H) 3.98−3.72 (m, 1H) 3.34 (t, *J* = 6.6 Hz, 2H) 3.16−2.99 (m, 1H) 3.16−2.99 (m, *J* = 12.7, 10.3 Hz, 1H) 1.99−1.89 (m, 1H) 1.84−1.54 (m, 7H) 1.48 (s, 9H).

*(S)-tert-Butyl 3-(3-Aminopropyl)-3-fluoropiperidine-1-carboxylate (**129**).* (*R*)-*tert*-Butyl 3-(3-azidopropyl)-3-fluoropiperidine-1-carboxylate (**128**, 5.0 g, 17.46 mmol) was dissolved in THF (50 mL), and triphenylphosphine (5.50 g, 20.95 mmol) was added. The mixture was then stirred at rt over the weekend. Water (50 mL) was added, and the mixture was stirred vigorously for 2 h and then diluted with EtOAc (100 mL) and brine (50 mL). The organic layer was separated, dried, and evaporated *in vacuo*. The crude product was dissolved in DCM (20 mL) and purified by silica chromatography eluting with 0−20% 2 M methanolic ammonia/DCM. Product-containing fractions were evaporated *in vacuo* to give (*S*)-*tert*-butyl 3-(3-aminopropyl)-3-fluoropiperidine-1-carboxylate (**129**, 4.0 g, 15.36 mmol, 88% yield) as a colorless oil. ^{1}H NMR (400 MHz, $CDCl_3$-*d*): δ 3.99−3.74 (m, 1H) 3.81 (br d, *J* = 10.8 Hz, 1H) 3.11−2.92 (m, 1H) 3.11−2.92 (m, *J* = 11.7, 10.3 Hz, 1H) 2.76−2.70 (m, *J* = 6.8 Hz, 2H) 1.98−1.88 (m, 1H) 1.86−1.74 (m, 1H) 1.71−1.50 (m, 6H) 1.47 (s, 9H) 1.39 (br s, 2H).

*(S)-tert-Butyl 3-Fluoro-3-(3-(3-(1-methyl-1H-1,2,3-triazol-4-yl)-4-((S)-1-(pyridin-2-yl)ethoxy)benzamido)propyl)piperidine-1-carboxylate (**62**).* General procedure C was followed using the following amounts: (*S*)-3-(1-methyl-1*H*-1,2,3-triazol-4-yl)-4-(1-(pyridin-2-yl)-ethoxy)benzoic acid (**66**, 100 mg, 0.308 mmol), HATU (141 mg, 0.370 mmol), DIPEA (0.162 mL, 0.925 mmol), DMF (5 mL), and (*S*)-*tert*-butyl 3-(3-aminopropyl)-3-fluoropiperidine-1-carboxylate (**129**, 88 mg, 0.339 mmol). The sample was purified by silica chromatography eluting with 0−25% 2 M NH_3 in 20:80 MeOH/DCM in DCM. The relevant fractions were combined and concentrated *in vacuo* to give the product (*S*)-*tert*-butyl 3-fluoro-3-(3-(3-(1-methyl-1*H*-1,2,3-triazol-4-yl)-4-((*S*)-1-(pyridin-2-yl)-ethoxy)benzamido)propyl)piperidine-1-carboxylate (**62**, 160 mg, 0.282 mmol, 92% yield) as a yellow/orange oil. LC−MS (high pH, ES^+) t_R = 1.12 min; *m*/*z* = 567.5; ^{1}H NMR (400 MHz, MeOD-d_4): δ 8.63 (d, *J* = 2.4 Hz, 1H) 8.56 (dt, *J* = 4.4, 1.5 Hz, 1H) 8.48 (s, 1H) 7.77 (td, *J* = 7.8, 1.5 Hz, 1H) 7.64 (dd, *J* = 8.8, 2.4 Hz, 1H) 7.43 (d, *J* = 8.3 Hz, 1H) 7.32 (ddd, *J* = 7.3, 4.9, 1.0 Hz, 1H) 6.93 (d, *J* = 8.8 Hz, 1H) 5.67 (q, *J* = 6.4 Hz, 1H) 4.21 (s, 3H) 3.86 (br dt, *J* = 13.2, 3.9 Hz, 1H) 3.93 (br t, *J* = 11.7 Hz, 1H) 3.38 (t, *J* = 6.8 Hz, 2H) 3.12−2.81 (m, 2H) 1.96−1.87 (m, 1H) 1.81 (d, *J* = 6.4 Hz, 3H) 1.76−1.51 (m, 7H) 1.43 (s, 9H).

*N-(3-((R)-3-Fluoropiperidin-3-yl)propyl)-3-(1-methyl-1H-1,2,3-triazol-4-yl)-4-((S)-1-(pyridin-2-yl)ethoxy)benzamide (**46**).* (*S*)-*tert*-Butyl 3-fluoro-3-(3-(3-(1-methyl-1*H*-1,2,3-triazol-4-yl)-4-((*S*)-1-(pyridin-2-yl)ethoxy)benzamido)propyl)piperidine-1-carboxylate (**62**, 160 mg, 0.282 mmol) was dissolved in DCM (5 mL), and TFA (0.5 mL, 6.49 mmol) was added. The reaction mixture was stirred at rt for 1 h. Saturated $NaHCO_3$ solution (10 mL) was added, and the mixture was stirred for 1 h. The reaction mixture was diluted with water (5 mL) and extracted with DCM (3 × 30 mL). Brine (5 mL) was added. The organics were washed with 10% LiCl solution (equal volume), dried *via* a hydrophobic frit, and concentrated *in vacuo*. The residue was taken up into MeOH (2 mL) and eluted through an NH_2 Isolute column (prewashed with MeOH) with MeOH (50 mL). The relevant fractions were combined and concentrated *in vacuo*. The residue was taken up into 3:1 MeOH/DMSO (1 mL) and purified by MDAP (high pH method). The relevant fractions were combined and concentrated *in vacuo* to give the product *N*-(3-((*R*)-3-fluoropiperidin-3-yl)propyl)-3-(1-methyl-1*H*-1,2,3-triazol-4-yl)-4-((*S*)-1-(pyridin-2-yl)ethoxy)benzamide (**46**, 24 mg, 0.051 mmol, 18% yield) as an off-white solid. LC−MS (high pH, ES^+) t_R = 0.85 min; *m*/*z* = 467.3; (100% pure) ^{1}H NMR (400 MHz, MeOD-d_4): δ 8.62 (d, *J* = 2.4 Hz, 1H) 8.57 (ddd, *J* = 4.9, 1.0, 1.0 Hz, 1H) 8.49 (s, 1H) 7.78 (td, *J* = 7.8, 1.5 Hz, 1H) 7.64 (dd, *J* = 8.8, 2.4 Hz, 1H) 7.45−7.42 (m, *J* = 8.3 Hz, 1H) 7.33 (ddd, *J* = 7.3, 4.9, 1.0 Hz, 1H) 6.94 (d, *J* = 8.8 Hz, 1H) 5.68 (q, *J* = 6.8 Hz, 1H) 4.22 (s, 3H) 3.37 (t, *J* = 6.8 Hz, 2H) 3.00−2.90 (m, *J* = 12.2, 2.9 Hz, 2H) 2.69−2.50 (m, 2H) 1.99−1.90 (m, 1H) 1.82 (d, *J* = 6.4 Hz, 3H) 1.76−1.51 (m, 7H).

*tert-Butyl 2-Benzyl-6-(1-methyl-1H-1,2,3-triazol-4-yl)-isonicotinate (**73**).* *tert*-Butyl 2-chloro-6-(1-methyl-1*H*-1,2,3-triazol-4-yl)isonicotinate (**69**, 400 mg, 1.357 mmol), $PdCl_2(PPh_3)_2$ (95 mg, 0.136 mmol), and benzylzinc(II) bromide (4.07 mL, 2.036 mmol) were dissolved in THF (6 mL). The reaction mixture was then irradiated for 0.5 h at 100 °C. The reaction mixture was partitioned between EtOAc (25 mL) and water (30 mL). The aqueous layer was removed; the organic layer was washed (1× water 20 mL, 2× sat. aq $NaHCO_3$ 20 mL), passed through a hydrophobic frit, and evaporated *in vacuo* to a red/brown oil. The sample was then dissolved in 5 mL of DCM and was purified by silica chromatography eluting with 0−50% EtOAc/cyclohexane. The product-containing fractions were combined, and the solvent was removed *in vacuo*. The sample was then dried under a stream of nitrogen for 16 h and was placed in a vacuum oven for 30 min to give *tert*-butyl 2-benzyl-6-(1-methyl-1*H*-1,2,3-triazol-4-yl)isonicotinate (**73**, 261 mg, 0.559 mmol, 41% yield) as a red/brown gum. LC−MS (formic, ES^+) t_R = 1.25 min; *m*/*z* = 351.3; ^{1}H NMR (400 MHz, DMSO-d_6): δ ppm 8.62 (s, 1H) 8.21 (d, *J* = 1.5 Hz, 1H) 7.59 (d, *J* = 1.5 Hz, 1H) 7.28−7.45 (m, 4H) 7.19−7.26 (m, 1H) 4.22 (obs. s, 2H) 4.13 (s, 3H) 1.57 (s, 9H).

*2-Benzyl-6-(1-methyl-1H-1,2,3-triazol-4-yl)isonicotinamide (**47**).* 2-Benzyl-6-(1-methyl-1*H*-1,2,3-triazol-4-yl)isonicotinic acid (**82**, 30 mg, 0.102 mmol), EDC (23.45 mg, 0.122 mmol), 1*H*-benzo[*d*]-[1,2,3]triazol-1-ol, ammonia salt (31.0 mg, 0.204 mmol), and DIPEA (0.053 mL, 0.306 mmol) were dissolved in DMF (4 mL). The reaction mixture was partitioned between EtOAc (25 mL) and water (30 mL). The organic layer was washed (1× water 20 mL, 2× sat. aq $NaHCO_3$ 20 mL), passed through a hydrophobic frit, and evaporated *in vacuo* to a white solid. The sample was then purified by silica chromatography 20−100% EtOAc/cyclohexane. The product-containing fractions were combined, and the solvent was removed *in vacuo*. The sample was then dried under a stream of nitrogen for 1 h and was placed in the vacuum oven for 30 min to give 2-benzyl-6-(1-methyl-1*H*-1,2,3-triazol-4-yl)isonicotinamide (**47**, 14 mg, 0.048 mmol, 47% yield) as a white solid. LC−MS (formic, ES^+) t_R = 0.77 min; *m*/*z* = 294.2; (98% pure) ^{1}H NMR (400 MHz, DMSO-d_6): δ ppm 8.59 (s, 1H) 8.35 (br s, 1H) 8.27 (d, *J* = 1.5 Hz, 1H) 7.71 (br s, 1H) 7.60 (d, *J* = 1.5 Hz, 1H) 7.27−7.38 (m, 4H) 7.18−7.25 (m, 1H) 4.17 (s, 2H) 4.13 (s, 3H).

*Methyl 2-Benzyl-6-bromoisonicotinate (**130**).* A yellow solution of methyl 2,6-dibromopyridine-4-carboxylate (2.5 g, 8.48 mmol) and tetrakis triphenyl phosphine palladium (0.40 g, 0.346 mmol) was sparged with nitrogen for 15 min and a solution of 0.5 M benzylzinc(II) bromide in THF (20 mL, 10.00 mmol) was added. The resulting brown solution was heated to 60 °C under nitrogen for 20 min to give a black solution. MeOH (5 mL) was added to quench

https://dx.doi.org/10.1021/acs.jmedchem.0c02156
J. Med. Chem. 2021, 64, 3249−3281

the reaction, and the mixture was cooled to rt. The reaction mixture was stood overnight and diluted with EtOAc, and the solution was washed twice with sat. aq NH_4Cl. The organic layer was dried over $MgSO_4$ and evaporated *in vacuo* to a yellow oil. Cyclohexane was added to the residue and a suspension formed. The suspension was stirred vigorously for 30 min and filtered. The filtrate was loaded onto a 100 g Biotage silica SNAP column and eluted with 0−10% EtOAc/cyclohexane. The product-containing fractions were evaporated *in vacuo* to give methyl 2-benzyl-6-bromoisonicotinate (**130**, 1.837 g, 6.00 mmol, 64% yield) as a yellow oil. LC−MS (TFA, ES^+) t_R = 1.24 min; m/z = 306.0, 308.0; ^{1}H NMR (400 MHz, DMSO-d_6): δ 7.82 (d, J = 1.5 Hz, 1H) 7.75 (d, J = 1.5 Hz, 1H) 7.36−7.27 (m, 5H) 4.20−4.18 (m, 2H) 3.88 (s, 3H).

*Methyl 2-Benzyl-6-((trimethylsilyl)ethynyl)isonicotinate (**131**).* Tetrakis triphenylphosphine palladium (0.122 g, 0.106 mmol) was added to a rapidly stirred yellow solution of methyl 2-benzyl-6-bromoisonicotinate (**130**, 1.62 g, 5.29 mmol), (trimethylsilyl)-acetylene (4.52 mL, 32.0 mmol), copper(I) iodide (0.040 g, 0.212 mmol), and diisopropylamine (4.52 mL, 31.7 mmol). The suspension was stirred for 3 h. The reaction mixture was filtered, and the remaining solid was washed with EtOAc. The filtrate was washed with water (×2) and brine, and an emulsion formed. The emulsion was passed through a phase separator as were the combined aqueous washings. The aqueous portion was extracted with DCM, and the combined organics were evaporated *in vacuo* to a black gum. The residue was dissolved in toluene and purified by silica chromatography eluting with 10−50% DCM/hexane. The product-containing fractions were evaporated *in vacuo* to give methyl 2-benzyl-6-((trimethylsilyl)-ethynyl)isonicotinate (**131**, 1756 mg, 4.89 mmol, 92% yield) as a black oil. LC−MS (TFA, ES^+) t_R = 1.46 min; m/z = 324.2; ^{1}H NMR (400 MHz, DMSO-d_6): δ 7.71 (s, 2H) 7.35−7.20 (m, 5H) 4.19 (s, 2H) 3.87 (s, 3H) 0.27 (s, 9H).

*2-Benzyl-6-(1-methyl-1H-1,2,3-triazol-4-yl)isonicotinate, Sodium Salt (**132**).* Methyl 2-benzyl-6-(1-methyl-1*H*-1,2,3-triazol-4-yl)-isonicotinate (**131**, 955 mg, 3.10 mmol) was suspended in isopropanol (50 mL) and heated to reflux. The resulting solution was removed from the heat and a solution of 2 M NaOH (3.10 mL, 6.19 mmol) was added. The mixture was cooled to rt with vigorous stirring over 30 min. A white precipitate formed and the suspension was stopped stirring. TBME (40 mL) was added; the suspension was mechanically broken up and stirred vigorously for 20 min. The mixture was then filtered; the solid was washed with TBME (3 × 10 mL) and dried *in vacuo* to give 2-benzyl-6-(1-methyl-1*H*-1,2,3-triazol-4-yl)isonicotinate, sodium salt (**132**, 994 mg, 2.83 mmol, 91% yield) as a white solid. LC−MS (TFA, ES^+) t_R = 0.84 min; m/z = 295.2; ^{1}H NMR (400 MHz, DMSO-d_6): δ ppm 8.19 (d, J = 1.5 Hz, 1H) 7.45 (d, J = 1.5 Hz, 1H) 7.26−7.35 (m, 5H) 7.16−7.24 (m, 1H) 4.04−4.15 (m, 5H).

*2-Benzyl-N-((1R,5S,6r)-3-oxabicyclo[3.1.0]hexan-6-yl)-6-(1-methyl-1H-1,2,3-triazol-4-yl)isonicotinamide (**48**).* A solution of 2-benzyl-6-(1-methyl-1*H*-1,2,3-triazol-4-yl)isonicotinate, sodium salt (**132**, 0.032 g, 0.1 mmol) and HATU (0.038 g, 0.100 mmol) dissolved in DMF (0.5 mL) was prepared. DIPEA (0.055 mL, 0.315 mmol) was added, and the mixture was shaken and added to preweighed (1*R*,5*S*,6*r*)-3-oxabicyclo[3.1.0]hexan-6-amine (**117**, 0.120 mmol). The reaction mixture was capped, shaken, and left to stand at rt for 2 h. HATU (20 mg) was added to the reaction mixture with DIPEA (30 μL). The mixture was capped, shaken, and left to stand at rt for 18 h. A solution of T_3P 50% in EtOAC (120 μL) and DIPEA (55 μL) was added to the reaction vial. The reaction mixture was capped, shaken, and stood at rt for 1 h. The solvent was removed from the reaction mixture. The sample was dissolved in DMSO (2 mL) and purified by high pH MDAP. The solvent was dried under a stream of nitrogen in the Radleys blowdown apparatus to give 2-benzyl-*N*-((1*R*,5*S*,6*r*)-3-oxabicyclo[3.1.0]hexan-6-yl)-6-(1-methyl-1*H*-1,2,3-triazol-4-yl)isonicotinamide (**48**, 9.6 mg, 0.026 mmol, 23% yield). LC−MS (formic, ES^+) t_R = 0.88 min; m/z = 376.0; (100% pure) ^{1}H NMR (500 MHz, DMSO-d_6): δ 8.24 (d, J = 1.4 Hz, 1H) 7.55 (d, J = 1.4 Hz, 1H) 7.35−7.30 (m, 4H) 7.22 (tt, J = 6.9, 1.9 Hz, 2H) 4.18 (s, 2H) 4.13 (s, 3H) 3.87 (d, J = 8.5 Hz, 1H) 3.64 (br d, J = 8.2 Hz, 2H) 2.64 (dt, J = 4.4, 2.5 Hz, 1H) 1.94 (s, 2H).

*2-Benzyl-6-(1-methyl-1H-1,2,3-triazol-4-yl)-N-(tetrahydro-2H-pyran-4-yl)isonicotinamide (**49**).* General procedure C was followed using the following amounts: 2-benzyl-6-(1-methyl-1*H*-1,2,3-triazol-4-yl)isonicotinic acid (**82**, 0.029 g, 0.1 mmol), HATU (0.038 g, 0.100 mmol), DMF (0.5 mL), DIPEA (0.055 mL, 0.315 mmol), and tetrahydro-2*H*-pyran-4-amine (0.120 mmol). The sample was purified by high pH MDAP. The solvent was dried under a stream of nitrogen in the Radleys blowdown apparatus to give 2-benzyl-6-(1-methyl-1*H*-1,2,3-triazol-4-yl)-*N*-(tetrahydro-2*H*-pyran-4-yl)isonicotinamide (**49**, 8.2 mg, 0.022 mmol, 20% yield). LC−MS (formic, ES^+) t_R = 0.89 min; m/z = 378.2; (100% pure) ^{1}H NMR (600 MHz, DMSO-d_6): δ 8.75 (br d, J = 7.9 Hz, 1H) 8.59 (s, 1H) 8.29−8.25 (m, J = 1.1 Hz, 1H) 7.60−7.56 (m, J = 1.1 Hz, 1H) 7.35−7.30 (m, 3H) 7.22 (t, J = 7.5 Hz, 1H) 4.18 (s, 2H) 4.13 (s, 3H) 4.06−3.98 (m, 1H) 3.88 (d, J = 11.7 Hz, 2H) 3.39 (t, J = 11.7 Hz, 2H) 1.77 (d, J = 12.8 Hz, 2H) 1.60 (qd, J = 11.7, 4.5 Hz, 2H).

*2-Benzyl-6-(1-methyl-1H-1,2,3-triazol-4-yl)-N-((tetrahydro-2H-pyran-4-yl)methyl)isonicotinamide (**50**).* General procedure C was followed using the following amounts: HATU (78 mg, 0.204 mmol), 2-benzyl-6-(1-methyl-1*H*-1,2,3-triazol-4-yl)isonicotinic acid (**82**, 50 mg, 0.170 mmol), (tetrahydro-2*H*-pyran-4-yl)methanamine (0.031 mL, 0.255 mmol), DIPEA (0.089 mL, 0.510 mmol), and DMF (4 mL). The sample was purified using normal-phase column chromatography, eluting with a gradient of 80−100% EtOAc/cyclohexane. The product-containing fractions were combined, and the solvent was removed *in vacuo*. The sample was then dried under a stream of nitrogen for 1 h and was then placed in the vacuum oven at 40 °C 1 h to give 2-benzyl-6-(1-methyl-1*H*-1,2,3-triazol-4-yl)-*N*-((tetrahydro-2*H*-pyran-4-yl)methyl)isonicotinamide (**50**, 50 mg, 0.12 mmol, 68% yield) as a white solid. LC−MS (formic, ES^+) t_R = 0.91 min; m/z = 392.3; (100% pure) ^{1}H NMR (400 MHz, DMSO-d_6): δ 8.87 (t, J = 5.9 Hz, 1H) 8.58 (s, 1H) 8.26 (d, J = 1.5 Hz, 1H) 7.57 (d, J = 1.5 Hz, 1H) 7.36−7.29 (m, 4H) 7.22 (tt, J = 6.8, 1.5 Hz, 1H) 4.18 (s, 2H) 4.13 (s, 3H) 3.85 (ddd, J = 11.7, 3.9, 2.0 Hz, 2H) 3.25 (dd, J = 11.7, 2.0 Hz, 2H) 3.17 (t, J = 6.4 Hz, 2H) 1.86−1.76 (m, J = 3.9, Hz, 1H) 1.60 (dd, J = 12.7, 2.0 Hz, 2H) 1.20 (qd, J = 12.2, 3.9 Hz, 2H).

*(R)-tert-Butyl 2-(2-(2-Benzyl-6-(1-methyl-1H-1,2,3-triazol-4-yl)-isonicotinamido)ethyl)morpholine-4-carboxylate (**75**).* General procedure C was followed using the following amounts: DIPEA (0.095 mL, 0.544 mmol), 2-benzyl-6-(1-methyl-1*H*-1,2,3-triazol-4-yl)-isonicotinic acid (**82**, 100 mg, 0.272 mmol), (*R*)-*tert*-butyl 2-(2-aminoethyl)morpholine-4-carboxylate (68.9 mg, 0.299 mmol), HATU (134 mg, 0.353 mmol), and DMF (3 mL). The sample was purified by silica chromatography using a gradient of 20−90% EtOAc/cyclohexane. The product-containing fractions were combined, and the solvent was removed under reduced pressure. The product was left to dry *in vacuo* for 2 h to give (*R*)-*tert*-butyl 2-(2-(2-benzyl-6-(1-methyl-1*H*-1,2,3-triazol-4-yl)isonicotinamido)ethyl)-morpholine-4-carboxylate (**75**, 104 mg, 0.164 mmol, 60% yield) as a yellow gum. LC−MS (formic, ES^+) t_R = 1.12 min; m/z = 507.4; ^{1}H NMR (400 MHz, $CDCl_3$-*d*): δ 8.19 (d, J = 1.5 Hz, 1H) 8.18 (s, 1H) 7.73−7.66 (m, 1H) 7.55 (ddd, J = 7.3, 4.4, 1.5 Hz, 3H) 7.48 (td, J = 7.8, 2.9 Hz, 3H) 7.53 (d, J = 1.0 Hz, 1H) 7.32 (d, J = 1.0 Hz, 1H) 7.25−7.21 (m, 1H) 4.23 (s, 2H) 4.19 (s, 3H) 3.98 (dd, J = 11.7, 2.9 Hz, 2H) 3.94−3.84 (m, 2H) 3.83−3.73 (m, 2H) 3.56 (td, J = 11.2, 2.4 Hz, 2H) 3.51−3.40 (m, 2H) 1.48 (s, 9H).

*(R)-2-Benzyl-6-(1-methyl-1H-1,2,3-triazol-4-yl)-N-(2-(morpholin-2-yl)ethyl)isonicotinamide (**51**).* TFA (0.032 mL, 0.411 mmol) was added to a suspension of (*R*)-*tert*-butyl 2-(2-(2-benzyl-6-(1-methyl-1*H*-1,2,3-triazol-4-yl)isonicotinamido)ethyl)morpholine-4-carboxylate (**75**, 104 mg, 0.205 mmol) in DCM (3 mL), and the mixture was stirred at rt under nitrogen for 3 h after which further TFA (0.032 mL, 0.411 mmol) was added. Stirring continued for 2 h after which further TFA (0.032 mL, 0.411 mmol) was added, and the reaction mixture was left to stand in solution overnight. The reaction mixture was quenched with sat. sodium bicarbonate solution (10 mL) and extracted with DCM (3 × 20 mL). The organic layer was passed

https://dx.doi.org/10.1021/acs.jmedchem.0c02156
J. Med. Chem. 2021, 64, 3249−3281

through a hydrophobic frit, and the solvent was removed under reduced pressure. The resulting oil was dissolved in DCM and purified by silica chromatography using a gradient of 0−16% 2 M methanolic ammonia/DCM. The product-containing fractions were combined, and the solvent was removed *in vacuo*. The product was left to dry *in vacuo* overnight to give (*R*)-2-benzyl-6-(1-methyl-1*H*-1,2,3-triazol-4-yl)-*N*-(2-(morpholin-2-yl)ethyl)isonicotinamide (**51**, 28.6 mg, 0.070 mmol, 34% yield) as a pale yellow solid. LC−MS (high pH, ES^+) t_R = 0.83 min; *m*/*z* = 407.4; (100% pure) ^{1}H NMR (400 MHz, DMSO-d_6): δ 8.84 (t, *J* = 5.4 Hz, 1H) 8.58 (s, 1H) 8.25 (d, *J* = 1.5 Hz, 1H) 7.56 (d, *J* = 1.5 Hz, 1H) 7.36−7.29 (m, 4H) 7.22 (tt, *J* = 6.4, 2.0 Hz, 1H) 4.18 (s, 2H) 4.13 (s, 3H) 3.71 (dt, *J* = 9.8, 2.0 Hz, 1H) 3.46−3.34 (m, 4H, obscured by water) 2.77 (dd, *J* = 12.2, 2.4 Hz, 1H), 2.65 (br s, 2H) 2.35 (dd, *J* = 12.2, 10.3 Hz, 1H) 1.60 (q, *J* = 7.3 Hz, 2H).

*(S)-tert-Butyl 2-(2-(2-Benzyl-6-(1-methyl-1H-1,2,3-triazol-4-yl)-isonicotinamido)ethyl)morpholine-4-carboxylate (**76**).* General procedure C was followed using the following amounts: DIPEA (83 μL, 0.476 mmol), 2-benzyl-6-(1-methyl-1*H*-1,2,3-triazol-4-yl)isonicotinic acid (**82**, 70 mg, 0.238 mmol), (*S*)-*tert*-butyl 2-(2-aminoethyl)-morpholine-4-carboxylate (**123**, 54.8 mg, 0.238 mmol), HATU (90 mg, 0.238 mmol), and DMF. The sample was purified by silica chromatography using a gradient of 33−100% EtOAc/cyclohexane. The product-containing fractions were combined, and the solvent was removed *in vacuo* to give (*S*)-*tert*-butyl 2-(2-(2-benzyl-6-(1-methyl-1*H*-1,2,3-triazol-4-yl)isonicotinamido)ethyl)morpholine-4-carboxylate (**76**, 108 mg, 0.185 mmol, 78% yield) as a pale yellow solid. LC−MS (formic, ES^+) t_R = 1.13 min; *m*/*z* = 507.4; ^{1}H NMR (400 MHz, $CDCl_3$-*d*): δ 8.18 (s, 2H) 7.55−7.50 (m, 2H) 7.34−7.30 (m, 4H) 4.23 (s, 2H) 4.20 (s, 3H) 4.01−3.96 (m, 2H) 3.84−3.75 (m, 2H) 3.56 (td, *J* = 11.7, 2.4 Hz, 2H) 3.49−3.41 (m, 2H) 1.87−1.71 (m, 3H) 1.48 (s, 9H).

*(S)-2-Benzyl-6-(1-methyl-1H-1,2,3-triazol-4-yl)-N-(2-(morpholin-2-yl)ethyl)isonicotinamide (**52**).* TFA (0.246 mL, 3.20 mmol) was added to a suspension of (*S*)-*tert*-butyl 2-(2-(2-benzyl-6-(1-methyl-1*H*-1,2,3-triazol-4-yl)isonicotinamido)ethyl)morpholine-4-carboxylate (**76**, 108 mg, 0.213 mmol) in DCM (2 mL), and the reaction mixture was stirred at rt for 5 h before the solvent was removed *in vacuo*. The resulting solid was dissolved in MeOH and purified using a 5 g Isolute SCX-2 cartridge using methanol followed by 2 M methanolic ammonia. The basic fractions were combined, and the solvent was removed *in vacuo*. The product was left to dry *in vacuo* for 90 min to give (*S*)-2-benzyl-6-(1-methyl-1*H*-1,2,3-triazol-4-yl)-*N*-(2-(morpholin-2-yl)ethyl)isonicotinamide (**52**, 57 mg, 0.140 mmol, 66% yield) as a white solid. LC−MS (formic, ES^+) t_R = 0.57 min; *m*/*z* = 407.4; (100% pure) ^{1}H NMR (400 MHz, DMSO-d_6): δ 8.89 (t, *J* = 5.4 Hz, 1H) 8.60 (s, 1H) 8.26 (d, *J* = 1.5 Hz, 1H) 7.57 (d, *J* = 1.5 Hz, 1H) 7.36−7.28 (m, 4H) 7.22 (tt, *J* = 6.8, 2.0 Hz, 1H) 4.17 (s, 2H) 4.13 (s, 3H) 3.74 (dd, *J* = 11.7, 2.0 Hz, 1H) 3.48−3.24 (obs. m, 7H) 2.81 (dd, *J* = 12.2, 1.5 Hz, 1H) 2.68−2.60 (m, *J* = 11.2, 11.2, 3.4 Hz, 1H) 2.38 (dd, *J* = 12.2, 10.3 Hz, 1H) 1.60 (br q, *J* = 7.3 Hz, 2H).

*(R)-3-(1-(tert-Butoxycarbonyl)-3-fluoropiperidin-3-yl)propanoic Acid (**133**).* (*R*)-*tert*-Butyl 3-(3-ethoxy-3-oxopropyl)-3-fluoropiperidine-1-carboxylate (**125**, 9.6 g, 31.6 mmol) was dissolved in ethanol (50 mL), and NaOH (47.5 mL, 95 mmol) was added. The solution was then stirred at rt for 4 h. The solvent was evaporated *in vacuo* and the residue was partitioned between water (100 mL) and ether (100 mL). The aqueous layer was acidified with 2 M HCl to pH 2 and then extracted with EtOAc (2 × 100 mL). The organic layer was washed with water (100 mL), then dried, and evaporated *in vacuo* to give (*R*)-3-(1-(*tert*-butoxycarbonyl)-3-fluoropiperidin-3-yl)propanoic acid (**133**, 8.6 g, 31.2 mmol, 99% yield) as a colorless solid. ^{1}H NMR (400 MHz, $CDCl_3$-*d*): δ 3.76 (dt, *J* = 13.2, 4.4 Hz, 1H) 3.06 (br d, *J* = 9.3 Hz, 2H) 2.55 (t, *J* = 7.8 Hz, 2H) 2.04−1.88 (m, 3H) 1.86−1.73 (m, 1H) 1.68−1.50 (m, 3H) 1.47 (s, 9H).

*(R)-tert-Butyl 3-(2-(((Benzyloxy)carbonyl)amino)ethyl)-3-fluoropiperidine-1-carboxylate (**134**).* Diphenyl phosphorazidate (8.08 mL, 37.5 mmol) was added to a mixture of (*R*)-3-(1-(*tert*-butoxycarbonyl)-3-fluoropiperidin-3-yl)propanoic acid (**133**, 8.6 g, 31.2 mmol) and Et_3N (13.06 mL, 94 mmol) in toluene (50 mL). The solution was then stirred for 30 min at rt, benzyl alcohol (6.50 mL, 62.5 mmol) was added, and the mixture was heated at reflux for 3 h. The reaction mixture was diluted with EtOAc (100 mL) and washed with water (100 mL), the organic layer was dried and evaporated *in vacuo*, and the residue was purified by silica chromatography eluting with 0−50% EtOAc/cyclohexane. Product-containing fractions were combined and evaporated *in vacuo* to give (*R*)-*tert*-butyl 3-(2(((benzyloxy)carbonyl)amino)ethyl)-3-fluoropiperidine-1-carboxylate (**134**, 8.9 g, 23.39 mmol, 75% yield) as a colorless gum. LC−MS (formic, ES^+) t_R = 1.22 min; *m*/*z* = 381.3; ^{1}H NMR (400 MHz, DMSO-d_6): δ 7.39−7.28 (m, *J* = 8.3, 5.9 Hz, 4H) 7.24 (t, *J* = 5.4 Hz, 1H) 5.02 (s, 2H) 3.74 (br d, *J* = 12.7 Hz, 2H) 3.18−3.11 (m, *J* = 6.8 Hz, 2H) 3.07−2.93 (m, 1H) 2.87 (br t, *J* = 10.0 Hz, 1H) 1.89−1.80 (m, 1H) 1.79−1.53 (m, 4H) 1.51−1.44 (m, 1H) 1.39 (s, 9H).

*(R)-tert-Butyl 3-(2-Aminoethyl)-3-fluoropiperidine-1-carboxylate (**135**).* (*R*)-*tert*-Butyl 3-(2-(((benzyloxy)carbonyl)amino)ethyl)-3-fluoropiperidine-1-carboxylate (**134**, 8.9 g, 23.39 mmol) was dissolved in ethanol (100 mL), added to Pd/C (2 g) under vacuum, and then hydrogenated at atmospheric pressure for 48 h. The mixture was filtered through celite under nitrogen, and the filtrate was evaporated *in vacuo* to give (*R*)-*tert*-butyl 3-(2-aminoethyl)-3-fluoropiperidine-1-carboxylate (**135**, 6.0 g, 24.36 mmol, 104% yield) as a colorless oil. ^{1}H NMR (400 MHz, DMSO-d_6): δ 3.75 (dt, *J* = 13.2, 3.9 Hz, 1H) 3.86−3.71 (m, 1H) 3.13−3.05 (m, 1H) 2.92−2.80 (m, 1H) 2.70−2.65 (m, *J* = 7.3 Hz, 2H) 1.87−1.77 (m, 1H) 1.72−1.53 (m, 4H), 1.50−1.43 (m, 1H), 1.39 (s, 9H).

*(R)-tert-Butyl 3-(2-(2-Benzyl-6-(1-methyl-1H-1,2,3-triazol-4-yl)-isonicotinamido)ethyl)-3-fluoropiperidine-1-carboxylate (**77**).* General procedure C was followed using the following amounts: DIPEA (0.089 mL, 0.510 mmol), 2-benzyl-6-(1-methyl-1*H*-1,2,3-triazol-4-yl)isonicotinic acid (**82**, 75 mg, 0.255 mmol), (*R*)-*tert*-butyl 3-(2-aminoethyl)-3-fluoropiperidine-1-carboxylate (**135**, 82 mg, 0.331 mmol), HATU (126 mg, 0.331 mmol), and DMF (2 mL). The sample was purified by silica chromatography using a gradient of 30−100% EtOAc/cyclohexane. The product-containing fractions were combined, and the solvent was removed *in vacuo* to give (*R*)-*tert*-butyl 3-(2-(2-benzyl-6-(1-methyl-1*H*-1,2,3-triazol-4-yl)isonicotinamido)-ethyl)-3-fluoropiperidine-1-carboxylate (**77**, 102 mg, 0.176 mmol, 69% yield) as a pale yellow solid. LC−MS (formic, ES^+) t_R = 1.17 min; *m*/*z* = 523.2; ^{1}H NMR (400 MHz, $CDCl_3$-*d*): δ 8.21−8.16 (m, 2H) 7.51 (d, *J* = 1.5 Hz, 1H) 7.31 (obs. s, 5H) 4.23 (s, 2H) 4.20 (s, 3H) 3.74−3.60 (m, 4H) 2.03−1.88 (m, 4H) 1.87−1.76 (m, 2H) 1.74−1.63 (m, 2H) 1.46 (s, 9H).

*(R)-2-Benzyl-N-(2-(3-fluoropiperidin-3-yl)ethyl)-6-(1-methyl-1H-1,2,3-triazol-4-yl)isonicotinamide (**53**).* TFA (0.150 mL, 1.952 mmol) was added to a suspension of (*R*)-*tert*-butyl 3-(2-(2-benzyl-6-(1-methyl-1*H*-1,2,3-triazol-4-yl)isonicotinamido)ethyl)-3-fluoropiperidine-1-carboxylate (**77**, 102 mg, 0.195 mmol) in DCM (3 mL). The reaction mixture was stirred at rt under nitrogen for 1 h and left to stand in solution overnight. The reaction mixture was concentrated *in vacuo* and purified using a 5 g Isolute SCX-2 cartridge using sequential methanol followed by 2 M methanolic ammonia. The basic fractions were combined, and the solvent was removed *in vacuo*. The impure product was dissolved in 1:1 DMSO/MeOH and purified by MDAP (high pH). The product-containing fraction was concentrated and dried *in vacuo* for 2 h to give (*R*)-2-benzyl-*N*-(2-(3-fluoropiperidin-3-yl)ethyl)-6-(1-methyl-1*H*-1,2,3-triazol-4-yl)-isonicotinamide (**53**, 36.4 mg, 0.086 mmol, 44% yield) as a white solid. LC−MS (high pH, ES^+) t_R = 0.91 min; *m*/*z* = 423.4; (100% pure) ^{1}H NMR (400 MHz, DMSO-d_6): δ 8.90 (t, *J* = 5.4 Hz, 1H) 8.60 (s, 1H) 8.25 (d, *J* = 1.5 Hz, 1H) 7.56 (d, *J* = 1.5 Hz, 1H) 7.36−7.28 (m, 4H) 7.22 (tt, *J* = 6.8, 2.0 Hz, 1H) 4.17 (s, 2H) 4.13 (s, 3H) 2.82−2.66 (m, 3H), 2.61 (t, *J* = 13.2 Hz, 1H) 2.23−2.05 (m, 1H) 1.91−1.76 (m, 3H) 1.73−1.62 (m, 1H) 1.62−1.51 (m, 2H) 1.44−1.36 (m, 1H).

*2-Benzyl-6-(1-methyl-1H-1,2,3-triazol-4-yl)-N-(3-(piperidin-4-yl)-propyl)isonicotinamide (**54**).* General procedure C was followed using the following amounts: 2-benzyl-6-(1-methyl-1*H*-1,2,3-triazol-4-yl)isonicotinate, sodium salt (**132**, 0.032 g, 0.1 mmol), HATU (0.038 g, 0.100 mmol), DMF (0.5 mL), DIPEA (0.055 mL, 0.315 mmol),

https://dx.doi.org/10.1021/acs.jmedchem.0c02156
J. Med. Chem. 2021, 64, 3249−3281

and 3-(piperidin-4-yl)propan-1-amine (0.120 mmol). The reaction mixture was capped, shaken, and left to stand at rt for 2 h. HATU (20 mg) was added to the reaction mixture with DIPEA (30 μL). The vessel was capped, shaken, and left to stand at rt for 18 h. A solution of T_3P 50% in EtOAc (120 μL) was added to the reaction vial, and DIPEA (55 μL) was also added. The reaction mixture was capped, shaken, and stood at rt for 1 h. The solvent was removed. The sample was dissolved in DMSO (2 mL) and purified by high pH MDAP. The solvent was dried under a stream of nitrogen in the Radleys blowdown apparatus. To the reaction mixture were added DCM (0.5 mL) and TFA (0.5 mL). The mixture was then capped, shaken, and left to stand at rt for 2 h. The solvent was removed to dryness. An SCX-2 SPE column [0.5 g, preconditioned with MeOH (1 mL)] was prepared, and the sample was dissolved in MeOH (0.5 mL) and added to the column, before it was washed thoroughly with a further MeOH (1 mL). The column was finally washed thoroughly with 2 M NH_3 in MeOH (1 mL) and these final washings only were collected. The solvent was removed to dryness to give 2-benzyl-6-(1-methyl-1*H*-1,2,3-triazol-4-yl)-*N*-(3-(piperidin-4-yl)propyl)isonicotinamide (**54**, 7.3 mg, 0.017 mmol, 16% yield). LC−MS (formic, ES^+) t_R = 0.58 min; m/z = 419.3; (100% pure) ^{1}H NMR (400 MHz, DMSO-d_6): δ 8.84 (t, J = 5.5 Hz, 1H) 8.58 (s, 1H) 8.25 (d, J = 1.5 Hz, 1H) 7.57 (d, J = 1.5 Hz, 1H) 7.37−7.28 (m, 4H) 7.22 (tt, J = 6.5, 2.0 Hz, 1H) 4.18 (s, 2H) 4.13 (s, 3H) 3.58−3.33 (m, 2H) 3.25 (td, J = 7.1, 6.0 Hz, 2H) 2.96 (dt, J = 12.1, 3.5 Hz, 2H) 1.62 (br d, J = 12.1 Hz, 2H) 1.57−1.50 (m, 2H) 1.39−1.28 (m, 1H) 1.26−1.18 (m, 2H) 1.02 (qd, J = 12.1, 4.5 Hz, 2H).

*(S)-2-Benzyl-N-(3-(3-fluoropiperidin-3-yl)propyl)-6-(1-methyl-1H-1,2,3-triazol-4-yl)isonicotinamide (**55**).* A solution of 2-benzyl-6-(1-methyl-1*H*-1,2,3-triazol-4-yl)isonicotinic acid (**82**, 0.029 g, 0.1 mmol) and HATU (0.038 g, 0.100 mmol) dissolved in DMF (0.5 mL) was prepared. DIPEA (0.055 mL, 0.315 mmol) was added before the mixture was shaken and added to preweighed (*R*)-3-(3-fluoropiperidin-3-yl)propan-1-amine (0.120 mmol). The reaction mixture was capped, shaken, and left to stand at rt for 18 h. The sample, in DMF, was taken up into DMSO (0.5 mL) and purified by high pH MDAP. The solvent was dried under a stream of nitrogen in the Radleys blowdown apparatus. To the concentrate were added DCM (0.5 mL) and TFA (0.5 mL). The mixture was capped, shaken, and left to stand at rt for 2 h, before the solvent was removed to dryness. An SCX-2 SPE column [0.5 g, preconditioned with MeOH (1 mL)] was prepared and the sample dissolved in MeOH (0.5 mL) was added. The column was washed with MeOH (1 mL) followed by 2 M NH_3 in MeOH (1 mL). The basic washes were collected, and the solvent was removed to dryness to give (*S*)-2-benzyl-*N*-(3-(3-fluoropiperidin-3-yl)propyl)-6-(1-methyl-1*H*-1,2,3-triazol-4-yl)-isonicotinamide (**55**, 7.1 mg, 0.016 mmol, 15% yield). LC−MS (formic, ES^+) t_R = 0.58 min; m/z = 437.2; (95% pure) ^{1}H NMR (600 MHz, DMSO-d_6): δ 8.91 (t, J = 5.3 Hz, 1H) 8.60−8.59 (m, 1H) 8.27−8.26 (m, 1H) 7.58−7.57 (m, 1H) 7.36−7.30 (m, J = 7.2 Hz, 4H) 7.22 (t, J = 7.2 Hz, 1H) 4.18 (s, 2H) 4.13 (s, 3H) 2.98−2.92 (m, 2H) 2.62−2.55 (m, 2H) 1.84−1.78 (m, 2H) 1.65−1.59 (m, J = 13.6 Hz, 6H) 1.53−1.47 (m, 2H) 1.44−1.38 (m, 1H).

BRD4 Mutant TR-FRET Assay.[73] Tandem bromodomains of 6His-Thr-BRD4(1−477) were expressed, with an appropriate mutation in BD2 (Y390A) to monitor compound binding to BD1 or in BD1 (97A) to monitor compound binding to BD2. Analogous Y → A mutants were used to measure binding to the other BET bromodomains: 6His-Thr-BRD2 (1−473 Y386A or Y113A), 6His-Thr-BRD3 (1−435 Y348A or Y73A), and 6His-FLAG-Tev-BRDT (1−397 Y309A or Y66A). The AlexaFluor 647-labeled BET bromodomain ligand was prepared as follows: to a solution of AlexaFluor 647 hydroxysuccinimide ester in DMF was added a 1.8-fold excess of *N*-(5-aminopentyl)-2-((4*S*)-6-(4-chlorophenyl)-8-methoxy-1-methyl-4*H*-benzo[*f*][1,2,4]triazolo[4,3-*a*][1,4]-diazepin-4-yl)acetamide, also in DMF, and when thoroughly mixed, the solution was basified by the addition of a threefold excess of diisopropylethylamine. Reaction progress was followed by electrospray LC/MS, and when judged completely, the product was isolated and purified by reversed-phase C18 high-performance LC (HPLC). The final compound was characterized by mass spectroscopy and analytical reversed-phase HPLC.

Compounds were titrated from 10 mM in 100% DMSO and 50 nL was transferred to a low volume black 384-well microtitre plate using a Labcyte Echo 555. A Thermo Scientific Multidrop Combi was used to dispense 5 μL of 20 nM protein in an assay buffer of 50 mM HEPES, 150 mM NaCl, 5% glycerol, 1 mM DTT, and 1 mM CHAPS, pH 7.4, and in the presence of 100 nM fluorescent ligand (~K_d concentration for the interaction between BRD4 BD1 and ligand). After equilibrating for 30 min in the dark at rt, the bromodomain protein/fluorescent ligand interaction was detected using TR-FRET following a 5 μL addition of 3 nM europium chelate-labeled anti-6His antibody (PerkinElmer, W1024, AD0111) in assay buffer. Time-resolved fluorescence (TRF) was then detected on a TRF laser-equipped PerkinElmer Envision multimode plate reader (excitation = 337 nm; emission 1 = 615 nm; emission 2 = 665 nm; dual wavelength bias dichroic = 400 nm, 630 nm). The TR-FRET ratio was calculated using the following equation: ratio = [(acceptor fluorescence at 665 nm)/(donor fluorescence at 615 nm)] × 1000. TR-FRET ratio data were normalized to high (DMSO) and low (compound control derivative of I-BET762) controls and IC_{50} values were determined for each of the compounds tested by fitting the fluorescence ratio data to a four-parameter model

$$y = A + (B - A)/(1 + (10c/x')D)$$

where "*A*" is the minimum, "*B*" is the Hill slope, "*c*" is the IC_{50}, and "*D*" is the maximum.

Physicochemical Properties. Permeability across a lipid membrane, chromatographic logD at pH 7.4, and CLND solubility by precipitation into saline were measured using published protocols.[65,74−76]

FaSSIF Solubility. This experiment determines the solubility of solid compounds in FaSSIF at pH 6.5 after 4 h equilibration at room temperature. A total of 1 mL of FaSSIF buffer (3 mM Sodium taurocholate, 0.75 mM lecithin in sodium phosphate buffer at pH 6.5) is added to manually weighed 1 mg of the solid compound in a 4 mL vial.[77] The resulting suspension is shaken at 900 rpm for 4 h at room temperature and then transferred to a Multiscreen HTS, 96-well solubility filter plate. The residual solid is removed by filtration. The supernatant solution is quantified by HPLC-UV using single-point calibration of a known concentration of the compound in DMSO. The dynamic range of the assay is 1−1000 μg/mL.

All animal studies were ethically reviewed and carried out in accordance with Animals (Scientific Procedures) Act 1986 and the GSK Policy on the Care, Welfare and Treatment of Animals.

The human biological samples were sourced ethically and their research use was in accordance with the terms of the informed consents under an IRB/EC-approved protocol.

Intrinsic Clearance (CL_{int}) Measurements. The human biological samples were sourced ethically and their research use was in accordance with the terms of the informed consents under an IRB/EC-approved protocol.

Microsome intrinsic clearance data were determined by Cyprotex UK. To test the metabolic stability of **12**, it was incubated in male Wistar Han rat and mixed gender-pooled human liver microsomes. Microsomes (final protein concentration 0.5 mg/mL), 0.1 M phosphate buffer pH 7.4, and test compound (final substrate concentration = 0.5 μM) were preincubated at 37 °C prior to the addition of NADPH (final concentration = 1 mM) to initiate the reaction. The test compound was incubated for 0, 5, 15, 30, and 45 min. The control (minus NADPH) was incubated for 45 min only. The reactions were stopped by the addition of 50 μL of methanol containing the internal standard at the appropriate time points. Following protein precipitation, the compound remaining in the supernatants was measured using specific LC−MS/MS methods as a ratio to the internal standard in the absence of a calibration curve. Peak area ratios (compound to IS) were fitted to an unweighted logarithmic decline in the substrate. Using the first-order rate constant, clearance was calculated by adjustment for protein

https://dx.doi.org/10.1021/acs.jmedchem.0c02156
J. Med. Chem. 2021, 64, 3249−3281

concentration, volume of the incubation, and hepatic scaling factor (52.5 mg microsomal protein/g liver for all species).

Hepatocyte intrinsic clearance data were determined by Cyprotex UK. The test compound (0.5 μM) was incubated with cryopreserved hepatocytes in suspension. Samples were removed at 6 time points over the course of a 60 min (rat) or 120 min (human) experiment, and the test compound was analyzed by LC−MS/MS. Cryopreserved pooled hepatocytes were purchased from a reputable commercial supplier and stored in liquid nitrogen prior to use. Williams E media was supplemented with 2 mM L-glutamine and 25 mM HEPES, and the test compound (final substrate concentration 0.5 μM; final DMSO concentration 0.25%) was preincubated at 37 °C prior to the addition of a suspension of cryopreserved hepatocytes (final cell density 0.5×10^6 viable cells/mL in Williams E media supplemented with 2 mM L-glutamine and 25 mM HEPES) to initiate the reaction. The final incubation volume was 500 μL. The reactions were stopped by transferring 50 μL of the incubate to 100 μL of acetonitrile at the appropriate time points. The termination plates were centrifuged at 2500 rpm at 4 °C for 30 min to precipitate the protein. The remaining incubate (200 μL) was crashed with 400 μL of acetonitrile at the end of the incubation. Following protein precipitation, the sample supernatants were combined in cassettes of up to 4 compounds and analyzed using Cyprotex generic LC−MS/MS conditions.

Intrinsic Clearance (CL_{int}) Data Analysis. From a plot of ln peak area ratio (compound peak area/internal standard peak area) against time, the gradient of the line was determined. Subsequently, half-life ($t_{1/2}$) and intrinsic clearance (CL_{int}) were calculated using the equations given below

$$\text{elimination rate constant } (k) = (-\text{gradient})$$

$$\text{half-life } (t_{1/2})\ (\text{min}) = \frac{0.693}{k}$$

$$\text{intrinsic clearance } (CL_{int})(\mu\text{L/min /million cells}) = \frac{V \times 0.693}{t_{1/2}}$$

where V = incubation volume (μL)/number of cells.

Fraction Unbound in Blood. Control blood from Wistar Han rats was obtained on the day of experimentation from in-house GSK stock animals. The fraction unbound in blood was determined using a rapid equilibrium dialysis (RED) technology plate (Linden Bioscience, Woburn, MA) at a concentration of 200 and 1000 ng/mL. Blood was dialyzed against phosphate-buffered saline solution by incubating the dialysis units at 37 °C for 4 h. Following incubation, aliquots of blood and buffer were matrix-matched prior to analysis by LC−MS/MS. The unbound fraction was determined using the peak area ratios in buffer and in blood as a mean value of the two concentrations investigated.

Human Serum Albumin Measurements. Chemically bonded human serum albumin (HSA) columns, with the dimensions of 50 mm × 3 mm id, were obtained from Chromtech, Ltd (U.K.). The mobile-phase flow rate was 1.8 mL/min. The starting mobile phase was 50 mM aqueous ammonium acetate, with the pH adjusted to 7.4. Mobile phase B was 100% 2-propanol (HPLC grade). The gradient retention time of the compound was recorded using the following gradient profile: 0−3 min linear gradient from 0 to 30% 2-propanol; 3 to 6 min constant mobile-phase composition of 30% 2-propanol; 6 to 6.5 min linear gradient back to 0% 2-propanol (100% ammonium acetate buffer); and 6.5 to 10 min 100% ammonium acetate buffer.

***In Vivo* DMPK Studies.** All animal studies were ethically reviewed and carried out in accordance with Animals (Scientific Procedures) Act 1986 and the GSK Policy on the Care, Welfare and Treatment of Animals.

For all *in vivo* studies, the temperature and humidity were nominally maintained at 21 ± 2 °C and 55 ± 10%, respectively. The diet for rodents was 5LF2 Eurodent Diet 14% (PMI Labdiet, Richmond, IN). There were no known contaminants in the diet or water at concentrations that could interfere with the outcome of the studies.

Rat Surgical Preparation for the IV Infusion Study. Male Wistar Han rats (supplied by Charles River UK Ltd.) were surgically prepared at GSK with implanted cannulae in the femoral vein (for drug administration) and jugular vein (for blood sampling). The rats received cefuroxime (116 mg/kg sc) and carprofen (7.5 mg/kg sc) as a preoperative antibiotic and analgesic, respectively. The rats were allowed to recover for at least 2 days prior to dosing and had free access to food and water throughout.

Rat IV *n* = 1 PK Study. Surgically prepared male Wistar Han rats received a 1 h intravenous (iv) infusion of compound **28**, **36**, or **29** as a discrete dose, formulated in DMSO and 10% (w/v) Kleptose HPB in saline aq [2:98% (v/v)] at a concentration of 0.2 mg/mL to achieve a target dose of 1 mg/kg. Serial blood samples (25 μL) were collected predose and up to 7 h after the start of the iv infusion. Diluted blood samples were analyzed for the parent compound using a specific LC−MS/MS assay (LLQ = 1−2 ng/mL). At the end of the study, the rats were euthanized using a Schedule 1 technique.

Rat PO *n* = 3 PK Study. Three naïve male Wistar Han rats with no surgical preparation received an oral gavage administration of compound **28**, **36**, or **29** as a discrete dose, suspended in 1% (w/v) methylcellulose aq at a concentration of 0.6 mg/mL to achieve a target dose of 3 mg/kg. Serial blood samples (25 μL) were collected via temporary tail vein cannulation up to 24 h after oral dosing and additional blood sampling via tail vein venepuncture up to 24 h after oral dosing. Diluted blood samples were analyzed for the parent compound using a specific LC−MS/MS assay (LLQ = 1 ng/mL). At the end of the study, the rats were euthanized using a Schedule 1 technique.

Blood Sample Analysis. Diluted blood samples (1:1 with water) were extracted using protein precipitation with acetonitrile containing an analytical internal standard. An aliquot of the supernatant was analyzed by reverse-phase LC−MS/MS using a heat-assisted electrospray interface in the positive ion mode. Samples were assayed against calibration standards prepared in control blood.

PK Data Analysis from PK Studies. PK parameters were obtained from the blood concentration−time profiles using non-compartmental analysis with WinNonlin Professional 6.3 (Pharsight, Mountain View, CA).

hWB MCP-1 Assay. The human biological samples were sourced ethically and their research use was in accordance with the terms of the informed consents under an IRB/EC-approved protocol.

Compounds to be tested were diluted in 100% DMSO to give a range of appropriate concentrations at 140×, the required final assay concentration, of which 1 μL was added to a 96-well tissue culture plate. A total of 130 μL of hWB, collected into a sodium heparin anticoagulant (1 unit/mL final), was added to each well and plates were incubated at 37 °C (5% CO_2) for 30 min before the addition of 10 μL of 2.8 μg/mL LPS (Salmonella typhosa), diluted in complete RPMI 1640 (final concentration 200 ng/mL), to give a total volume of 140 μL per well. After further incubation for 24 h at 37 °C, 140 μL of phosphate-buffered saline was added to each well. The plates were sealed, shaken for 10 min, and then centrifuged (2500 rpm × 10 min). A total of 100 μL of the supernatant was removed and MCP-1 levels were assayed immediately by immunoassay (MesoScale Discovery technology).

■ ASSOCIATED CONTENT

Supporting Information

The Supporting Information is available free of charge at https://pubs.acs.org/doi/10.1021/acs.jmedchem.0c02156.

X-ray crystallographic data and methods, DiscoverX BROMOscan Bromodomain Profiling of **36**, and LC−MS and NMR spectra for **28**, **36**, and **39** (PDF)

Molecular formula strings (CSV)

Accession Codes

Authors will release the unpublished PDB ID, atomic coordinates, and experimental data upon article publication.

https://dx.doi.org/10.1021/acs.jmedchem.0c02156
J. Med. Chem. 2021, 64, 3249−3281

AUTHOR INFORMATION

Corresponding Author

Helen E. Aylott − *Epigenetics Discovery Performance Unit, GlaxoSmithKline, Medicines Research Centre, Hertfordshire SG1 2NY, U.K.*; orcid.org/0000-0002-6362-1790; Email: helen.x.aylott@gsk.com

Authors

Stephen J. Atkinson − *Epigenetics Discovery Performance Unit, GlaxoSmithKline, Medicines Research Centre, Hertfordshire SG1 2NY, U.K.*

Paul Bamborough − *Platform Technology and Science, GlaxoSmithKline, Medicines Research Centre, Hertfordshire SG1 2NY, U.K.*; orcid.org/0000-0001-9479-2894

Anna Bassil − *Epigenetics Discovery Performance Unit, GlaxoSmithKline, Medicines Research Centre, Hertfordshire SG1 2NY, U.K.*

Chun-wa Chung − *Platform Technology and Science, GlaxoSmithKline, Medicines Research Centre, Hertfordshire SG1 2NY, U.K.*; orcid.org/0000-0002-2480-3110

Laurie Gordon − *Platform Technology and Science, GlaxoSmithKline, Medicines Research Centre, Hertfordshire SG1 2NY, U.K.*

Paola Grandi − *IVIVT Cellzome, Platform Technology and Science, GlaxoSmithKline, Heidelberg 69117, Germany*

James R. J. Gray − *Quantitative Pharmacology, Immunoinflammation Therapy Area Unit, GlaxoSmithKline, Medicines Research Centre, Hertfordshire SG1 2NY, U.K.*

Lee A. Harrison − *Epigenetics Discovery Performance Unit, GlaxoSmithKline, Medicines Research Centre, Hertfordshire SG1 2NY, U.K.*; orcid.org/0000-0003-1804-0687

Thomas G. Hayhow − *Epigenetics Discovery Performance Unit, GlaxoSmithKline, Medicines Research Centre, Hertfordshire SG1 2NY, U.K.*

Cassie Messenger − *Platform Technology and Science, GlaxoSmithKline, Medicines Research Centre, Hertfordshire SG1 2NY, U.K.*

Darren Mitchell − *Epigenetics Discovery Performance Unit, GlaxoSmithKline, Medicines Research Centre, Hertfordshire SG1 2NY, U.K.*

Alexander Phillipou − *Platform Technology and Science, GlaxoSmithKline, Medicines Research Centre, Hertfordshire SG1 2NY, U.K.*

Alex Preston − *Epigenetics Discovery Performance Unit, GlaxoSmithKline, Medicines Research Centre, Hertfordshire SG1 2NY, U.K.*; orcid.org/0000-0003-0334-0679

Rab K. Prinjha − *Epigenetics Discovery Performance Unit, GlaxoSmithKline, Medicines Research Centre, Hertfordshire SG1 2NY, U.K.*

Francesco Rianjongdee − *Epigenetics Discovery Performance Unit, GlaxoSmithKline, Medicines Research Centre, Hertfordshire SG1 2NY, U.K.*

Inmaculada Rioja − *Epigenetics Discovery Performance Unit, GlaxoSmithKline, Medicines Research Centre, Hertfordshire SG1 2NY, U.K.*

Jonathan T. Seal − *Epigenetics Discovery Performance Unit, GlaxoSmithKline, Medicines Research Centre, Hertfordshire SG1 2NY, U.K.*; orcid.org/0000-0003-0148-5487

Ian D. Wall − *Platform Technology and Science, GlaxoSmithKline, Medicines Research Centre, Hertfordshire SG1 2NY, U.K.*

Robert J. Watson − *Epigenetics Discovery Performance Unit, GlaxoSmithKline, Medicines Research Centre, Hertfordshire SG1 2NY, U.K.*

James M. Woolven − *Platform Technology and Science, GlaxoSmithKline, Medicines Research Centre, Hertfordshire SG1 2NY, U.K.*

Emmanuel H. Demont − *Epigenetics Discovery Performance Unit, GlaxoSmithKline, Medicines Research Centre, Hertfordshire SG1 2NY, U.K.*; orcid.org/0000-0001-7307-3129

Complete contact information is available at: https://pubs.acs.org/10.1021/acs.jmedchem.0c02156

Author Contributions

The manuscript was written through contributions of all authors. All authors have given approval to the final version of the manuscript.

Funding

All authors were GlaxoSmithKline full-time employees when this study was performed.

Notes

The authors declare no competing financial interest.

ACKNOWLEDGMENTS

We would like to thank Darrian Hollywood, Fiona Shilliday, and other members of Platform Technology Sciences group at GSK for protein reagent generation, assay, and crystallization support; Tony Cooper and Heather Barnett for support with chemistry arrays; Eric Hortense, Richard Briers, Steve Jackson, and Sean Hindley for analytical and purification support; Sean Lynn, Richard Upton, and Stephen Richards for assistance with NMR analysis; and Matthew Bowen for assistance with experimentals.

ABBREVIATIONS

AMP, artificial membrane permeability; BD1, bromodomain 1 (N-terminal bromodomain); BD2, bromodomain 2 (C-terminal bromodomain); BET, bromo and extraterminal domain; BRD2,3,4,T, bromodomain containing protein 2,3,4,T; CL_b, blood clearance; CL_{int}, intrinsic clearance; CLND, chemiluminescent nitrogen detection; DIAD, diisopropyl azodicarboxylate; dppb, 1,4-bis(diphenylphosphino)-butane; EDC, *N*-(3-dimethylaminopropyl)-*N*′-ethylcarbodiimide; EDG, electron-donating group; EWG, electron-withdrawing group; FACS, flow cytometry staining buffer; fu_b, fraction unbound in blood; HATU, 1-[bis(dimethylamino)-methylene]-1*H*-1,2,3-triazolo[4,5-*b*]pyridinium 3-oxide hexafluorophosphate; hWB, human whole blood; *k*, elimination rate constant; KAc, acetylated lysine; LLE_{at}, Astex lipophilic ligand efficiency; MCP-1, monocyte chemoattractant protein-1; MDAP, mass-directed auto preparation; MLA, mouse lymphoma assay; STAB, sodium triacetoxyborohydride; *V*, incubation volume; V_{ss}, volume of distribution at the steady state; WPF, tryptophan-proline-phenylalanine; 2-MeTHF, 2-methyltetrahydrofuran

REFERENCES

(1) Filippakopoulos, P.; Picaud, S.; Mangos, M.; Keates, T.; Lambert, J.-P.; Barsyte-Lovejoy, D.; Felletar, I.; Volkmer, R.; Müller, S.; Pawson, T.; Gingras, A.-C.; Arrowsmith, C. H.; Knapp, S. Histone recognition and large-scale structural analysis of the human bromodomain family. *Cell* **2012**, *149*, 214−231.

(2) Boi, M.; Gaudio, E.; Bonetti, P.; Kwee, I.; Bernasconi, E.; Tarantelli, C.; Rinaldi, A.; Testoni, M.; Cascione, L.; Ponzoni, M.; Mensah, A. A.; Stathis, A.; Stussi, G.; Riveiro, M. E.; Herait, P.; Inghirami, G.; Cvitkovic, E.; Zucca, E.; Bertoni, F. The BET bromodomain inhibitor OTX015 affects pathogenetic pathways in preclinical B-cell tumor models and synergizes with targeted drugs. *Clin. Cancer Res.* **2015**, *21*, 1628−1638.
(3) Chaidos, A.; Caputo, V.; Gouvedenou, K.; Liu, B.; Marigo, I.; Chaudhry, M. S.; Rotolo, A.; Tough, D. F.; Smithers, N. N.; Bassil, A. K.; Chapman, T. D.; Harker, N. R.; Barbash, O.; Tummino, P.; Al-Mahdi, N.; Haynes, A. C.; Cutler, L.; Le, B.; Rahemtulla, A.; Roberts, I.; Kleijnen, M.; Witherington, J. J.; Parr, N. J.; Prinjha, R. K.; Karadimitris, A. Potent antimyeloma activity of the novel bromodomain inhibitors I-BET151 and I-BET762. *Blood* **2014**, *123*, 697−705.
(4) Cheng, Z.; Gong, Y.; Ma, Y.; Lu, K.; Lu, X.; Pierce, L. A.; Thompson, R. C.; Muller, S.; Knapp, S.; Wang, J. Inhibition of BET bromodomain targets genetically diverse glioblastoma. *Clin. Cancer Res.* **2013**, *19*, 1748−1759.
(5) da Motta, L. L.; Ledaki, I.; Purshouse, K.; Haider, S.; De Bastiani, M. A.; Baban, D.; Morotti, M.; Steers, G.; Wigfield, S.; Bridges, E.; Li, J.-L.; Knapp, S.; Ebner, D.; Klamt, F.; Harris, A. L.; McIntyre, A. The BET inhibitor JQ1 selectively impairs tumour response to hypoxia and downregulates CA9 and angiogenesis in triple negative breast cancer. *Oncogene* **2016**, *36*, 122−132.
(6) Filippakopoulos, P.; Qi, J.; Picaud, S.; Shen, Y.; Smith, W. B.; Fedorov, O.; Morse, E. M.; Keates, T.; Hickman, T. T.; Felletar, I.; Philpott, M.; Munro, S.; McKeown, M. R.; Wang, Y.; Christie, A. L.; West, N.; Cameron, M. J.; Schwartz, B.; Heightman, T. D.; La Thangue, N.; French, C. A.; Wiest, O.; Kung, A. L.; Knapp, S.; Bradner, J. E. Selective inhibition of BET bromodomains. *Nature* **2010**, *468*, 1067−1073.
(7) Picaud, S.; Da Costa, D.; Thanasopoulou, A.; Filippakopoulos, P.; Fish, P. V.; Philpott, M.; Fedorov, O.; Brennan, P.; Bunnage, M. E.; Owen, D. R.; Bradner, J. E.; Taniere, P.; O'Sullivan, B.; Müller, S.; Schwaller, J.; Stankovic, T.; Knapp, S. PFI-1, A highly selective protein interaction inhibitor, targeting BET bromodomains. *Cancer Res.* **2013**, *73*, 3336−3346.
(8) Prinjha, R. K.; Witherington, J.; Lee, K. Place your BETs: the therapeutic potential of bromodomains. *Trends Pharmacol. Sci.* **2012**, *33*, 146−153.
(9) Rhyasen, G. W.; Hattersley, M. M.; Yao, Y.; Dulak, A.; Wang, W.; Petteruti, P.; Dale, I. L.; Boiko, S.; Cheung, T.; Zhang, J.; Wen, S.; Castriotta, L.; Lawson, D.; Collins, M.; Bao, L.; Ahdesmaki, M. J.; Walker, G.; O'Connor, G.; Yeh, T. C.; Rabow, A. A.; Dry, J. R.; Reimer, C.; Lyne, P.; Mills, G. B.; Fawell, S. E.; Waring, M. J.; Zinda, M.; Clark, E.; Chen, H. AZD5153: A novel bivalent BET bromodomain inhibitor highly active against hematologic malignancies. *Mol. Cancer Ther.* **2016**, *15*, 2563−2574.
(10) Segura, M. F.; Fontanals-Cirera, B.; Gaziel-Sovran, A.; Guijarro, M. V.; Hanniford, D.; Zhang, G.; González-Gomez, P.; Morante, M.; Jubierre, L.; Zhang, W.; Darvishian, F.; Ohlmeyer, M.; Osman, I.; Zhou, M.-M.; Hernando, E. BRD4 Sustains melanoma proliferation and represents a new target for epigenetic therapy. *Cancer Res.* **2013**, *73*, 6264−6276.
(11) Zuber, J.; Shi, J.; Wang, E.; Rappaport, A. R.; Herrmann, H.; Sison, E. A.; Magoon, D.; Qi, J.; Blatt, K.; Wunderlich, M.; Taylor, M. J.; Johns, C.; Chicas, A.; Mulloy, J. C.; Kogan, S. C.; Brown, P.; Valent, P.; Bradner, J. E.; Lowe, S. W.; Vakoc, C. R. RNAi Screen identifies Brd4 as a therapeutic target in acute myeloid leukaemia. *Nature* **2011**, *478*, 524−528.
(12) Bandukwala, H. S.; Gagnon, J.; Togher, S.; Greenbaum, J. A.; Lamperti, E. D.; Parr, N. J.; Molesworth, A. M. H.; Smithers, N.; Lee, K.; Witherington, J.; Tough, D. F.; Prinjha, R. K.; Peters, B.; Rao, A. Selective inhibition of CD4+ T-cell cytokine production and autoimmunity by BET protein and c-Myc inhibitors. *Proc. Natl. Acad. Sci. U.S.A.* **2012**, *109*, 14532−14537.
(13) Belkina, A. C.; Nikolajczyk, B. S.; Denis, G. V. BET Protein function is required for inflammation: Brd2 genetic disruption and BET inhibitor JQ1 impair mouse macrophage inflammatory responses. *J. Immunol.* **2013**, *190*, 3670−3678.
(14) Chan, C. H.; Fang, C.; Qiao, Y.; Yarilina, A.; Prinjha, R. K.; Ivashkiv, L. B. BET Bromodomain inhibition suppresses transcriptional responses to cytokine-Jak-STAT signaling in a gene-specific manner in human monocytes. *Eur. J. Immunol.* **2015**, *45*, 287−297.
(15) Klein, K.; Kabala, P. A.; Grabiec, A. M.; Gay, R. E.; Kolling, C.; Lin, L.-L.; Gay, S.; Tak, P. P.; Prinjha, R. K.; Ospelt, C.; Reedquist, K. A. The bromodomain protein inhibitor I-BET151 suppresses expression of inflammatory genes and matrix degrading enzymes in rheumatoid arthritis synovial fibroblasts. *Ann. Rheum. Dis.* **2016**, *75*, 422−429.
(16) Mele, D. A.; Salmeron, A.; Ghosh, S.; Huang, H.-R.; Bryant, B. M.; Lora, J. M. BET Bromodomain inhibition suppresses T(H)17-mediated pathology. *J. Exp. Med.* **2013**, *210*, 2181−2190.
(17) Meng, S.; Zhang, L.; Tang, Y.; Tu, Q.; Zheng, L.; Yu, L.; Murray, D.; Cheng, J.; Kim, S. H.; Zhou, X.; Chen, J. BET Inhibitor JQ1 blocks inflammation and bone destruction. *J. Dent. Res.* **2014**, *93*, 657−662.
(18) Nadeem, A.; Al-Harbi, N. O.; Al-Harbi, M. M.; El-Sherbeeny, A. M.; Ahmad, S. F.; Siddiqui, N.; Ansari, M. A.; Zoheir, K. M. A.; Attia, S. M.; Al-Hosaini, K. A.; Al-Sharary, S. D. Imiquimod-induced psoriasis-like skin inflammation is suppressed by BET bromodomain inhibitor in mice through RORC/IL-17A pathway modulation. *Pharmacol. Res.* **2015**, *99*, 248−257.
(19) Nicodeme, E.; Jeffrey, K. L.; Schaefer, U.; Beinke, S.; Dewell, S.; Chung, C.-w.; Chandwani, R.; Marazzi, I.; Wilson, P.; Coste, H.; White, J.; Kirilovsky, J.; Rice, C. M.; Lora, J. M.; Prinjha, R. K.; Lee, K.; Tarakhovsky, A. Suppression of inflammation by a synthetic histone mimic. *Nature* **2010**, *468*, 1119−1123.
(20) Schilderink, R.; Bell, M.; Reginato, E.; Patten, C.; Rioja, I.; Hilbers, F. W.; Kabala, P. A.; Reedquist, K. A.; Tough, D. F.; Tak, P. P.; Prinjha, R. K.; de Jonge, W. J. BET Bromodomain inhibition reduces maturation and enhances tolerogenic properties of human and mouse dendritic cells. *Mol. Immunol.* **2016**, *79*, 66−76.
(21) Tough, D. F.; Prinjha, R. K. Immune disease-associated variants in gene enhancers point to BET epigenetic mechanisms for therapeutic intervention. *Epigenomics* **2017**, *9*, 573−584.
(22) Tough, D. F.; Tak, P. P.; Tarakhovsky, A.; Prinjha, R. K. Epigenetic drug discovery: breaking through the immune barrier. *Nat. Rev. Drug Discovery* **2016**, *15*, 835−853.
(23) Zhang, Q.-g.; Qian, J.; Zhu, Y.-c. Targeting bromodomain-containing protein 4 (BRD4) benefits rheumatoid arthritis. *Immunol. Lett.* **2015**, *166*, 103−108.
(24) Alqahtani, A.; Choucair, K.; Ashraf, M.; Hammouda, D. M.; Alloghbi, A.; Khan, T.; Senzer, N.; Nemunaitis, J. Bromodomain and extra-terminal motif inhibitors: a review of preclinical and clinical advances in cancer therapy. *Future Sci. OA* **2019**, *5*, FSO372.
(25) Doroshow, D. B.; Eder, J. P.; LoRusso, P. M. BET Inhibitors: a novel epigenetic approach. *Ann. Oncol.* **2017**, *28*, 1776−1787.
(26) Liu, Z.; Wang, P.; Chen, H.; Wold, E. A.; Tian, B.; Brasier, A. R.; Zhou, J. Drug discovery targeting bromodomain-containing protein 4. *J. Med. Chem.* **2017**, *60*, 4533−4558.
(27) Andrieu, G.; Belkina, A. C.; Denis, G. V. Clinical trials for BET inhibitors run ahead of the science. *Drug Discovery Today: Technol.* **2016**, *19*, 45−50.
(28) Piha-Paul, S. A.; Sachdev, J. C.; Barve, M.; LoRusso, P.; Szmulewitz, R.; Patel, S. P.; Lara, P. N.; Chen, X.; Hu, B.; Freise, K. J.; Modi, D.; Sood, A.; Hutti, J. E.; Wolff, J.; O'Neil, B. H. First-in-human study of mivebresib (ABBV-075), an oral pan-inhibitor of bromodomain and extra terminal proteins, in patients with relapsed/refractory solid tumors. *Clin. Cancer Res.* **2019**, *25*, 6309−6319.
(29) Postel-Vinay, S.; Herbschleb, K.; Massard, C.; Woodcock, V.; Soria, J.-C.; Walter, A. O.; Ewerton, F.; Poelman, M.; Benson, N.; Ocker, M.; Wilkinson, G.; Middleton, M. First-in-human phase I study of the bromodomain and extraterminal motif inhibitor BAY 1238097: emerging pharmacokinetic/pharmacodynamic relationship

https://dx.doi.org/10.1021/acs.jmedchem.0c02156
J. Med. Chem. 2021, 64, 3249−3281

and early termination due to unexpected toxicity. *Eur. J. Cancer* **2019**, *109*, 103−110.
(30) Amans, D.; Atkinson, S. J.; Harrison, L. A.; Hirst, D. J.; Law, R. P.; Lindon, M.; Preston, A.; Seal, J. T.; Wellaway, C. R. 2,3-Disubstituted 1-acyl-4-amino-1,2,3,4-tetrahydroquinoline derivatives and their use as bromodomain inhibitors. WO 2014140076 A1, 2014.
(31) Amans, D.; Bamborough, P.; Barker, M. D.; Bit, R. A.; Brown, J. A.; Campbell, M.; Garton, N. S.; Lindon, M. J.; Shipley, T. J.; Theodoulou, N. H.; Wellaway, C. R.; Westaway, S. M. Furopyridines as bromodomain inhibitors. WO 2014140077 A1, 2014.
(32) Atkinson, S. J.; Aylott, H. E.; Cooper, A. W. J.; Demont, E. H.; Harrison, L. A.; Hayhow, T. G. C.; Lindon, M. J.; Preston, A. G.; Seal, J. T.; Wall, I. D.; Watson, R. J.; Woolven, J. M. Pyridinone dicarboxamide for use as bromodomain inhibitors. WO 2017037116 A1, 2017.
(33) Atkinson, S. J.; Demont, E. H.; Harrison, L. A.; Hayhow, T. G. C.; House, D.; Lindon, M. J.; Preston, A. G.; Seal, J. T.; Wall, I. D.; Watson, R. J.; Woolven, J. M. Pyridinone dicarboxamide for use as bromodomain inhibitors. WO 2017050714 A1, 2017.
(34) Combs, A. P.; Sparks, R. B.; Maduskuie, T. P., Jr.; Rodgers, J. D. Tricyclic heterocycles as bet protein inhibitors. WO 2014143768 A1, 2014.
(35) Gerner Seitzberg, J.; Titilola Akinleminu Kronborg, T.; Poljak, V.; Friberg, G.; Teuber, L. Compounds active towards bromodomains. WO 2016016316 A1, 2016.
(36) Siegel, S.; Baeurle, S.; Cleve, A.; Haendler, B.; Fernandez-Montalvan, A. E. 1-Phenyl-3h-2,3-benzodiazepines and their use as bromodomain inhibitors. WO 2015121268 A1, 2015.
(37) Wang, L.; Dai, Y.; Holms, J.; Liu, D.; McClellan, W.; McDaniel, K.; Hasvold, L.; Fidanze, S. D.; Sheppard, G.; Marjanovic, J. Bromodomain inhibitors. WO 2014206345 A1, 2014.
(38) Petretich, M.; Demont, E. H.; Grandi, P. Domain-selective targeting of BET proteins in cancer and immunological diseases. *Curr. Opin. Chem. Biol.* **2020**, *57*, 184−193.
(39) Baud, M. G. J.; Lin-Shiao, E.; Cardote, T.; Tallant, C.; Pschibul, A.; Chan, K.-H.; Zengerle, M.; Garcia, J. R.; Kwan, T. T. L.; Ferguson, F. M.; Ciulli, A. A bump-and-hole approach to engineer controlled selectivity of BET bromodomain chemical probes. *Science* **2014**, *346*, 638−641.
(40) Miller, T. C. R.; Simon, B.; Rybin, V.; Grötsch, H.; Curtet, S.; Khochbin, S.; Carlomagno, T.; Müller, C. W. A bromodomain−DNA interaction facilitates acetylation-dependent bivalent nucleosome recognition by the BET protein BRDT. *Nat. Commun.* **2016**, *7*, 13855−13868.
(41) Olp, M. D.; Jackson, V.; Smith, B. C. Nucleosome scaffolding by Brd4 tandem bromodomains in acetylation-dependent chromatin compartmentalization. *bioRxiv* **2019**, 699967.
(42) Runcie, A. C.; Zengerle, M.; Chan, K.-H.; Testa, A.; van Beurden, L.; Baud, M. G. J.; Epemolu, O.; Ellis, L. C. J.; Read, K. D.; Coulthard, V.; Brien, A.; Ciulli, A. Optimization of a "bump-and-hole" approach to allele-selective BET bromodomain inhibition. *Chem. Sci.* **2018**, *9*, 2452−2468.
(43) Cheung, K.; Lu, G.; Sharma, R.; Vincek, A.; Zhang, R.; Plotnikov, A. N.; Zhang, F.; Zhang, Q.; Ju, Y.; Hu, Y.; Zhao, L.; Han, X.; Meslamani, J.; Xu, F.; Jaganathan, A.; Shen, T.; Zhu, H.; Rusinova, E.; Zeng, L.; Zhou, J.; Yang, J.; Peng, L.; Ohlmeyer, M.; Walsh, M. J.; Zhang, D. Y.; Xiong, H.; Zhou, M.-M. BET N-Terminal bromodomain inhibition selectively blocks Th17 cell differentiation and ameliorates colitis in mice. *Proc. Natl. Acad. Sci. U.S.A.* **2017**, *114*, 2952−2957.
(44) Divakaran, A.; Talluri, S. K.; Ayoub, A. M.; Mishra, N. K.; Cui, H.; Widen, J. C.; Berndt, N.; Zhu, J.-Y.; Carlson, A. S.; Topczewski, J. J.; Schonbrunn, E. K.; Harki, D. A.; Pomerantz, W. C. K. Molecular Basis for the N-Terminal Bromodomain-and-Extra-Terminal-Family Selectivity of a Dual Kinase-Bromodomain Inhibitor. *J. Med. Chem.* **2018**, *61*, 9316−9334.
(45) Gacias, M.; Gerona-Navarro, G.; Plotnikov, A. N.; Zhang, G.; Zeng, L.; Kaur, J.; Moy, G.; Rusinova, E.; Rodriguez, Y.; Matikainen, B.; Vincek, A.; Joshua, J.; Casaccia, P.; Zhou, M.-M. Selective chemical modulation of gene transcription favors oligodendrocyte lineage progression. *Chem. Biol.* **2014**, *21*, 841−854.
(46) Raux, B.; Voitovich, Y.; Derviaux, C.; Lugari, A.; Rebuffet, E.; Milhas, S.; Priet, S.; Roux, T.; Trinquet, E.; Guillemot, J.-C.; Knapp, S.; Brunel, J.-M.; Fedorov, A. Y.; Collette, Y.; Roche, P.; Betzi, S.; Combes, S.; Morelli, X. Exploring selective inhibition of the first bromodomain of the human bromodomain and extra-terminal domain (BET) proteins. *J. Med. Chem.* **2016**, *59*, 1634−1641.
(47) Zhang, G.; Plotnikov, A. N.; Rusinova, E.; Shen, T.; Morohashi, K.; Joshua, J.; Zeng, L.; Mujtaba, S.; Ohlmeyer, M.; Zhou, M.-M. Structure-guided design of potent diazobenzene inhibitors for the BET bromodomains. *J. Med. Chem.* **2013**, *56*, 9251−9264.
(48) Bai, P.; Lu, X.; Liu, Y.; Lan, Y.; Wang, H.; Fiedler, S.; Striar, R.; Wang, C. Discovery of a positron emission tomography radiotracer selectively targeting the BD1 bromodomains of BET proteins. *ACS Med. Chem. Lett.* **2021**, *12*, 282.
(49) Liu, Z.; Chen, H.; Wang, P.; Li, Y.; Wold, E. A.; Leonard, P. G.; Joseph, S.; Brasier, A. R.; Tian, B.; Zhou, J. Discovery of orally bioavailable chromone derivatives as potent and selective BRD4 inhibitors: scaffold hopping, optimization, and pharmacological evaluation. *J. Med. Chem.* **2020**, *63*, 5242−5256.
(50) Hügle, M.; Lucas, X.; Weitzel, G.; Ostrovskyi, D.; Breit, B.; Gerhardt, S.; Einsle, O.; Günther, S.; Wohlwend, D. 4-Acyl pyrrole derivatives yield novel vectors for designing inhibitors of the acetyl-lysine recognition site of BRD4(1). *J. Med. Chem.* **2016**, *59*, 1518−1530.
(51) Baud, M. G. J.; Lin-Shiao, E.; Zengerle, M.; Tallant, C.; Ciulli, A. New synthetic routes to triazolo-benzodiazepine analogues: expanding the scope of the bump-and-hole approach for selective bromo and extra-terminal (BET) bromodomain inhibition. *J. Med. Chem.* **2016**, *59*, 1492−1500.
(52) Kharenko, O. A.; Gesner, E. M.; Patel, R. G.; Norek, K.; White, A.; Fontano, E.; Suto, R. K.; Young, P. R.; McLure, K. G.; Hansen, H. C. RVX-297- A novel BD2 selective inhibitor of BET bromodomains. *Biochem. Biophys. Res. Commun.* **2016**, *477*, 62−67.
(53) McLure, K. G.; Gesner, E. M.; Tsujikawa, L.; Kharenko, O. A.; Attwell, S.; Campeau, E.; Wasiak, S.; Stein, A.; White, A.; Fontano, E.; Suto, R. K.; Wong, N. C. W.; Wagner, G. S.; Hansen, H. C.; Young, P. R. RVX-208, An inducer of ApoA-I in humans, is a BET bromodomain antagonist. *PLoS One* **2013**, *8*, No. e83190.
(54) Jiang, F.; Hu, Q.; Zhang, Z.; Li, H.; Li, H.; Zhang, D.; Li, H.; Ma, Y.; Xu, J.; Chen, H.; Cui, Y.; Zhi, Y.; Zhang, Y.; Xu, J.; Zhu, J.; Lu, T.; Chen, Y. Discovery of benzo[cd]indol-2(1H)-ones and pyrrolo-[4,3,2-de]quinolin-2(1H)-ones as bromodomain and extra-terminal domain (BET) inhibitors with selectivity for the first bromodomain with potential high efficiency against acute gouty arthritis. *J. Med. Chem.* **2019**, *62*, 11080−11107.
(55) Watson, R. J.; Bamborough, P.; Barnett, H.; Chung, C.-w.; Davis, R.; Gordon, L.; Grandi, P.; Petretich, M.; Phillipou, A.; Prinjha, R. K.; Rioja, I.; Soden, P.; Werner, T.; Demont, E. H. GSK789: A selective inhibitor of the first bromodomains (BD1) of the bromo and extra terminal domain (BET) proteins. *J. Med. Chem.* **2020**, *63*, 9045−9069.
(56) Wellaway, C. R.; Bamborough, P.; Bernard, S. G.; Chung, C.-w.; Craggs, P. D.; Cutler, L.; Demont, E. H.; Evans, J. P.; Gordon, L.; Karamshi, B.; Lewis, A. J.; Lindon, M. J.; Mitchell, D. J.; Rioja, I.; Soden, P. E.; Taylor, S.; Watson, R. J.; Willis, R.; Woolven, J. M.; Wyspiańska, B. S.; Kerr, W. J.; Prinjha, R. K. Structure-based design of a bromodomain and extraterminal domain (BET) inhibitor selective for the N-terminal bromodomains that retains an anti-inflammatory and anti-proliferative phenotype. *J. Med. Chem.* **2020**, *63*, 9020−9044.
(57) Law, R. P.; Atkinson, S. J.; Bamborough, P.; Chung, C.-w.; Demont, E. H.; Gordon, L. J.; Lindon, M.; Prinjha, R. K.; Watson, A. J. B.; Hirst, D. J. Discovery of tetrahydroquinoxalines as bromodomain and extra-terminal domain (BET) inhibitors with selectivity for the second bromodomain. *J. Med. Chem.* **2018**, *61*, 4317−4334.
(58) Faivre, E. J.; McDaniel, K. F.; Albert, D. H.; Mantena, S. R.; Plotnik, J. P.; Wilcox, D.; Zhang, L.; Bui, M. H.; Sheppard, G. S.;

https://dx.doi.org/10.1021/acs.jmedchem.0c02156
J. Med. Chem. 2021, 64, 3249−3281

Wang, L.; Sehgal, V.; Lin, X.; Huang, X.; Lu, X.; Uziel, T.; Hessler, P.; Lam, L. T.; Bellin, R. J.; Mehta, G.; Fidanze, S.; Pratt, J. K.; Liu, D.; Hasvold, L. A.; Sun, C.; Panchal, S. C.; Nicolette, J. J.; Fossey, S. L.; Park, C. H.; Longenecker, K.; Bigelow, L.; Torrent, M.; Rosenberg, S. H.; Kati, W. M.; Shen, Y. Selective inhibition of the BD2 bromodomain of BET proteins in prostate cancer. *Nature* **2020**, *578*, 306−310.

(59) Sheppard, G. S.; Wang, L.; Fidanze, S. D.; Hasvold, L. A.; Liu, D.; Pratt, J. K.; Park, C. H.; Longenecker, K.; Qiu, W.; Torrent, M.; Kovar, P. J.; Bui, M.; Faivre, E.; Huang, X.; Lin, X.; Wilcox, D.; Zhang, L.; Shen, Y.; Albert, D. H.; Magoc, T. J.; Rajaraman, G.; Kati, W. M.; McDaniel, K. F. Discovery of N-ethyl-4-[2-(4-fluoro-2,6-dimethylphenoxy)-5-(1-hydroxy-1-methyl-ethyl)phenyl]-6-methyl-7-oxo-1H-pyrrolo[2,3-c]pyridine-2-carboxamide (ABBV-744), a BET bromodomain inhibitor with selectivity for the second bromodomain. *J. Med. Chem.* **2020**, *63*, 5585−5623.

(60) Gilan, O.; Rioja, I.; Knezevic, K.; Bell, M. J.; Yeung, M. M.; Harker, N. R.; Lam, E. Y. N.; Chung, C.-w.; Bamborough, P.; Petretich, M.; Urh, M.; Atkinson, S. J.; Bassil, A. K.; Roberts, E. J.; Vassiliadis, D.; Burr, M. L.; Preston, A. G. S.; Wellaway, C.; Werner, T.; Gray, J. R.; Michon, A.-M.; Gobbetti, T.; Kumar, V.; Soden, P. E.; Haynes, A.; Vappiani, J.; Tough, D. F.; Taylor, S.; Dawson, S.-J.; Bantscheff, M.; Lindon, M.; Drewes, G.; Demont, E. H.; Daniels, D. L.; Grandi, P.; Prinjha, R. K.; Dawson, M. A. Selective targeting of BD1 and BD2 of the BET proteins in cancer and immunoinflammation. *Science* **2020**, *368*, 387−394.

(61) Preston, A.; Atkinson, S. J.; Bamborough, P.; Chung, C.-w.; Gordon, L. J.; Grandi, P.; Gray, J. R. J.; Harrison, L. A.; Lewis, A. J.; Lugo, D.; Messenger, C.; Michon, A.-M.; Mitchell, D. J.; Prinjha, R. K.; Rioja, I.; Seal, J.; Taylor, S.; Thesmar, P.; Wall, I. D.; Watson, R. J.; Woolven, J. M.; Demont, E. H. GSK973 Is an inhibitor of the second bromodomains (BD2s) of the bromodomain and extra-terminal (BET) family. *ACS Med. Chem. Lett.* **2020**, *11*, 1581−1587.

(62) Preston, A.; Atkinson, S.; Bamborough, P.; Chung, C.-w.; Craggs, P. D.; Gordon, L.; Grandi, P.; Gray, J. R. J.; Jones, E. J.; Lindon, M.; Michon, A.-M.; Mitchell, D. J.; Prinjha, R. K.; Rianjongdee, F.; Rioja, I.; Seal, J.; Taylor, S.; Wall, I.; Watson, R. J.; Woolven, J.; Demont, E. H. Design and Synthesis of a Highly Selective and In Vivo-Capable Inhibitor of the Second Bromodomain of the Bromodomain and Extra Terminal Domain Family of Proteins. *J. Med. Chem.* **2020**, *63*, 9070−9092.

(63) Harrison, L. A.; Atkinson, S. J.; Bassil, A. K.; Chung, C.-w.; Grandi, P.; Gray, J. R.; Liverier, E.; Lugo, D.; Michon, A.-M.; Mitchell, D. J.; Preston, A.; Prinjha, R. K.; Rioja, I.; Seal, J.; Taylor, S.; Wall, I.; Watson, R. J.; Woolven, J.; Demont, E. H. The identification of a series of N-methylpyridine-2-carboxamides as potent and selective inhibitors of the second bromodomain (BD2) of the bromo and extra terminal domain (BET) proteins. *J. Med. Chem.* **2021**, accepted for publication.

(64) Seal, J. T.; Atkinson, S. J.; Aylott, H.; Bamborough, P.; Chung, C.-w.; Copley, R. C. B.; Gordon, L.; Grandi, P.; Gray, J. R. J.; Harrison, L. A.; Hayhow, T. G.; Lindon, M.; Messenger, C.; Michon, A.-M.; Mitchell, D.; Preston, A.; Prinjha, R. K.; Rioja, I.; Taylor, S.; Wall, I. D.; Watson, R. J.; Woolven, J. M.; Demont, E. H. The optimisation of a novel, weak bromo and extra terminal domain (BET) bromodomain fragment ligand to a potent and selective second bromodomain (BD2) inhibitor. *J. Med. Chem.* **2020**, *63*, 9093−9126.

(65) Young, R. J.; Green, D. V. S.; Luscombe, C. N.; Hill, A. P. Getting physical in drug discovery II: the Impact of chromatographic hydrophobicity measurements and aromaticity. *Drug Discovery Today* **2011**, *16*, 822−830.

(66) Mortenson, P. N.; Murray, C. W. Assessing the lipophilicity of fragments and early hits. *J. Comput.-Aided Mol. Des.* **2011**, *25*, 663−667.

(67) Albrecht, B. K.; Gehling, V. S.; Hewitt, M. C.; Vaswani, R. G.; Côté, A.; Leblanc, Y.; Nasveschuk, C. G.; Bellon, S.; Bergeron, L.; Campbell, R.; Cantone, N.; Cooper, M. R.; Cummings, R. T.; Jayaram, H.; Joshi, S.; Mertz, J. A.; Neiss, A.; Normant, E.; O'Meara, M.; Pardo, E.; Poy, F.; Sandy, P.; Supko, J.; Sims, R. J.; Harmange, J.-C.; Taylor, A. M.; Audia, J. E. Identification of a benzoisoxazoloazepine inhibitor (CPI-0610) of the bromodomain and extra-terminal (BET) family as a candidate for human clinical trials. *J. Med. Chem.* **2016**, *59*, 1330−1339.

(68) Gehling, V. S.; Hewitt, M. C.; Vaswani, R. G.; Leblanc, Y.; Côté, A.; Nasveschuk, C. G.; Taylor, A. M.; Harmange, J.-C.; Audia, J. E.; Pardo, E.; Joshi, S.; Sandy, P.; Mertz, J. A.; Sims, R. J.; Bergeron, L.; Bryant, B. M.; Bellon, S.; Poy, F.; Jayaram, H.; Sankaranarayanan, R.; Yellapantula, S.; Bangalore Srinivasamurthy, N.; Birudukota, S.; Albrecht, B. K. Discovery, design, and optimization of isoxazole azepine BET inhibitors. *ACS Med. Chem. Lett.* **2013**, *4*, 835−840.

(69) Hewings, D. S.; Wang, M.; Philpott, M.; Fedorov, O.; Uttarkar, S.; Filippakopoulos, P.; Picaud, S.; Vuppusetty, C.; Marsden, B.; Knapp, S.; Conway, S. J.; Heightman, T. D. 3,5-Dimethylisoxazoles act as acetyl-lysine-mimetic bromodomain ligands. *J. Med. Chem.* **2011**, *54*, 6761−6770.

(70) Mirguet, O.; Gosmini, R.; Toum, J.; Clément, C. A.; Barnathan, M.; Brusq, J.-M.; Mordaunt, J. E.; Grimes, R. M.; Crowe, M.; Pineau, O.; Ajakane, M.; Daugan, A.; Jeffrey, P.; Cutler, L.; Haynes, A. C.; Smithers, N. N.; Chung, C.-W.; Bamborough, P.; Uings, I. J.; Lewis, A.; Witherington, J.; Parr, N.; Prinjha, R. K.; Nicodème, E. Discovery of epigenetic regulator I-BET762: lead optimization to afford a clinical candidate inhibitor of the BET bromodomains. *J. Med. Chem.* **2013**, *56*, 7501−7515.

(71) Fletcher, J. T.; Walz, S. E.; Keeney, M. E. Monosubstituted 1,2,3-triazoles from two-step one-pot deprotection/click additions of trimethylsilylacetylene. *Tetrahedron Lett.* **2008**, *49*, 7030−7032.

(72) Whiting, M.; Harwood, K.; Hossner, F.; Turner, P. G.; Wilkinson, M. C. Selection and development of the manufacturing route for EP1 antagonist GSK269984B. *Org. Process Res. Dev.* **2010**, *14*, 820−831.

(73) Chung, C.-w.; Coste, H.; White, J. H.; Mirguet, O.; Wilde, J.; Gosmini, R. L.; Delves, C.; Magny, S. M.; Woodward, R.; Hughes, S. A.; Boursier, E. V.; Flynn, H.; Bouillot, A. M.; Bamborough, P.; Brusq, J.-M. G.; Gellibert, F. J.; Jones, E. J.; Riou, A. M.; Homes, P.; Martin, S. L.; Uings, I. J.; Toum, J.; Clément, C. A.; Boullay, A.-B.; Grimley, R. L.; Blandel, F. M.; Prinjha, R. K.; Lee, K.; Kirilovsky, J.; Nicodeme, E. Discovery and characterization of small molecule inhibitors of the BET family bromodomains. *J. Med. Chem.* **2011**, *54*, 3827−3838.

(74) Valkó, K.; Bevan, C.; Reynolds, D. Chromatographic Hydrophobicity Index by Fast-Gradient RP-HPLC: A High-Throughput Alternative to log P/log D. *Anal. Chem.* **1997**, *69*, 2022−2029.

(75) Bunally, S.; Young, R. J. The role and impact of high throughput biomimetic measurements in drug discovery. *ADMET and DMPK* **2018**, *6*, 74−84.

(76) Valko, K.; Nunhuck, S.; Bevan, C.; Abraham, M. H.; Reynolds, D. P. Fast gradient HPLC method to determine compounds binding to human serum albumin. Relationships with octanol/water and immobilized artificial membrane lipophilicity. *J. Pharm. Sci.* **2003**, *92*, 2236−2248.

(77) Sou, T.; Bergström, C. A. S. Automated assays for thermodynamic (equilibrium) solubility determination. *Drug Discovery Today: Technol.* **2018**, *27*, 11−19.

https://dx.doi.org/10.1021/acs.jmedchem.0c02156
J. Med. Chem. 2021, 64, 3249−3281